**UNIVERSIDAD COMPLUTENSE DE MADRID**
FACULTAD DE CIENCIAS BIOLÓGICAS


# TESIS DOCTORAL

## Non-genetic factors modulate the role of NR5A2 in pancreatic inflammation

## Factores no genéticos modulan el papel de NR5A2 en inflamación pancreática/

MEMORIA PARA OPTAR AL GRADO DE DOCTOR

PRESENTADA POR

**Irene Millán Crespo**

Director

**Francisco Real Arribas**

Madrid

# UNIVERSIDAD COMPLUTENSE DE MADRID

FACULTAD DE CIENCIAS BIOLÓGICAS



# TESIS DOCTORAL

Non-genetic factors modulate the role of NR5A2 in pancreatic inflammation
Factores no genéticos modulan el papel de NR5A2 en inflamación pancreática

MEMORIA PARA OPTAR AL GRADO DE DOCTORA

PRESENTADA POR


Irene Millán Crespo

DIRECTOR

Francisco Real Arribas

Universidad Complutense de Madrid (UCM)

Facultad de Ciencias Biológicas


Doctoral Thesis/Tesis Doctoral

# NON-GENETIC FACTORS MODULATE THE ROLE OF NR5A2 IN PANCREATIC INFLAMMATION

# FACTORES NO GENÉTICOS MODULAN EL PAPEL DE NR5A2 EN INFLAMACIÓN PANCREÁTICA

Irene Millán Crespo

Thesis Director/Director de tesis

Francisco Real Arribas

Programa de doctorado en Bioquímica, Biología Molecular y Biomedicina

Madrid, 2022

The project that gave rise to these results received the support of a fellowship from "la Caixa" Foundation (ID 100010434). The fellowship code is LCF/BQ/DE18/11670009.

A mi abuela Alicia

# ACKNOWLEDGEMENTS

En primer lugar, me gustaría darle las gracias a **Paco** por darme la oportunidad de unirme a este laboratorio. Gracias por confiar en mí, por tu paciencia y por tu esfuerzo en formarnos para convertirnos en mejores científicos. Ahora me doy cuenta de que lo cómodo para ti habría sido conformarte con cualquier cosa, o como me decía mi madre de pequeña: darnos para cenar bocadillos de nocilla. Muchas gracias por ser crítico, por involucrarte en nuestros proyectos, pero a la vez fomentar que propongamos nuestras propias ideas y tener en cuenta nuestras preferencias.

Gracias a todos los miembros de laboratorio de Carcinogénesis Epitelial, por crear un ambiente de trabajo tan agradable y divertido. **Mark**, thanks for being so helpful and fun! You came to the lab in a bad moment for this project and helped me to regain the motivation needed to continue. I'm really grateful for that! A **Miriam**, una de las mejores personas que he conocido nunca, muchísimas gracias por ayudarme a organizar mis ideas cuando no veía la luz, por tu buen rollo y tus buenos consejos. A **Cintia Massillo**, que ha participado en muchos de los experimentos presentados en esta tesis. Gracias por darlo todo durante tu estancia y por adaptarte tan bien a mi forma de trabajar (incluso a la ingesta de palmeras de chocolate, jaja). A Cata, Mago y Mónicus, mis compañeras desde el principio de la tesis. A **Cata**, por ponerle un toque de cordura a todas las situaciones. Gracias a **Francisco** y a ti por hacernos partícipes de vuestra vida (y por los pistachos, jaja). A **Mago**, por las risas, por los bailes y por ser el pegamento del labo incluso después de haberte ido. A **Mónicus**, muchísimas gracias por tu apoyo durante los momentos más duros de la escritura. Ha sido bonito compartir este camino contigo y tenerte como referencia en cada paso que me tocaba dar. Eres una campeona y un ejemplo a seguir. Gracias a la nueva generación de predocs, que nos van a dejar a todos los anteriores a la altura del betún. A **Catalina**, por hacerte la sueca cuando me como tus cereales. A **Auba**, Ms. Intensity, por ofrecerme tu ayuda con experimentos delicados. A **Cris B.**, por sacar lo mejor de mis chapas y hacerme reír con tus posados de culturista e intentos de hablar griego. A **Maria,** por ser tan divertida a la par que sensata, pero sobre todo por acompañarme al cerro San Pedro jaja (¡gracias a **Alberto** también!). A **Leti**, que cuando nos queramos dar cuenta formará parte de esta categoría, gracias por el buen rollo que transmites. Y por supuesto, gracias a mi **Sonius** querida, por ser tan buena persona, amiga y compañera. Por quererme tanto, por escuchar sin juzgar y

por ser una fuente de inspiración, talento y diversión. Lo mejor de este laboratorio es coincidir contigo todos los días. Gracias también a todos los postdocs del laboratorio. A **Ele**, por no tener miedo a decir lo que piensas y apoyar a tus compañeros cuando nadie se atreve. A **Irene**, por ser todo un ejemplo de esfuerzo y sacrificio, ¡una súper mujer! A **Elena**, por estar siempre dispuesta a ayudar y conseguir que los experimentos difíciles den menos miedo. A **Sladjana**, una pedazo de investigadora, a la par que divertida y atenta. A **Cris S.**, por asegurarte de que no pasemos hambre. A **Lavi**, por tu buen rollo y simpatía. A **Gabriel**, por el interés que has mostrado siempre en este proyecto. A **Luis**, por la tranquilidad y simpatía que te caracterizan. A **Jaime**, por tu ayuda con temas de bioinformática, tu buen criterio y transparencia. A nuestros técnicos de laboratorio. A **Natalia**, por todo la ayuda con los ratoncitos, desde el diseño hasta la realización de los experimentos. A **Tania**, **Miguelín** y **Leti** (de nuevo), por los innumerables cortes de páncreas. **Miguelín**, sin duda me has descubierto una nueva dimensión de la originalidad. Gracias también a todos los estudiantes y residentes que han pasado por el laboratorio a lo largo de los años (**Fran, Ester, Santi, Pablo, Maxime, Tatiana, Martina, Mirabai, Sonia**). Gracias a **Cristina Álvaro**, por ser tan simpática y resolutiva.

Gracias al personal de las distintas unidades del CNIO, así como todos aquellos profesionales que trabajan para facilitar nuestro trabajo. A todos los miembros del animalario, por vuestro esfuerzo y dedicación. A **Yoli, Oliva, Sheila** e **Isa**, por cuidar de mis ratoncitos y tener una paciencia inmensa conmigo. A **Isabel Blanco** y **Gema Luque**, por hacerlo todo tan fácil. A los miembros de lavado, por recibirme todas las mañanas de tratamientos con una sonrisa. A **Lola** por ayudarme tantísimo con los experimentos de citometría. A **Eduardo**, por todo el tiempo invertido en evaluar cortes histológicos. A **Enrique** y **Osvaldo**, por vuestra ayuda durante los primeros meses en la unidad de Bioinformática. Al personal de seguridad, con los que he compartido muchos turnos de fin de semana. Al personal de limpieza, especialmente a **Gloria** y a **Natalia**; las tardes son mucho más divertidas con vosotras. Al equipo de **Mantenimiento e Instrumentación**, los grandes solucionadores de problemas. Al personal de IT, especialmente a **Félix** por su carisma y humor.

Muchas gracias a **Guillermo Velasco, Carles Úbeda, Alejo Efeyan, Salvador Iborra, Elisa Espinet, Oscar Palomares, Evangelina López de Maturana, Iván Ballesteros,**

**Gonzalo Gómez** y **Gabriel Piedrafita** por aceptar la invitación de formar parte del tribunal de mi tesis.

Many thanks to **David Olmeda**, **Anabel Rojas**, **Erwin Wagner** and **Latifa Bakiri** for the scientific discussion and advice during the thesis committee meetings, and to our collaborators: **Nuria Malats**, **Evangelina López de Maturana**, **Lola Alonso**, **Sylvie Rabot**, **Sandra Rodríguez** and **Cintia Massillo**. Gracias también al **Wiener Lab** (Argentina) por donar los reactivos para la medición de triglicéridos en plasma.

A la Obra Social de la Fundación "la Caixa", por darme la oportunidad de formar parte de su magnífico programa de becas.

A nuestros vecinos de Melanoma, especialmente a **Marta**, **Xavi**, **Naiara** por las consultorías de citometría, el préstamo de reactivos, las risas y los buenos momentos. También a **Dani** y **Davide**, por amenizar las tardes con vuestras bromas a la pobre Gloria. A todos mis compañeros de la beca de la Caixa, en especial a **Pablo**, **Miquel** y **Vicky. Vicky**, it has been fun to share these years with you! Thank you for being up to every plan, from a quick trip to Segovia to learning sevillanas from a school video. You have been the best possible flatmate! A **Alberto Hernández** y a **Marina Gomá**, por ayudarme a preparar la entrevista de la beca. A **Bruna** y **Marta** (de nuevo), por nuestros desayunos formativo-terapéuticos. A **Sergio**, por instalarme los mejores programas. A todos los compañeros de otros laboratorios que me han acompañado a lo largo de estos años: **Pedro, Santi, Iñaki, Kurt, Raúl**, **Simone, Lauritz, Jessica, Raquel, Claudia, Thelma, Álvaro Curiel, Verónica, Iole, Montero, José Carlos** y muchos otros**.**

Gracias a toda mi familia, por su apoyo incondicional. A mi **madre**, por creer en mí y preocuparse siempre por mi bienestar. A mi **padre**, por apoyarme en todas las decisiones e impulsarme a tomar aquellas que dan un poco de vértigo, como la de hacer un doctorado. A **Enrique**, por ser tan generoso y dejar que arrase la nevera cuando los experimentos no me dejan tiempo para hacer la compra. A **Bea**, por el coaching emocional. A **Natalia**, por las llamadas de camino al trabajo. A **Rudy** y a **Gon**. A mis sobrinas, **Sofía**, **Lily** y **Alejandra**, por ser la mayor fuente de felicidad sin ni siquiera intentarlo.

A mis amigas de Tres Cantos (Popeyas y Popeye) y de la universidad (Divinas), por animarme tanto en los malos momentos y compartir mi alegría en los buenos. ¡Qué suerte tener tan buenas amigas!

A **Miguel**, por haber sido una parte esencial de mi vida durante todos estos años, por hacer esfuerzos por no dormirte cuando te cuento mi proyecto y combatirme con bromas cuando me pongo muy pesada. Gracias por todo tu cariño y apoyo.

A todos vosotros, gracias por ayudarme a llegar hasta aquí.

# TABLE OF CONTENTS

# SUMMARY

Genome-wide association studies have identified pancreatic ductal adenocarcinoma (PDAC) susceptibility variants in the vicinity of the *NR5A2* gene, which codes for an orphan nuclear receptor involved in acinar differentiation. *Nr5a2* heterozygous mice (*Nr5a2*$^{+/-}$) display more severe damage upon induction of pancreatitis and are sensitized to the effects of mutant *Kras*. The pancreas of *Nr5a2*$^{+/-}$ mice displays a pre-inflammatory state that mimics transcriptomic changes present in the pancreas of subjects carrying *NR5A2* risk alleles. Here, I aimed to determine the contribution of non-genetic factors to pancreatic inflammation in these mice.

First, I investigated the effects of administration of a high fat diet (HFD). Wild type (*wt*) and *Nr5a2*$^{+/-}$ mice displayed similar changes in body weight gain, insulin resistance, glucose intolerance, and hypercholesterolemia. However, *Nr5a2*$^{+/-}$ mice presented an attenuated hepatic steatosis. While HFD administration exacerbated experimental pancreatitis in *wt* mice, this was not observed in *Nr5a2*$^{+/-}$ mice. These results indicate that *Nr5a2* heterozygosity does not cooperate with HFD to induce pancreatic inflammation.

In addition, I investigated the role of the gut microbiome, which has emerged as a critical modulator of pancreatic disease. I depleted the gut microbiome using broad-spectrum antibiotics (ABX) and assessed the effects on the pancreas in basal conditions and upon induction of pancreatitis, through the use of histologic and transcriptomic analyses. ABX administration had no major effects on pancreas histology but it induced a transcriptomic sub-inflammatory state in the pancreas both in *wt* and in *Nr5a2*$^{+/-}$ mice. In addition, ABX-mediated gut microbiome depletion rescued pancreatitis at the histological and transcriptomic level in *Nr5a2*$^{+/-}$ mice. Transcriptomic analyses of the pancreas revealed that ABX treatment led to an up-regulation of oxidative phosphorylation in basal conditions; the same pathways were down-regulated upon pancreatitis induction only in *Nr5a2*$^{+/-}$ mice. These findings suggest that the effects of ABX could result from the modulation of mitochondrial function. Immunoprofiling showed that *Nr5a2*$^{+/-}$ mice presented increased levels of circulating and splenic T and CD4+ T cells, that were normalised upon ABX administration. These immune cell populations have been reported to participate in the pathogenesis of pancreatitis, suggesting that ABX may protect *Nr5a2*$^{+/-}$ mice from pancreatitis through the modulation of the activity of these immune cell populations. The composition and

diversity of the fecal microbiome and the abundance of intrapancreatic bacteria was comparable across genotypes, supporting the notion that *Nr5a2* heterozygosity does not promote pancreatic inflammation through the generation of dysbiosis.

Overall, this work reveals a complex interaction between *Nr5a2* haploinsufficiency and non-genetic factors and indicates that a genetic defect that increases susceptibility to pancreatic disease can be rescued through manipulation of the gut microbiota. Understanding the mechanisms involved may provide an opportunity to act on modifiable factors to prevent pancreatic disease.

# RESUMEN

Los estudios de asociación del genoma completo han identificado variantes de susceptibilidad al adenocarcinoma ductal pancreático (PDAC) próximos al gen *NR5A2*, que codifica un receptor nuclear huérfano involucrado en la diferenciación acinar. Los ratones heterocigotos para *Nr5a2* (*Nr5a2*$^{+/-}$) muestran un daño más grave tras la inducción de pancreatitis y están sensibilizados a los efectos de *Kras* mutante. El páncreas de ratones *Nr5a2*$^{+/-}$ muestra un estado preinflamatorio que imita los cambios transcriptómicos presentes en el páncreas de sujetos que portan alelos de riesgo para *NR5A2*. El objetivo principal de esta tesis es determinar la contribución de factores no genéticos a la inflamación pancreática en estos ratones.

Primero, investigué los efectos de la administración de una dieta alta en grasas (HFD). Los ratones wild type (*wt*) y *Nr5a2*$^{+/-}$ experimentaron cambios similares en el aumento de peso corporal, resistencia a la insulina, intolerancia a la glucosa e hipercolesterolemia. Sin embargo, los ratones *Nr5a2*$^{+/-}$ presentaban menos esteatosis hepática. Si bien la administración de HFD exacerbó la pancreatitis experimental en los ratones *wt*, esto no se observó en los ratones *Nr5a2*$^{+/-}$. Estos resultados indican que la heterocigosidad para *Nr5a2* no coopera con HFD en la inducción de inflamación pancreática.

Por otro lado, exploré el papel de la microbiota intestinal, que se ha propuesto como un modulador crítico de la enfermedad pancreática. Para ello, eliminé la microbiota intestinal usando antibióticos de amplio espectro (ABX) y evalué los efectos sobre el páncreas en condiciones basales y tras la inducción de pancreatitis, mediante el uso de análisis histológicos y transcriptómicos. La administración de ABX no tenía efectos importantes sobre la histología del páncreas, pero inducía un estado subinflamatorio a nivel transcriptómico en el páncreas tanto en ratones *wt* como en *Nr5a2*$^{+/-}$. Además, la eliminación de la microbiota intestinal mediante el uso de ABX rescataba la pancreatitis a nivel histológico y transcriptómico en ratones *Nr5a2*$^{+/-}$. Los análisis transcriptómicos del páncreas revelaron que el tratamiento con ABX aumentaba la expresión de firmas de fosforilación oxidativa en condiciones basales. Únicamente en ratones *Nr5a2*$^{+/-}$, la inducción de una pancreatitis regulaba estas mismas rutas transcripcionales en la dirección opuesta. Estos hallazgos sugieren que los efectos de los ABX podrían resultar de la modulación de la función mitocondrial. De acuerdo a nuestros análisis de poblaciones inmunitarias, los ratones *Nr5a2*$^{+/-}$ presentaban niveles elevados de células T

y T CD4+ en sangre y bazo, que se normalizan tras la administración de ABX. La literatura indica que estas poblaciones de células inmunitarias participan en la evolución de la pancreatitis, lo que sugiere que los ABX podrían proteger a los ratones *Nr5a2*$^{+/-}$ de la pancreatitis a través de la modulación de la actividad de estas poblaciones de células inmunitarias. Los ratones *wt* y *Nr5a2*$^{+/-}$ presentaban una cantidad normal de bacterias en el páncreas y no mostraban alteraciones en la composición o diversidad de la microbiota intestinal, lo que respalda la idea de que la heterocigosis en *Nr5a2* no promueve la inflamación pancreática a través de la generación de disbiosis.

En general, estos estudios revelan una interacción compleja entre la haploinsuficiencia de *Nr5a2* y los factores no genéticos, e indica que un defecto genético que aumenta el riesgo de enfermedad pancreática se puede rescatar mediante la manipulación de la microbiota intestinal. Adquirir un mayor entendimiento de los mecanismos involucrados podría ofrecernos la oportunidad de prevenir la enfermedad pancreática mediante la modulación de factores modificables.

# ABBREVIATIONS

| | |
|---|---|
| ABX | Antibiotic(s) |
| ALR | AIM2-like receptors |
| ADM | Acinar-to-ductal metaplasia |
| AF-2 | Activating function-2 |
| AmphB | Amphotericin B |
| AP | Acute pancreatitis |
| AUC | Area under curve |
| B | Basal |
| BMI | Body mass index |
| CACs | Centroacinar cells |
| ChIP | Chromatin immunoprecipitation |
| CLR | C-type lectin receptor |
| CD | Control diet |
| CCK | Cholecystokinin |
| CP | Chronic pacreatitis |
| DAMPs | Damage-associated molecular patterns |
| DBD | DNA-binding domain |
| DLPC | Dilauroyl phosphatidyl choline |
| ER | Endoplasmic reticulum |
| ERK | Extracellular signal-regulated kinases |
| FDR | False discovery rate |
| FISH | Fluorescence *in situ* hybridization |
| FITC | Fluorescein isothiocyanate |
| GLP-1 | Glucagon peptide 1 |
| GTT | Glucose tolerance test |
| GSEA | Gene set enrichment analysis |
| GWAS | Genome-wide association studies |
| h | Hours |
| HFD | High-fat diet |
| HDAC3 | Histone deacetylase 3 |
| HOMA-IR | Homeostatic assessment for insulin resistance |
| HRE | Hormone response element |

| | |
|---|---|
| H&E | Hematoxylin and eosin |
| i.p. | Intraperitoneal |
| LBD | Ligand-binding domain |
| LPS | Bacterial lipopolysaccharide |
| LRH-1 | Liver homolog receptor 1 (NR5A2) |
| M | Metronidazole |
| min | Minutes |
| MBF-1 | Multiprotein bridging factor 1 |
| MPC | Multipotent progenitor cells |
| mpIgR | Mouse poly immunoglobulin receptor |
| N | Neomycin |
| NASH | Non-alcoholic steatohepatitis |
| NFALD | Non-fatty acid liver disease |
| NLR | NOD-like receptor |
| NR | Nuclear receptor |
| OCT | Optimal cutting temperature compound |
| PAMPs | Pathogen-associated molecular patterns |
| PanIN | Pancreatic intraepithelial neoplasia |
| PCA | Principal component analysis |
| PCG-1 α | PPARɣ coactivator 1α |
| PDAC | Pancreatic ductal adenocarcinoma |
| PE | Phosphatidyl ethanolamine |
| PG | Phosphatidyl glycerol |
| PI | Phosphatidyl inositol |
| PKA | Protein kinase A |
| PPARɣ | Proliferator-activated receptor gamma |
| PYY | Peptide tyrosine-tyrosine |
| PRRs | Patter recognition receptors |
| qPCR | quantitative PCR |
| RLR | RIG-I-like receptor |
| RNA-seq | RNA-sequencing |
| RT | Room temperature |

| | |
|---|---|
| RT-qPCR | Reverse transcription-quantitative PCR |
| SBAs | Secondary bile acids |
| SCFAs | Short chain fatty acids |
| SHP | Short heterodimer partner (NR0B2) |
| SNP | Single-nucleotide polymorphisms |
| TF | Transcription factor |
| TGF-β | Transforming growth factor- β |
| TLR | Toll-like receptor |
| TSS | Transcriptional start site |
| V | Vancomycin |
| *wt* | wild type |
| 16S rDNA | 16S ribosomal DNA gene |
| 16 rRNA | 16S ribosomal RNA |

# INTRODUCTION

# 1. Pancreas biology

The pancreas is a glandular organ involved in the regulation of two major physiological processes: food digestion and glucose homeostasis. It is located in the upper left abdomen, surrounded by the spleen, stomach and small intestine and connected to the duodenum by the ampulla of Vater, a conical structure where the main pancreatic duct confluences with the bile duct (Fig. I1A) (Slack, 1995). In humans, the pancreas constitutes a well-defined organ that can be macroscopically divided into three parts – head, body and tail – based on their proximity to the duodenum. This organization is less evident in rodents, in which the pancreas is diffusely localised throughout the mesentery adjacent to the duodenum (Dolenšek, Rupnik and Stožer, 2015). The pancreas is mainly composed of two types of glandular tissue: an exocrine compartment that secretes digestive enzymes into the duodenum, and an endocrine compartment that releases hormones into the bloodstream. It is irrigated by numerous blood vessels, which travel alongside an intricate lymphatic network. In addition, the pancreas has an extensive sympathetic and parasympathetic nerve supply (Slack, 1995).

## 1.1. Exocrine pancreas

The exocrine pancreas constitutes more than 95% of the pancreatic tissue and is composed of three epithelial cell types: acinar, ductal and centroacinar cells.

**Acinar cells** are the most abundant cell type in the pancreas. They are organised in functional clusters – called acini – specialised in the large-scale production of digestive enzymes (Fig. I1B). Acinar cells have a pyramidal shape, with a basal nucleus, an extensive rough endoplasmic reticulum (ER) and a prominent Golgi apparatus. They have a polarised appearance in hematoxylin and eosin (H&E) stains, where the basophilic nature of the perinuclear region contrasts with the numerous eosinophilic granules located in the apical part (Slack, 1995; Whitley, 2014). Despite their low proliferative rate, adult acinar cells display a significant regenerative capacity in response to damage (Storz, 2017).

**Ductal cells** form the epithelial lining of pancreatic ducts, a complex network of tubes that deliver acinar enzymes into the digestive tract. Upon secretin hormonal stimulation,

ductal cells secrete a bicarbonate rich solution that dilutes acinar enzymes and neutralises stomach acidity. These cells also secrete mucins, which protect and lubricate the epithelial lining (Slack, 1995; Grapin-Botton, 2005).

**Centroacinar cells** (CACs) are specialised ductal pancreatic cells located between the acinus and the terminal ductal tree (Fig. I1B). This poorly characterised cell type, display a unique cell morphology with cytoplasmic projections that extend into the pancreatic parenchyma, connecting them to neighbouring cells from the exocrine and endocrine compartments (Leeson and Leeson, 1986; Delaspre *et al.*, 2015; Beer, Parsons and Rovira, 2016). CACs have been proposed as multipotent progenitors in rodents, since they proliferate in response to different types of pancreatic injury (Gasslander *et al.*, 1990; Hayashi *et al.*, 2003; Nagasao *et al.*, 2005), although their progenitor status in mammals is under debate. Recently, the mitochondrial enzyme ALDH1B1 was reported as a unique centroacinar specific marker. ALDH1B1-expressing cells have been found to contribute to the three major pancreatic lineages – acinar, ductal and endocrine – in homeostatic mouse pancreas, supporting the role of CACs as multipotent progenitors (Mameishvili *et al.*, 2019).

## 1.2. Endocrine pancreas

Endocrine cells constitute 1-2% of the total pancreas weight and are mainly organised into islets of Langerhans, which are well defined spheroidal clusters embedded within acinar tissue that release hormones into the bloodstream (Fig. I1C and I1D). In addition, individual endocrine cells may be found adjacent to ducts, acini or connective tissue. Islets are composed of multiple hormone-secreting cell types that act in a coordinated manner through paracrine communication to regulate glucose homeostasis, including: α cells (which secrete glucagon), β cells (insulin), δ cells (somatostatin), ε cells (ghrelin) and PP or F cells (pancreatic polypeptide) (Haschek-Hock *et al.*, 2022). Alpha and β cells control glucose availability, while the remaining cell types regulate their secretory properties (Da Silva Xavier, 2018). The control of glucose homeostasis is highly reliant on the microvasculature present within the islets, which facilitates rapid glucose sensing and hormonal release into the circulation (Puri and Hebrok, 2010).

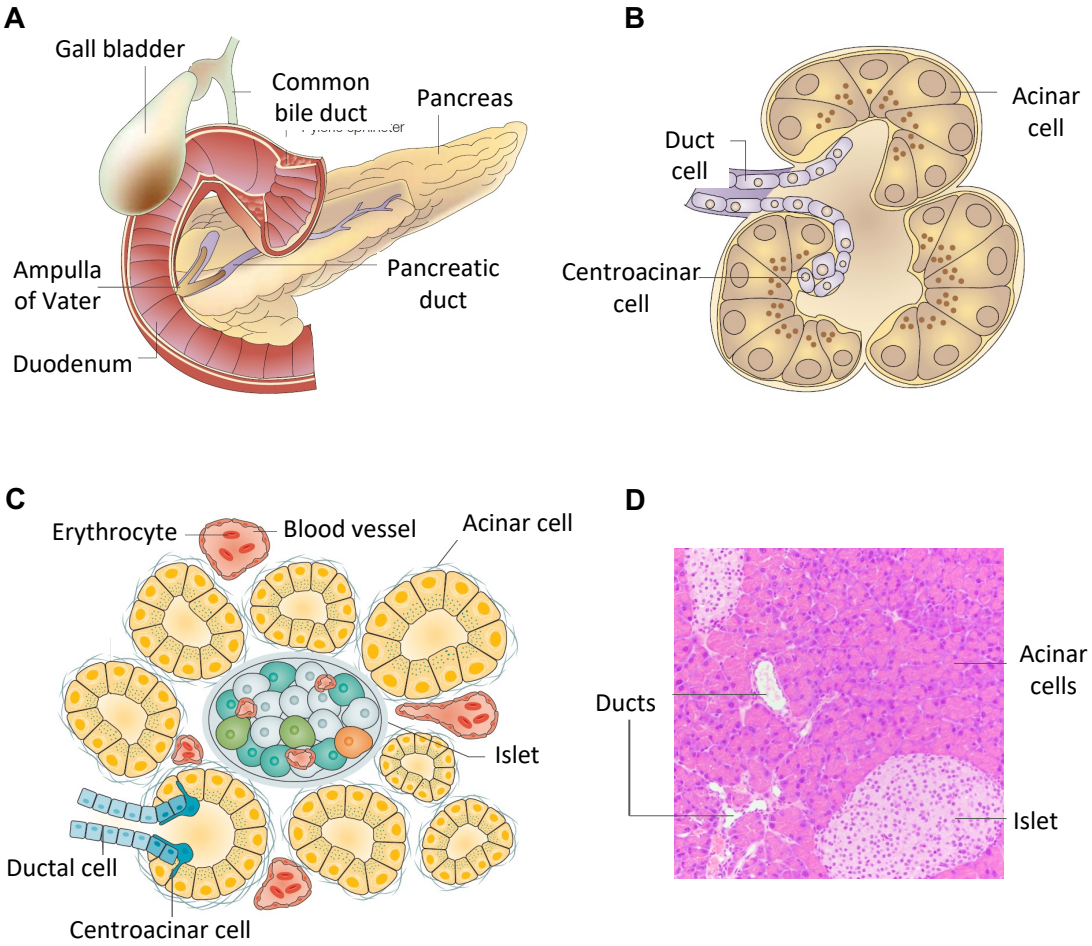


**Figure I1: Anatomy and histology of the pancreas. (A)** Macroscopic representation of the pancreas. **(B)** Schematic representation of terminal duct connected to acini. **(C)** Schematic representation of blood vessels and islets embedded in the exocrine compartment. **(D)** H&E staining of a pancreas section showing endocrine and exocrine (ducts and acini) compartments. *Schemes adapted from Bardeesy and DePinho (2002) and Ramzy and Kieffer (2017).*

## 1.3. Acinar cell function

Pancreatic acinar cells produce most of the digestive enzymes required for intestinal digestion. This includes proteases (e.g. trypsin, chymotrypsin, carboxypeptidase, elastase), lipases, glycosidases (e.g. amylase) and nucleases (e.g. DNase, RNAse) (Whitcomb and Lowe, 2007). To meet the enormous demand for these enzymes, acinar cells have the highest rate of protein synthesis of all mammalian cell types, which is accomplished through an intense transcription, an abundant number of ribosomes, a large rough ER and a highly functional storage and secretion system (Case, 1978).

Upon translation, immature proteins are delivered into the lumen of the rough ER, where folding and post-translational modifications occur. Digestive enzymes are then transported to the Golgi apparatus, where they are concentrated and packaged into

zymogen granules (Logsdon and Ji, 2013). Most digestive enzymes are produced as catalytically inactive precursor proteins and stored as zymogen granules in the apical part of the cell, ready for release into the acini lumen upon chemical stimulation. The most common stimuli are the hormone cholecystokinin (CCK) and the neurotransmitter acetylcholine, which are produced by intestinal endocrine cells in response to fat consumption or released by parasympathetic neurons in response to meal anticipation, respectively. In response to these molecules, the ER releases $Ca^{2+}$ ions into the cytoplasm, causing an increase in intracellular $Ca^{2+}$ levels that triggers zymogen granule fusion and exocytosis (Williams, 2010). Under normal physiological conditions, precursor enzymes remain inactive until they enter the duodenum, where trypsinogen - the inactive precursor of trypsin – is activated by enteropeptidases located in the enterocyte brush border, leading to the subsequent cleavage of other proenzymes (Whitcomb and Lowe, 2007).

# 2. Mouse pancreas development

## 2.1. Morphogenesis

Mouse pancreatic organogenesis, differentiation and maturation is divided in three developmental periods: a primary transition from embryonic day (E) 8.5 to E12.5, a secondary transition from E12.5 to E16.5 and a tertiary transition from E16.5 to postnatal life (Fig. I2) (Dassaye, Naidoo and Cerf, 2016).

Pancreatic organogenesis is initiated in the primary transition, with the evagination of the foregut endoderm into ventral and dorsal buds that eventually fuse. During this process, multipotent progenitor cells (MPCs) proliferate creating a pseudostratified epithelium with multiple microlumens that eventually fuse into tubular structures. Concomitantly, signalling from the underlying mesoderm promotes compartmentalization of the pancreatic epithelium into tip and trunk domains. Cells located at the tip are thought to include MPCs, which have the ability to give rise to the three pancreatic lineages, whereas ductal-endocrine bipotent progenitors constitute the trunk (Benitez, Goodyer and Kim, 2012; Dassaye, Naidoo and Cerf, 2016).

The secondary transition involves expansion, branching, differentiation and acinar cell lineage allocation. Around E13.5, the remaining multipotent progenitors present at the tip domain proliferate or differentiate into acinar progenitors (Zhou *et al.*, 2007). Differentiated endocrine cells delaminate from the trunk and assemble into cell clusters that will give rise to mature islets (Benitez, Goodyer and Kim, 2012; Dassaye, Naidoo and Cerf, 2016).

During the tertiary transition, differentiated pancreatic cells experience additional remodelling and maturation. Acinar and beta cell proliferation and differentiation continue after birth, but gradually decrease until weaning. Thereafter, acinar and beta cell mass is maintained through self-replication (Teta *et al.*, 2007; Houbracken and Bouwens, 2017).

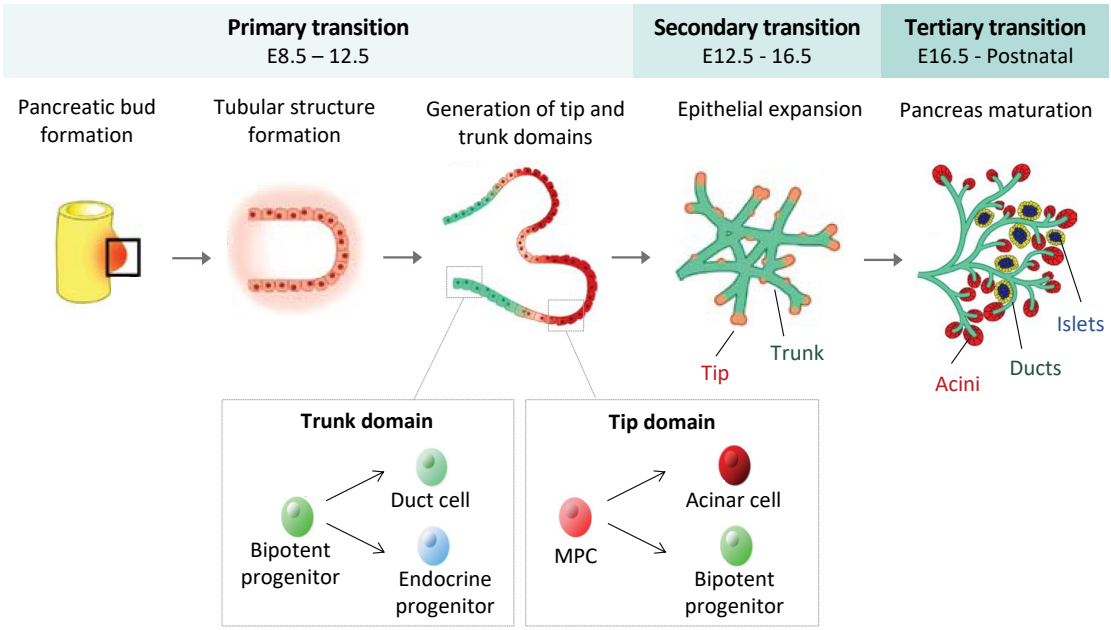


**Figure I2: Mouse pancreas development.** During the primary transition the gut endoderm evaginates into a dorsal and a ventral bud that eventually fuse into tubular structures with "tip" and "trunk" domains with different potency capabilities. The secondary transition involves epithelial expansion and the differentiation of remaining MPCs into acinar cells. The tertiary transition is a period of pancreas remodelling and maturation. *Adapted from Pan and Wright (2021).*

## 2.2. Transcriptional regulation of pancreas development

Pancreatic development is a dynamic process coordinated by extrinsic signals produced by non-pancreatic tissues – such as mesenchyme and blood vessels – and intrinsic transcriptional regulation (Puri and Hebrok, 2010; Magenheim *et al.*, 2011). The most

relevant transcription factors (TFs) involved in pancreas morphogenesis are PDX1 and PTF1A. Apart from their crucial role in early pancreatic development, these TFs also participate in other functions in later developmental stages. Hence, their promoters are commonly used as drivers for pancreatic-specific expression of selected genes.

**PDX1** is a homeodomain transcription factor that is expressed at early stages of mouse pancreatic development, in the pre-pancreatic endodermal epithelium (E8.5). Germline *Pdx1* ablation arrests pancreas development shortly after the emergence of pancreatic buds (Ohlsson, Karlsson and Edlund, 1993; Jonsson *et al.*, 1994; Fujitani *et al.*, 2006). At later gestational stages, *Pdx1* expression is required for acinar cell specification (Hale *et al.*, 2005). In the adult, *Pdx1* expression is mostly restricted to the duodenal epithelium and pancreatic β cells, where it maintains β cell identity by inducing insulin transcription (Ahlgren *et al.*, 1998; Gannon *et al.*, 2008) and suppressing alpha cell identity (Gao *et al.*, 2014). In fact, exogenous expression of *Pdx1* in adult mouse pancreas induces reprogramming of acinar cells into endocrine progenitors (Miyazaki, Tashiro and Miyazaki, 2016).

**PTF1A** (or P48) is a basic helix-loop-helix (bHLH) transcription factor involved in cell fate development in multiple organs, including pancreas, brain, retina and spinal cord (Jin and Xiang, 2019). *Ptf1a* is expressed in early murine pancreas development at E9.5 shortly after *Pdx1* expression, where it determines whether multipotent progenitor cells acquire a pancreatic commitment or revert to an intestinal fate (Kawaguchi *et al.*, 2002). At later developmental stages, *Ptf1a* is expressed in the tips of the pancreatic epithelium and subsequently in derived acinar cells (Krapp *et al.*, 1998; Zhou *et al.*, 2007). PTF1A is preferably found as part of the PTF1 complex, which is the major regulator of acinar cell differentiation (Masui *et al.*, 2007).

## 2.3. Transcriptional control of acinar differentiation

Acinar cell specification starts during the primary transition, with the enhancement of *Ptf1a* expression in multipotent progenitors present at the tips of the branching epithelium. Simultaneously, *Ptf1a* inactivation in the trunk domain directs cells into suppressing the acinar fate (Schaffer *et al.*, 2010). At this stage, PTF1A partners with TFC12 and RBPJ to form a trimeric complex (PTF1-J) that activates the expression of a pancreas

restricted RBPJ paralogue, RBPJL. The role of PTF1-J in pancreatic organogenesis is so crucial, that disruption of protein interaction eliminates transcriptional activity and truncates pancreatic development (Beres *et al.*, 2006; Masui *et al.*, 2007).

As multipotent cells acquire an acinar commitment, RBPJ becomes gradually replaced by its paralogue RBPJL in the PTF1 complex (Masui *et al.*, 2007). The subsequently derived PTF1-L complex induces the expression of auto regulatory loops that maintain the stable commitment and differentiation of acinar cells (Masui *et al.*, 2008). PTF1 -L interacts with the same consensus motifs as PTF1-J (Minoguchi *et al.*, 1997), although it has a stronger transcriptional activity. The role of PTF1-L in acinar differentiation was explored in *Rbpjl* mutant mice, which display a smaller pancreas and incompletely differentiated acinar cells. Chromatin immunoprecipitation (ChIP) experiments indicate that RBPJ replaces RBPJL at the majority of PTF1 binding sites in *Rbpjl* null adult pancreas. However, transcriptomic sequencing analysis revealed a unique role of the RBPJL version of PTF1 (PTF1-L) in the completion of acinar cell differentiation (Beres *et al.*, 2006). The PTF1-L complex drives the final stages of acinar cell differentiation by stimulating mitochondrial metabolism and creatine phosphate energy stores, inducing the expression of acinar secretory genes, improving intracellular transport, packaging and secretion and supressing hepatic genes (MacDonald, Swift and Real, 2010; Masui *et al.*, 2010).

## 2.4. Maintenance of acinar differentiation in adult pancreas

In addition to the PTF1 complex, other transcription factors contribute to pancreatic organogenesis, acinar differentiation and maintenance of acinar identity, including NR5A2, GATA6, HNF1A and MIST1.

**NR5A2**, also known as liver receptor homolog 1 (LRH-1) and very rarely referred to as hB1B in the literature, is a nuclear receptor that plays a crucial role in pancreatic organogenesis and acinar cell maturation. *Nr5a2* inactivation in the early pancreatic epithelium halts pancreatic development (Hale *et al.*, 2014), while *Nr5a2* inactivation at later developmental stages destabilises the acinar phenotype (Hale *et al.*, 2014). In addition, NR5A2 directly regulates the expression of the acinar program in adult acinar cells (Cobo *et al.*, 2018). The role of *Nr5a2* in pancreas development and maintenance of acinar identity is further detailed in a subsequent chapter.

**GATA6** is a zinc finger transcription factor involved in pancreatic organogenesis (Decker *et al.*, 2006; Carrasco *et al.*, 2012; Xuan *et al.*, 2012). GATA6 is required to complete acinar cell differentiation and to maintain acinar identity in adult pancreas. It directly binds to the promoters of acinar genes, such as *Rbpjl* and the digestive enzyme *Pnlip*. Pancreas-specific inactivation of *Gata6* does not impact pancreatic development, but results in a massive replacement of acinar cells by fat in ageing mice (Martinelli, Cañamero, Del Pozo, *et al.*, 2013).

**HNF1A** is a homeobox transcription factor whose deletion does not produce profound defects in pancreatic development, but down-regulates the acinar transcriptional program in the pancreas (Molero *et al.*, 2012; Kalisz *et al.*, 2020). In addition, *Hnf1a*-deficient acinar cells display an increased expression of proliferation markers. These defects are thought to result from a downstream effect on *Nr5a2* expression, rather than from a direct regulation of acinar genes (Molero *et al.*, 2012; Kalisz *et al.*, 2020).

**MIST1** (or BHLHA15) is bHLH transcription factor whose expression in the pancreas is restricted to acinar cells (Lemercier *et al.*, 1997). It regulates acinar cell polarity, accumulation of zymogen granules within the apical part and gap junction-mediated intercellular communication. Consequently, *Mist* ablation destabilizes acinar organization and function (Pin *et al.*, 2001; Rukstalis *et al.*, 2003; Johnson *et al.*, 2004).

# 3. Pathology of the exocrine pancreas

The most common diseases of the exocrine pancreas are pancreatitis and pancreatic ductal adenocarcinoma (PDAC). Both disorders are highly associated with acinar cell biology: pancreatitis results from premature digestive enzyme activation within acinar cells and acinar cell plasticity contributes to PDAC development.

## 3.1. Acute and chronic pancreatitis

Pancreatitis is an inflammatory disorder of the pancreas that can manifest as an acute or chronic condition. The major histological features of acute pancreatitis (AP) are acinar cell necrosis, edema and the presence of inflammatory infiltrates. Although this condition is generally mild and self-resolving, 10-15% of cases progress to severe AP, which is associated with pancreatic necrosis, multiorgan failure and increased mortality (Zerem,

2014). Chronic pancreatitis (CP) is characterised by a progressive and irreversible substitution of the normal pancreatic parenchyma with fibrosis, resulting in a permanent loss of exocrine and endocrine function (Vonlaufen, Wilson and Apte, 2008). Although acute and chronic pancreatitis were initially considered two independent entities, they are now understood as a disease continuum: one third of the patients with recurrent episodes of AP develop CP (Sankaran *et al.*, 2015).

### 3.1.1. Factors involved in pancreatitis

Multiple genetic and environmental factors contribute to the development of acute and chronic pancreatitis. The most common environmental factors include alcohol abuse, tobacco smoking and physical obstruction of the pancreatic duct, which is frequently observed in patients with gallstone disease. Other causes include hyperlipidaemia, hypercalcemia, autoimmunity, drugs and infections. In addition, genetic factors also play a role, either through a direct effect on acinar cells or an indirect effect on the regulation of environmental factors (Lee and Papachristou, 2019; Weiss, Laemmerhirt and Lerch, 2019). For instance, serum lipid concentrations are highly dependent on genetic factors (Gan, 2006).

Based on the etiology of the disease, pancreatitis has traditionally been classified as alcoholic, hereditary, obstructive, hyperlipidemic and idiopathic (with no identifiable cause). However, increasing evidence supports the notion that more than a single cause converges in most patients. This has led to the reconsideration of traditional classification systems and to understand pancreatitis as a multifactorial condition, in which numerous risk modifiers – rather than etiologies - contribute to pancreatic disease (Forsmark and Pham, 2018). In support with this, even though most cases of pancreatitis are due to alcohol abuse, only a small percentage of alcoholics (2-3%) (Lankisch *et al.*, 2002) develop AP, suggesting that other factors are required for the development of the disease.

### 3.1.2. Molecular events that lead to pancreatitis

Most factors leading to pancreatitis converge in the activation proenzymes within the acinar cells leading to autodigestion of the pancreatic parenchyma and subsequent induction of tissue regeneration. These events often lead to a pathological elevation in serum levels of pancreatic enzymes, such as amylase and lipase, which is used as a

diagnostic criterion for acute and chronic pancreatitis. The most common cellular mechanisms of pancreatitis are the elevation of $Ca^{2+}$ signalling and premature trypsinogen activation (reviewed by Lee and Papachristou, 2019; Zheng *et al.*, 2021).

### *Calcium signalling*

Under physiological conditions, $Ca^{2+}$ release form the ER is required to induce zymogen exocytosis and stimulate mitochondrial energy production. Alcohol abuse and physical obstruction of the pancreatic duct – causing bile acid reflux into the pancreas – can disrupt pancreatic homeostasis and cause a pathological increase in intracellular levels of $Ca^{2+}$. This overload of $Ca^{2+}$ ions increases mitochondrial permeability by opening transition pores that eventually cause changes in membrane potential disrupting mitochondrial function. This results in a subsequent inactivation of ATP-dependent mechanisms such as calcium clearance, autophagy and UPR response. This sustained stress results in intracellular activation of pancreatic enzymes (Lee and Papachristou, 2019; Zheng *et al.*, 2021).

### *Premature trypsinogen activation*

Multiple pancreatic insults – such as pancreatic ductal obstruction, alcohol and other toxins – can cause partial lysosome fusion with zymogen granules. This event can occur as a result of other toxin-associated cellular events, such as decreased exocytosis of zymogen granules, cytoskeletal dysfunction or increased lysosome production. Subsequently, the lysosomal enzyme cathepsin B (CTSB) activates trypsinogen into trypsin, leading to the activation of other pro-enzymes within the acinar cell (Lee and Papachristou, 2019; Zheng *et al.*, 2021).

## 3.1.3. Experimental models of AP

Due to the difficulties of obtaining human pancreatic tissue during AP, most of our understanding of the early cellular events of the disease have been investigated in animal models. Multiple models have been developed in the past three decades, including those induced by secretagogues (i.e. substances that induce acinar secretion, such as cerulein), L-arginine, deoxycholate, alcohol, genetic modifications, as well as others that involve

surgical procedures that obstruct the main pancreatic duct, such as closed duodenal loop or pancreatic duct ligation (reviewed by Su, Cuthbertson and Christophi, 2006).

*The cerulein-induced model*

Pancreatitis induced by cerulein is the most popular experimental model of AP in rodents, due to its low invasiveness and reproducibility. In this model, digestive enzyme secretion is induced by administering supraphysiological doses of cerulein – a CCK analogue – at repeated intervals. At supramaximal doses, cerulein inhibits enzyme release leading to a premature activation of digestive enzymes within the pancreas (Saluja *et al.*, 1989). The most common protocol of cerulein administration - consisting of seven hourly intraperitoneal (i.p.) doses at 50 µg/kg - leads to a pathological increase in serum amylase levels and histologic alterations such as edema, inflammation and the presence of ductal-like structures whose origin and relevance in pancreatic regeneration will be discussed in a subsequent section (Flandez *et al.*, 2014). Owing to the mild and transient nature of these alterations, which generally resolve within 2-5 days, this procedure constitutes the classical model of mild AP. In addition, variations of this protocol have been used for different purposes: multiple episodes may be combined to model severe AP (Flandez *et al.*, 2014) while a single dose of cerulein (50 µg/kg) may be useful to investigate early transcriptional responses (Cobo *et al.*, 2018).

### 3.1.4. Molecular events during cerulein-induced mild AP

Multiple studies have reported the molecular and cellular events associated to cerulein administration. This section will focus on those that follow cerulein-induced mild AP, since this is the protocol that has been used for most experiments included in this thesis.

Early events involve intracellular proenzyme activation and acinar atrophy. This is thought to occur through the colocalization of zymogen granules and lysosomes shortly after cerulein administration, leading to premature trypsinogen activation (Halangk *et al.*, 2000). Cerulein has been reported to prevent enzyme secretion (O'Konski and Pandol, 1993), suggesting that colocalization could result from the accumulation of zymogen granules within acinar cells. In fact, other secretagogues that are unable to block secretion do not induce pancreatitis (O'Konski and Pandol, 1993; Grady *et al.*, 1996). Acinar damage resulting from intracellular proenzyme activation, results in a leak of

digestive enzymes into the circulation, leading to an increase in serum amylase levels that can be detected as early as 1 hour (h) after the first cerulein injection. Repeated cerulein doses further increase amylase levels, which peak at 8 h after the first cerulein injection (Halangk *et al.*, 2000).

In parallel to these events, acinar cells release inflammatory cytokines that recruit inflammatory cells to the pancreas during early stages of pancreatitis, subsequently promoting inflammation and disease (Gukovskaya *et al.*, 1997; Han and Logsdon, 1999). Modest immune infiltration was detected as early as 1 h after the cerulein infusion at supramaximal doses in mice (Mayerle *et al.*, 2005), and reach its maximum approximately 24 h after the induction of a mild AP (Flandez *et al.*, 2014).

In this model, acinar damage is associated with a transient down-regulation of the acinar program that gradually restores with histological recovery. This involves a reduction in the transcripts that encode digestive enzymes and acinar transcription factors – such as RBPJ-L, PDX1 and PTF1A, whose expression is lowest 7-24 h after the first cerulein injection (Jensen *et al.*, 2005; Molero *et al.*, 2007, 2012; Fendrich *et al.*, 2008; Flandez *et al.*, 2014).

### 3.1.5. Acinar dedifferentiation in post-pancreatitis regeneration

Increasing evidence suggest that acinar cells activate regenerative mechanisms in response to pancreatic damage. Although the classical model for acinar regeneration postulates that new acinar cells mainly derive from proliferation of residual differentiated acinar cells (Desai *et al.*, 2007; Strobel *et al.*, 2007; Blaine *et al.*, 2010), increasing evidence suggests a role for acinar dedifferentiation in this process.

Adult acinar cells present a wide plasticity in comparison to other pancreatic cell types (reviewed by Storz, 2017). In response to mild AP, acinar cells transiently lose polarity and acquire a cuboidal morphology of ductal appearance. This process is termed acinar-to-ductal metaplasia (ADM) since it involves down-regulation of the acinar transcriptional program and the acquisition of ductal and pancreatic progenitor markers (Houbracken *et al.*, 2011; Liou *et al.*, 2013). Multiple studies have proposed that these lesions contribute to pancreatic regeneration through the activation of developmental programs, such as

the NOTCH (Siveke *et al.*, 2008), HEDGEHOG (Fendrich *et al.*, 2008) and WNT (Morris *et al.*, 2010) signalling pathways.

Loss of acinar differentiation (dedifferentiation) and reactivation of developmental signalling pathways may offer a mechanism by which the acinar cells can undergo regeneration and repair. In addition, acinar dedifferentiation may provide cells with the opportunity to arrest protein synthesis and repair damage (Stanger and Hebrok, 2013). However, dedifferentiation renders cells vulnerable to inflammation and pancreatic oncogenesis (Morris, Wang and Hebrok, 2010). This will be further discussed in subsequent sections.

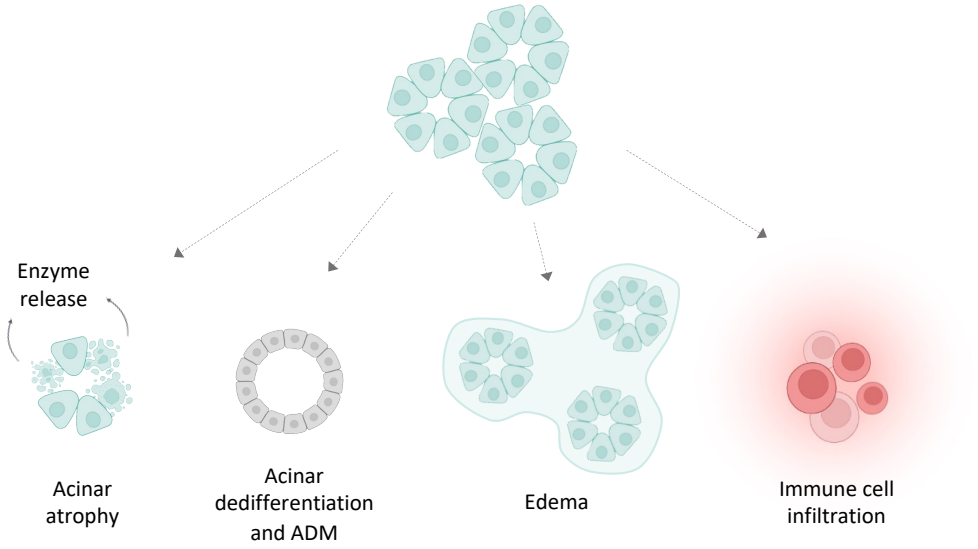


**Figure I3: Schematic representation of the effects of cerulein-induced pancreatitis.** In response to cerulein-induced damage, injured acinar cells release digestive enzymes into the circulation, down-regulate the acinar transcriptional program giving rise to ADM, accumulate interstitial fluid (edema) and release cytokines that recruit immune cells to the pancreas.

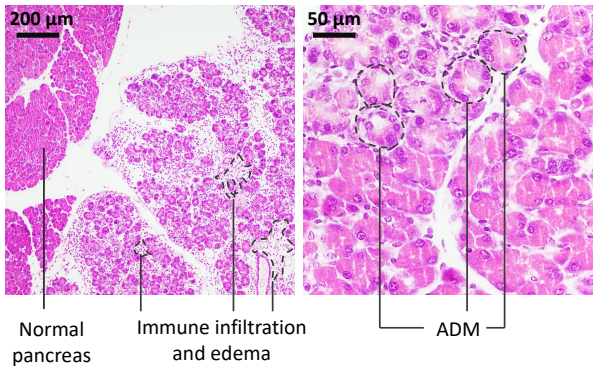


**Figure I4: Common histological alterations in the pancreas in response to cerulein-induced pancreatitis.** In response to cerulein-induced pancreatitis the pancreas displays histological alterations such as edema, inflammatory cell infiltration, and acinar-to-ductal metaplasia (ADM). Edema is identified as interstitial space in the exocrine parenchyma; inflammatory cell infiltration by the density of nuclei that populate the interstitial space; ADM can be recognised as the presence of lumens within the acini and loss of eosinophilia.

## 3.2. Pancreatic ductal adenocarcinoma (PDAC)

### 3.2.1. Epidemiology and risk factors

Pancreatic ductal adenocarcinoma (PDAC) is the most common type of pancreatic cancer and one of the most lethal human diseases. It has a five year survival rate lower than 10%, mainly due to its resistance to conventional therapies and the lack of early symptoms (Rawla, Sunkara and Gaduputi, 2019). Due to increasing incidence, pancreatic cancer is expected to constitute the second cause of cancer-related death by 2030 (Rahib *et al.*, 2014). The best strategy to prevent pancreatic cancer is to act on modifiable risk factors, such as smoking, alcohol consumption, dietary factors, occupational exposure to carcinogens, obesity, type 2 diabetes and CP. Non-modifiable risk factors include advanced age, gender, ethnicity, type I diabetes, genetic factors and family history, which is present in around 10% of the patients (reviewed by Rawla, Sunkara and Gaduputi, 2019).

#### *Pancreatitis as a major risk factor for PDAC development*

The association with CP is particularly relevant from a clinical perspective, as this condition has been reported in a recent meta-analysis to increase the risk of developing PDAC by 22-fold excluding patients diagnosed with pancreatic cancer within two years of CP diagnosis. An even stronger association (66-fold) was reported for patients with hereditary pancreatitis (Gandhi *et al.*, 2022). Likewise, cerulein induced pancreatitis has been commonly used as a tool to accelerate carcinogenesis in mouse models of pancreatic neoplasia (Guerra *et al.*, 2007, 2011; Carrière *et al.*, 2011; Flandez *et al.*, 2014).

### 3.2.2. PDAC initiation and progression

PDAC originates from precursor lesions derived from initiating events in normal pancreatic cells. Pancreatic intraepithelial neoplasias (PanINs) are non-invasive epithelial neoplasms and constitute the most common type of precursor lesions (Basturk *et al.*, 2015). They are graded based on the level of dysplasia as PanIN-1, -2 and -3, and are associated with activating point mutations in the *Kras* oncogene and progressive loss of tumor suppressors (reviewed by Hruban *et al.*, 2000; Maitra and Hruban, 2008).

### *Genetic landscape of PDAC*

Activating point mutations in the *KRAS* oncogene are considered the first genetic event in pancreatic carcinogenesis, as they are detected in more than 90% of PanIN lesions (Kanda *et al.*, 2012) and PDAC (Waddell *et al.*, 2015; Bailey *et al.*, 2016; The Cancer Genome Atlas Research Network and Raphael, 2017). KRAS activating mutations suppress the protein's ability to hydrolyse guanidine triphosphate (GTP), resulting in constitutive activation of the mitogen activated protein kinase (MAPK) and the phosphoinositide-3-kinase (PI3K) pathways independent of growth factor signalling (Malumbres and Barbacid, 2003). The identification of *KRAS* mutations as the earliest event of pancreatic carcinogenesis and the advent of the Cre-lox technology led to the development of tissue-specific mouse models of *Kras* oncogenic activation. Over the last two decades, these models have become standard tools for the study of PDAC initiation, cellular origin and progression (Guerra *et al.*, 2003; Hingorani *et al.*, 2003).

The most common inactivated tumor suppressors are *CDKN2A*, *TP53* and *SMAD4*. Genetic inactivation of *CDKN2A* has been reported in more than 90% of pancreatic cancers, either through homozygous deletion, genetic mutations combined with heterozygosity or promoter silencing (Schutte *et al.*, 1997). This gene codes for a cyclin-dependent kinase (CDK) inhibitor that decelerates cell cycle progression by inhibiting RB phosphorylation (Kim and Sharpless, 2006). *TP53* was found to be inactivated in 50-75% of pancreatic tumors mostly through genetic mutation and loss of the second allele (Dong *et al.*, 2011). Recently, *TP53* function was reported to be loss in 72-74% of PDAC cases (Waddell *et al.*, 2015; The Cancer Genome Atlas Research Network and Raphael, 2017). P53 regulates cell cycle progression, apoptosis and genomic stability and its genetic inactivation allows cells to divide even in the presence of damaged DNA, leading to rapid accumulation of genetic alterations (Redston *et al.*, 1994). *SMAD4* is lost in approximately 55 % of pancreatic cancers, either through mutation and loss of the second allele or homozygous deletion (Hahn *et al.*, 1996; Lüttges *et al.*, 2001). SMAD4 is a transcriptional mediator of the transforming growth factor-β (TGF-β) signalling pathway, which critically restrains growth in mammalian tissues. SMAD4 loss abrogates TGF-β signalling thereby promoting proliferation and cancer progression (Miyaki and Kuroki, 2003).

In addition to these alterations, genomic characterization of pancreatic cancer revealed a complex mutational landscape, where inactivation of the above mentioned genes coexist with low frequency mutations in other loci (Waddell *et al.*, 2015; Bailey *et al.*, 2016; The Cancer Genome Atlas Research Network and Raphael, 2017). Despite this heterogeneity, genomic alterations converge in common molecular pathways, such as DNA damage repair, TGF-β signalling, cell cycle, epigenetic regulation and axon guidance (Jones *et al.*, 2008; Biankin *et al.*, 2012; Waddell *et al.*, 2015).

*The classical model of PDAC development*

The observation that the genomic alterations associated with pancreatic cancer are already present in PanIN lesions led to the development of the classical model of PDAC development, which proposes that invasive PDAC originates from PanIN lesions though sequential acquisition of genetic mutations (Hruban *et al.*, 2000). Based on this model, *KRAS* mutations initiate pancreatic transformation and promote the loss of tumor suppressors, thereby inducing progression to invasive PDAC. *CDKN2A* inactivation is associated with the progression from PanIN-1 to PanIN-2 lesions (Moskaluk, Hruban and Kern, 1997; Schutte *et al.*, 1997), and the inactivation of *TP53* and *SMAD4* with the transition to PanIN-3 and invasive PDAC (Wilentz *et al.*, 2000; Lüttges *et al.*, 2001). Despite its popularity, multiple studies have questioned the accuracy of the linear progression model and proposed alternative models for PDAC development, although these will not be discussed in this thesis (Real, 2003; Real, Cibrián-Uhalte and Martinelli, 2008; Notta *et al.*, 2016; Notta, Hahn and Real, 2017).

### 3.2.3. Acinar dedifferentiation as the initiating event of pancreatic neoplasia

Despite the ductal characteristics of PanINs, increasing evidence demonstrates that these lesions originate from acinar cells (reviewed by Grimont, Leach and Chandwani, 2022). Initial studies found that targeting an oncogenic $Kras^{G12D}$ allele to pancreatic progenitor cells – using the *Pdx1-Cre* transgene, in which the Cre recombinase is driven by the *Pdx1* promoter - recapitulated PanIN progression in mice (Hingorani *et al.*, 2003). However, oncogenic *Kras* activation in ductal cells – achieved by fusing the cytokeratin 19 promoter to a mutant *Kras* allele – failed to initiate pancreatic transformation, only leading to periductal immune infiltration (Brembeck *et al.*, 2003). Later on, expression of the mutant

*Kras*$^{G12V}$ allele in acinar and centroacinar cells during development – using the *Elastase* promoter coupled to a tetracycline regulated system – was found to generate PanIN lesions that progressed to invasive PDAC. However, conditional *Kras*$^{G12V}$ expression in adult acinar and centroacinar cells failed to induce pancreatic neoplasia unless combined with CP (Guerra *et al.*, 2007). These studies evidenced the role of acinar cells as a potential source of PanINs and provided rationale for the already established association between CP and PDAC risk in humans (Gandhi *et al.*, 2022).

These results, together with the observation that AP leads to a transient down-regulation of the acinar program and the appearance of ADM structures (Molero *et al.*, 2007, 2012; Flandez *et al.*, 2014) led our group to hypothesise that pancreatitis contributed to pancreatic neoplasia by inducing acinar dedifferentiation. In addition, multiple studies reported the existence of genetic variants that predispose for pancreatic cancer development located in the vicinity of acinar genes (Petersen *et al.*, 2010; Zhang *et al.*, 2016; Chen *et al.*, 2018; López de Maturana *et al.*, 2021). In the last two decades, through the use of mouse models with genetic inactivation of transcription factors involved in the maintenance of acinar differentiation – such as *Gata6, Hnf1a* and *Nr5a2* –, we and others have provided increasing evidence supporting this notion. For instance, pancreas-specific homozygous inactivation of *Gata6* (Martinelli, Cañamero, del Pozo, *et al.*, 2013; Martinelli *et al.*, 2016), constitutive *Nr5a2* heterozygosity (Flandez *et al.*, 2014; Cobo *et al.*, 2018), *Hnf1a* deletion (Molero *et al.*, 2012; Kalisz *et al.*, 2020) and *Mist1* inactivation (Pin *et al.*, 2001; Shi *et al.*, 2009) were found to cooperate with inflammation and *Kras* driven tumorigenesis by compromising the acinar cell transcriptional program. These studies indicate a potential tumor suppressive role for acinar cell differentiation.

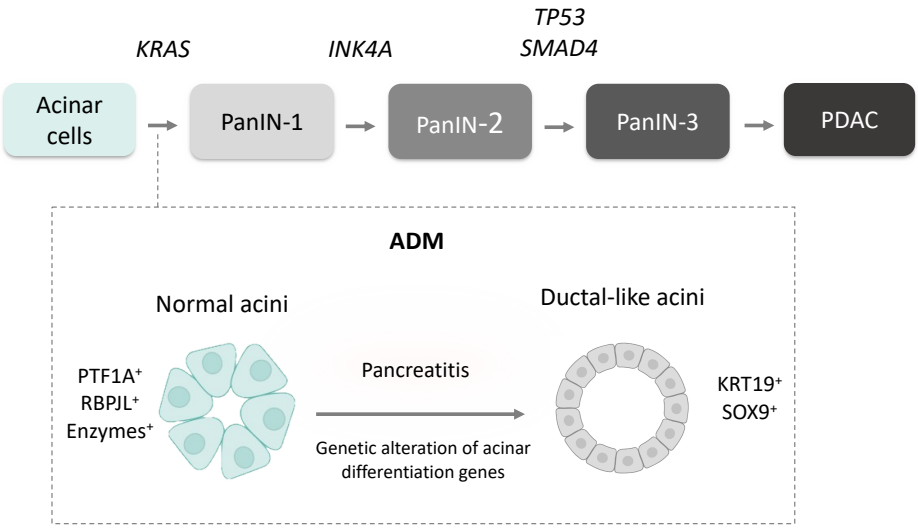


**Figure I5: Pancreatic ductal adenocarcinoma (PDAC) initiation and progression.** Most cases of invasive PDAC originate from intraepithelial neoplastic lesions (PanINs) that accumulate mutations as the disease progresses. Mutational activation of the *KRAS* oncogene is considered the earliest event in pancreatic oncogenesis. Acinar cells constitute the major source of origin of PanIN lesions. Genetic alterations in acinar differentiation genes and pancreatitis promote mutant *Kras* driven tumorigenesis in adult murine pancreas. This is thought to occur through the generation of acino-to-ductal metaplasia (ADM), a process that involves loss of acinar identity and acquisition of ductal- and progenitor-like markers.

# 4. Pathophysiology of obesity

Obesity is a health condition that involves excessive fat accumulation. It is generally defined using the body mass index (BMI: kg/m2), where a BMI above 25 is considered overweight and above 30 is considered obese (WHO, 2020), although lower cut-off values have been identified for Asian populations (Nishida *et al.*, 2004).

The incidence of obesity has increased dramatically in the past decades. Based on estimates from The World Health Organization, 39% of the adult population was overweight in 2016, and 13% were obese (WHO, 2020). In the Unites States, the country with the highest incidence of obesity according to the OECD (Organisation for Economic Co-operation and development), more than two thirds of the adult population were obese in 2015 (OECD Obesity Update, 2017). Due to its association with multiple diseases, obesity has become a serious health issue worldwide.

## 4.1. Diseases associated to obesity

Obesity is associated with the incidence of several co-morbidities including hyperlipidaemia, hypertension, cardiovascular disease, type 2 diabetes, metabolic

syndrome, non-fatty acid liver disease (NFALD), and cancer (Patterson *et al.*, 2004; Mata and Jasul, 2017).

### 4.1.1. Hyperlipidaemia

Hyperlipidaemia is a condition characterised by the accumulation of lipids and lipoproteins in the blood (Ezeh and Ezeudemba, 2021). Lipids include cholesterol, triglycerides, phospholipids, and cholesterol esters, while lipoproteins are macromolecules that result from the interaction of these lipids with proteins. Their structure enables lipids to be transported through the circulation to peripheral tissues (Feingold, 2021).

### 4.1.2. Type 2 diabetes

Type 2 diabetes involves dysregulation of glucose, lipid and protein metabolism and results from insulin resistance, impaired insulin secretion or a combination of both (DeFronzo *et al.*, 2015).

#### *Insulin resistance*

Insulin resistance is a condition in which cells are unable to respond to insulin. Under normal circumstances, β cells secrete insulin in response to an increase in blood glucose levels. This hormone then promotes glucose transport into insulin-dependent tissues, such as the liver, muscle and adipose tissue. This results in a normalization of blood glucose levels, and subsequent inhibition of insulin secretion. Under certain situations cells may become resistant to insulin, rendering them incapable of using blood glucose for energy consumption. In this context, insulin fails to restore baseline glucose levels, which further stimulates insulin secretion (Sinaiko and Caprio, 2012; Rahman *et al.*, 2021).

Insulin resistance is the primary metabolic defect associated to obesity. It is present in 89% of obese individuals, while its prevalence in non-obese individuals – lean or overweight - is 56% (Calori *et al.*, 2011). The association between obesity and insulin resistance is well stablished, and has been reported in adults (Bonadonna *et al.*, 1990), adolescents (Lim *et al.*, 2015) and children (Sinaiko *et al.*, 2001).

In many patients, insulin resistance precedes the development of type 2 diabetes for several years and even decades (Beck-Nielsen and Groop, 1994; Turner and Clapham,

1998). During this time, hyperinsulinemia can deteriorate other tissues that did not present insulin resistance, leading to the development of other conditions, such as hypertension or hypertriglyceridemia (McFarlane, Banerji and Sowers, 2001; Sarafidis and Lasaridis, 2006). Therefore, individuals with insulin resistance generally present other conditions prior to the development of overt type 2 diabetes.

Multiple indices have been validated to evaluate insulin resistance in an indirect manner, among which the homeostasis assessment insulin resistance model (HOMA-IR) is the most common. This method uses fasting glucose and insulin levels to calculate how much insulin the pancreas must produce to control blood glucose levels (Gutch *et al.*, 2015).

### *Diagnosis of type 2 diabetes*

Type 2 diabetes is diagnosed based on the following criteria: increased fasting plasma glucose levels, high values in the hemoglobin A1C test – which measures average glucose levels over the past months – and based on the result of oral glucose tolerance tests (GTT), which evaluates an individual's ability to metabolize glucose. This test involves measuring blood glucose levels at different time points after oral glucose administration in fasting conditions. Reduced or delayed glucose clearance is indicative of impaired glucose tolerance. In mice, GTT is a common method to evaluate glucose metabolism, with the sole difference that glucose is generally administered intraperitoneally rather than orally (Benedé-Ubieto *et al.*, 2020).

## 4.1.3. Metabolic syndrome

Metabolic syndrome is a group of multiple conditions that predispose for the development of type 2 diabetes and cardiovascular disease. It is diagnosed based on the presence of at least 3 of the following criteria: hypertriglyceridemia, hypercholesterolemia, hyperglycaemia, increased waist circumference and hypertension (Kanwar and Kowdley, 2016). Insulin resistance is considered an initiating event of this condition, as it promotes tissue deterioration through hyperinsulinemia (McFarlane, Banerji and Sowers, 2001; Sarafidis and Lasaridis, 2006).

#### 4.1.4. Non-alcoholic fatty liver disease (NAFLD)

Non-alcoholic fatty liver disease (NAFLD) is considered the hepatic component of the metabolic syndrome. It includes a wide spectrum of hepatic conditions in which hepatic steatosis – adipose tissue deposition in the liver - and inflammation progresses to non-alcoholic steatohepatitis (NASH), fibrosis, cirrhosis, and even hepatocellular carcinoma (Fassio *et al.*, 2004; Yatsuji *et al.*, 2009; Ahmed, Wong and Harrison, 2015). NASH has been proposed to develop through a multifactorial mechanism that involves insulin resistance, oxidative stress, mitochondrial dysfunction, genetic determinants, nutrition, ER stress, inflammation and changes in the gut microbiota (Tilg and Moschen, 2010).

### 4.2. Obesity and pancreatic disease

*Obesity and pancreatic cancer*

Obesity has been consistently reported to increase the incidence of pancreatic cancer (Xu *et al.*, 2018; Wiese *et al.*, 2021), as confirmed in multiple meta (Larsson, Orsini and Wolk, 2007; Aune *et al.*, 2012) and large pooled analysis (Arslan *et al.*, 2010; Genkinger *et al.*, 2011). Animal studies have supported this notion, since high fat diet (HFD) induced obesity increases the incidence of pancreatic neoplasia in mouse models of *Kras*-driven tumorigenesis (Dawson *et al.*, 2013; Philip *et al.*, 2013). However, the effect of obesity on pancreatic cancer outcome and mortality remains inconclusive (Wiese *et al.*, 2021).

Multiple mechanisms have been proposed to explain how obesity could contribute to pancreatic cancer initiation, including chronic inflammation, cytokines, insulin resistance, hyperlipidaemia and alterations in the gut microbiome (Xu *et al.*, 2018).

*Obesity and pancreatitis*

The association between obesity and pancreatitis has mainly been explored in an acute – rather than chronic - setting (Wiese *et al.*, 2021). Based on recent meta-analyses, obesity is associated with an increased AP incidence (Aune *et al.*, 2021), as well as severity and mortality (Chen, Xiong and Wu, 2012; Dobszai *et al.*, 2019). Animal studies have supported this association, since HFD-induced obesity increases the severity of pancreatitis in rodents (Rouse *et al.*, 2014; Hong *et al.*, 2020; Xu *et al.*, 2021). However, another meta-analysis indicated that, after correcting for confounding variables, obesity

is not independently associated to severity and mortality (Smeets *et al.*, 2019), suggesting a mechanism mediated through the development of other pathologies. Obesity has been proposed to contribute to pancreatitis through gallstone formation, hyperlipidaemia, type 2 diabetes and its treatments, therapeutic interventions (Khatua, El-Kurdi and Singh, 2017), the induction of an inflammatory status (Hong *et al.*, 2020), alterations in the gut microbiome (Ye *et al.*, 2019) or through the generation of liver steatosis (Hou *et al.*, 2019).

The associations between pancreatic cancer, pancreatitis and obesity are very relevant from the clinical standpoint, since they provide an opportunity to act on a modifiable risk factor to prevent pancreatic disease.

# 5. The role of the gut microbiome on host physiology

The human gut is inhabited by an extensive community of microorganisms, comprised of trillions of bacteria, fungi and viruses that coexist with the host for potential mutual benefit (Thursby and Juge, 2017). This ecosystem is referred to as the gut microbiota, or microbiome (when also accounting for their genomes and gene products). In the past two decades, it has emerged as a critical modulator of human health, since it contributes to multiple physiological processes including brain function (Rogers *et al.*, 2016), metabolism (Martin *et al.*, 2019) and immunity (Zheng, Liwinski and Elinav, 2020).

## 5.1. Mechanisms of action

The major mechanisms by which the gut microbiome affects host physiology are: i) the production of microbiome-derived metabolites that modulate tissue homeostasis in a direct manner or through the regulation of gut hormone release and ii) the interaction with pattern recognition receptors (PRRs) that activate cell signaling processes, and subsequently affect innate and adaptive immune responses.

### 5.1.1. Microbiome-derived metabolites modulate tissue homeostasis

The gut microbiome contributes to energy harvest by converting inaccessible nutrients such as plant carbohydrates into absorbable metabolites. The most common bacteria-derived metabolites are the short chain fatty acids (SCFAs) propionate, acetate and butyrate. These molecules exert important physiological functions in multiple tissues:

acetate is transported through the circulation to peripheral tissues where it contributes to cholesterol metabolism, propionate participates in gluconeogenesis in the liver, and butyrate serves as the major energy source for colonocytes (Martin *et al.*, 2019). Since the intestinal barrier is the first line of defense against commensal organisms and pathogens, butyrate is also involved in immune regulation (Arpaia *et al.*, 2013; Smith *et al.*, 2013; Haghikia *et al.*, 2015; Fung, Olson and Hsiao, 2017). Secondary bile acids (SBAs) constitute other common metabolites produced by the gut microbiome. Primary bile acids are produced by liver hepatocytes and then released to the gut lumen, where they assist lipid absorption. Once in the intestine, microbiome-derived hydrolases convert them into SBAs, which - as opposed to primary bile acids - diffuse through the intestinal epithelium. Thus, the gut microbiome regulates bile acid metabolism by promoting bile salt reuse (Martin *et al.*, 2019). The gut microbiome is also a source of various vitamins, such as B vitamins, which are involved in multiple biochemical processes including neurotransmitter metabolism (Rudzki *et al.*, 2021).

Apart from regulating tissue homeostasis in a direct manner, these metabolites modulate the secretory activity of enteroendocrine cells, subsequently affecting gut hormonal release. This includes multiple hormones with critical roles in glucose homeostasis, satiety, obesity and brain function such as glucagon peptide 1 (GLP-1), peptide tyrosine-tyrosine (PYY), serotonin and CCK (Martin *et al.*, 2019). GLP-1 is generally released by the colonic epithelium after a meal to induce insulin and inhibit glucagon secretion in the pancreas (Leech *et al.*, 2011). PYY acts in the hypothalamus regulating food satiety. Obese individuals display reduced circulating levels of this hormone as a result from attenuated colonic secretion (Batterham *et al.*, 2006). Enteroendocrine cells constitute the major source of serotonin, which apart from controlling mood and anxiety, promotes immune cell function and diet-induced obesity (Banskota, Ghia and Khan, 2019). These cells also regulate appetite, gastric motility and – as mentioned above – acinar secretion by releasing CCK (Martin *et al.*, 2019).

### 5.1.2. Cellular recognition of conserved microbial ligands regulates immunity

In addition to modulating host physiology in a metabolite-dependent manner, commensal and pathogenic microorganisms can also have a direct effect in cell signaling. Conserved ligands present on microbial surfaces – referred to as pathogen-associated

molecular patterns (PAMPs) - can interact with pattern recognition receptors (PRRs) to activate intracellular signaling pathways. PRRs are mainly expressed in innate immune cells – mostly antigen presenting macrophages and dendritic cells – and non-immune cells such as fibroblasts and epithelial cells. In immune cells, PAMP activation results in the production of inflammatory cytokines. This process does not only activate the innate immune system, but also modulates antigen-specific adaptive immune responses (Gordon, 2002; Li and Wu, 2021). This crosstalk between the immune system and the gut microbiome is essential to establish immune tolerance during development (Zheng, Liwinski and Elinav, 2020) and to prevent pathogen infections (Gordon, 2002; Li and Wu, 2021). On the other hand, the interaction between microbial patterns and PRRs in enteroendocrine cells modulates gut hormone secretion, thereby affecting tissue homeostasis in an immune-independent manner (Kidd *et al.*, 2009; Larraufie *et al.*, 2017; Lebrun *et al.*, 2017). Interestingly, these mechanisms can also be activated upon tissue damage, since PRRs also recognize damage-associated molecular patterns (DAMPs) produced by tumor, stressed or dying cells (Li and Wu, 2021).

Multiple classes of PRRs can be found in mammals, among which toll-like receptors (TLRs) are the best characterized. TLRs localize to the cell membrane or intracellular compartments such as the ER, endolysosomes or lysosomes. They interact with multiple microbial components including lipids, lipoproteins, proteins, peptidoglycans and nucleic acids. For example, bacterial lipopolysaccharide (LPS) – which constitutes a component of the cell wall in Gram negative bacteria – is a potent activator of TLR4, while TLR5 recognizes flagellin, the major component of bacterial flagella. TLR expression in immune cells – mostly dendritic cells and macrophages – results in the induction of the transcription factors NF-kB and IRFs, which orchestrate innate immune responses (Kawasaki and Kawai, 2014; Fitzgerald and Kagan, 2020). By contrast, activation of TLR in enteroendocrine cells modulates gut hormone secretions, including GLP-1 (Lebrun *et al.*, 2017), serotonin (Kidd *et al.*, 2009) and PYY (Larraufie *et al.*, 2017).

In addition to TLRs, PRRs also include cytosolic NOD-like receptors (NLRs), intracellular RIG-I-like receptors (RLRs), C-type lectin receptors (CLRs) and AIM2-like receptors (ALRs) (Li and Wu, 2021).

## 5.2. Influence of environmental gut microbiome perturbation in host disease

Due to its role in host homeostasis, the gut microbiome is emerging as a critical determinant of human health. An imbalance in the composition of this community – termed dysbiosis - is associated not only with gastrointestinal diseases such as inflammatory bowel disease or irritable bowel syndrome (Vich Vila *et al.*, 2018), but also with multiple conditions in other tissues, including diabetes (Qin *et al.*, 2012; Karlsson *et al.*, 2013), obesity (Turnbaugh *et al.*, 2009) and pancreatic diseases (Akshintala *et al.*, 2019). The richness and diversity of the gut microbiota is highly dependent on genetic and environmental factors, such as diet, medications, age and the immune system (Schepis *et al.*, 2021). For instance, plant-based diets rapidly increase the abundance of species enriched in carbohydrate hydrolases, while animal-based diets – which are rich in proteins and fat – increase bile acid content, thereby selecting for bile acid-resistant species (David *et al.*, 2014).

## 5.3. Methods for microbiome analysis

Traditionally, microbiology has relied on culture methods for the identification of bacteria involved in human disease. Samples are sent to a laboratory, where bacteria are enriched in liquid and agar mediums for subsequent biochemical characterization. This method has many limitations: a bias towards culturable bacteria, long incubation periods and the absence of quantitative results. Although this technique is the gold standard in clinical laboratories, it does not enable the identification of complex microbial communities (Gupta *et al.*, 2019). Recently, the advent of sequencing-based technologies has made it possible to profile entire communities, including unculturable bacteria. These alternatives provide relative taxonomic abundance and are becoming increasingly sensitive and cost effective. The most common techniques for microbiome analysis are gene amplicon sequencing and shotgun metagenomics (Bharti and Grimm, 2021).

Gene amplicon sequencing involves analyzing genetic variation in genes that are functionally conserved across microbial species. The most common amplicon used for bacterial identification is the 16S ribosomal DNA gene (16S rDNA), which encodes a prokaryotic ribosomal subunit required for cellular function and survival. This technique – referred to as 16S rDNA sequencing – uses highly conserved primer binding sites to

amplify variable regions of the gene that can discriminate taxonomic classification (Bharti and Grimm, 2021). Recently, 16S ribosomal RNA (16rRNA) sequencing – rather than rDNA - has also helped to identify metabolically active species in bacterial communities (Kang *et al.*, 2013; Wang *et al.*, 2017; Malayil *et al.*, 2020).

Shotgun metagenomics involves breaking the genome into small pieces that are sequenced individually. It provides a better taxonomic resolution than gene amplicon sequencing analysis, since it is based on the diversity of multiple genes. It also enables the identification of non-bacterial microorganisms and viruses (Bharti and Grimm, 2021). Despite these major advantages, 16S rDNA sequencing constitutes the most cost-effective alternative to explore changes in microbial populations across multiple samples.

### 5.4. The gut microbiome-pancreatic axis

Although traditionally considered a sterile organ, recent studies have pointed to the existence of microbiota within the pancreas (Pushalkar *et al.*, 2018; Sethi *et al.*, 2018; Thomas *et al.*, 2018). The anatomic connection between the main pancreatic duct and the duodenum constitutes a possible route of migration (Pushalkar *et al.*, 2018), although translocation may also occur via the mesenteric veins and lymph nodes (Diehl *et al.*, 2013). Increasing evidence supports the existence of a close connection between the gut microbiome and the pancreas, where one influences the other. Pancreatic secretions may modify the composition of the gut microbiome, while this has emerged as critical modulator of pancreatic disease (Akshintala *et al.*, 2019).

## 6. NR5A2/LRH1

### 6.1. NR5A2: a member of the nuclear receptor family

NR5A2 is a member of the nuclear receptor (NR) superfamily, which constitutes a large group of transcription factors that are involved in a variety of biological processes including development, metabolism and homeostasis. Most NRs are ligand-regulated transcription factors that are activated by steroid hormones, such as androgen, estrogen and progesterone, and other lipophilic molecules, such as retinoic acid, thyroid hormone or vitamin D. These ligands diffuse through the plasma membrane and activate their receptors inside the cell, rather than acting through cell membrane receptors as most

intercellular messengers. Once activated, the majority of NRs function as transcription factors, modulating gene expression through a direct interaction with the DNA (Sever and Glass, 2013). Recent advancements in crystallography have enabled the identification of lipid-soluble ligands for numerous NRs that were initially believed to be orphan. This has opened the door to novel therapeutic strategies for inflammation, metabolic disorders and cancer (Burris, Busby and Griffin, 2012; Roshan-Moniri *et al.*, 2014).

NRs have a conserved structure composed of an amino-terminal transactivation domain (A/B domain), a central DNA-binding domain containing two zinc fingers (C domain, or DBD), a variable hinge region (D domain) and a carboxy-terminal ligand-binding domain (the E domain, or LBD) that also contributes to protein dimerization (Fig. I6A) (Mangelsdorf *et al.*, 1995). These receptors form monomers, homodimers, or heterodimers that recognize repeated consensus sequences in the DNA, termed hormone response elements (HREs).

## 6.2. NR5A2 location in the genome, isoforms and structure

*NR5A2* is located on chromosome 1. The human gene encompasses eight exons, while nine are present in the mouse orthologue (Ensemble identifier: ENSG00000116833 and ENSMUSG00000026398). Four alternative splicing isoforms of 541, 495, 469 and 369 amino acids have been described for the human gene (UniProt identifier: O00482), among which the 495 amino acid one (UniProt identifier: O00482-1) has been reported as the most abundant (Li *et al.*, 1998; Nitta *et al.*, 1999). This isoform is identical to the largest one (UniProt identifier: O00482-2), except for a deletion in the transactivation domain that does not affect transcriptional activity (Nitta *et al.*, 1999). On the other hand, a single 560 amino acid isoform has been described for the mouse gene (UniProt identifier: P45448). Additional potential isoforms are annotated in UniProt, although their existence is based on computationally analysis (UniProt identifier: O00482 and P45448).

The most common isoforms in human and mouse share the same molecular structure, consistent with the modular architecture of NRs but with some peculiarities (Fig. I6B): the LBD contains a ligand binding pocket and a conserved activating function-2 (AF-2) region that mediates co-regulator recruitment and the DBD includes an Ftz-F1 domain that enables NR5A2 to interact with DNA as a monomer – contrary to most NRs - with

response elements containing the Ftz-F1 consensus motif YCAAGGYCR (Y = pyrimidine, R = purine) (Sun, Demagny and Schoonjans, 2021).

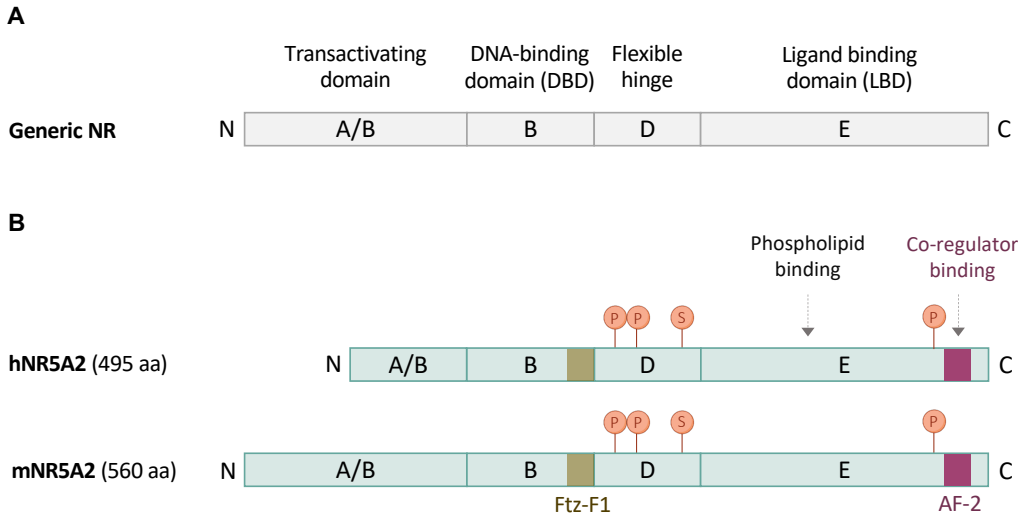


**Figure I6: Conserved structure of most nuclear receptors (NRs) and most abundant human and mouse NR5A2 isoforms.** (A) Most nuclear receptors have a modular structure that involves an N-terminal transactivation domain (A/B domain), a central DNA-binding domain (C domain, or DBD), a variable hinge region (D domain) and a C-terminal ligand-binding domain (the E domain, or LBD). (B) The most abundant NR5A2 isoforms in human and mouse share the same molecular structure, consistent with the modular architecture of NRs but with some peculiarities: the LBD contains an AF-2 region that modulates co-regulator recruitment, and an Ftz-F1 motif located within the DBD dictates specificity towards Ftz-F1 consensus DNA motifs. Conserved phosphorylation (P) and SUMOylation (S) sites are represented in orange.

## 6.3. Regulation of NR5A2 activity

The transcriptional activity of NR5A2 is modulated by naturally occurring phospholipids, transcriptional co-regulators and post-translational modification events. The interconnections between these processes coordinate NR5A2 activity in multiple tissues (reviewed by Lazarus et al. 2012; Sun, Demagny, and Schoonjans 2021).

### 6.3.1. Phospholipids as potential NR5A2 ligands

NR5A2 has traditionally been considered a constitutively active orphan nuclear receptor, since evidence for potential endogenous ligands remained inconclusive for decades. However, an increasing number of studies support the existence of several phospholipids that could act as natural ligands for NR5A2. Overall, ligand binding appears to induce a conformational change in NR5A2 that promotes its association with transcriptional co-activators, thereby enhancing its transcriptional activity (Ortlund *et al.*, 2005).

Over the last two decades, crystallographic studies allowed the identification of several phospholipids that can interact and activate human, but not mouse NR5A2. These potential endogenous ligands include different phosphatidyl inositol (PI) species, as well as the common bacterial phospholipids phosphatidyl glycerol (PG) and phosphatidyl ethanolamine (PE) (Krylova *et al.*, 2005; Ortlund *et al.*, 2005; Wang *et al.*, 2005; Musille *et al.*, 2012; Sablin *et al.*, 2015). Mutations within the human NR5A2 ligand binding domain reduce its transcriptional activity by preventing co-activator recruitment (Ortlund *et al.*, 2005). On the other hand, structural disruption of the ligand binding domain of mouse NR5A2 does not impact transcriptional potency, suggesting that ligand binding is dispensable for basal activity. Indeed, mouse NR5A2 presents a large empty pocket that adopts a constitutive active conformation despite the absence of ligand (Sablin *et al.*, 2003). This divergence between mouse and human NR5A2 orthologues is probably due to differences in the amino acid sequence, which affect ligand specificity (Sablin *et al.*, 2015). Recently, the dietary phospholipid dilauroyl phosphatidyl choline (DLPC) was found to act as a potent activator of both human and mouse NR5A2 (Turnbaugh *et al.*, 2009). Structurally, DLPC association to NR5a2 is a dynamic process that dictates co-regulator preference (Musille *et al.*, 2012), further supporting the role of DLPC as a modulator of NR5A2 activity.

### 6.3.2. Co-regulator recruitment

The role of NR5A2 is critically regulated by the recruitment of co-regulators, a diverse group of proteins that can enhance (co-activators) or reduce (co-repressors) its transcriptional activity. These interactions occur at the AF-2 domain through helical LXXLL motifs (where L is leucine and X is any amino acid) (Ortlund *et al.*, 2005; Shin and Osborne, 2008), a consensus sequence that facilitates protein interaction with nuclear receptors (Goodwin *et al.*, 2000).

Several proteins have been described to interact and repress NR5A2 activity in a tissue-dependent manner. For example, the short heterodimer partner (SHP or NR0B2) is expressed in pancreas, liver and heart and constitutes one the best characterised co-repressors of NR5A2 activity. NR0B2 is an unusual member of the nuclear receptor family that lacks the DNA-binding domain and thus requires an association with other transcription factors to regulate gene expression (Seol, Choi and Moore, 1996). NR0B2

reduces NR5A2 transcriptional activity through a dual mechanism that involves competition with co-activators as well as a direct repression of NR5A2 transactivation (Lee and Moore, 2002). Notably, NR5A2 is required for NR0B2 expression (Lee and Moore, 2002), which creates a negative regulatory loop that enables the latter to control its own expression by limiting the transcriptional activity of NR5A2 (Goodwin *et al.*, 2000; Lu *et al.*, 2000). Other co-repressors include DAX-1 (or NR0B1) - a putative NR0B2 paralogue that is expressed in embryonic stem cells, ovary and testis -, PROX1 – a homeobox transcription factor expressed in heart liver and hippocampus, and the nuclear receptor co-repressors NCOR1 and NCOR2 (reviewed by Stein and Schoonjans 2015). Recent *in vitro* overexpression experiments demonstrate that NR5A2 can also interact with c-Jun, as well as with the NF-kb subunits p50 and p65 to repress reporter activity (Huang, Lee and Chung, 2014).

In addition to co-repressors, several proteins have been found to potentiate NR5A2 activity, including steroid receptor coactivators (SRC-1, SRC-2, and SRC-3), peroxisome proliferator-activated receptor gamma (PPARɣ) coactivator 1α (PGC-1α), multiprotein bridging factor 1 (MBF-1), and β-catenin (reviewed in Stein and Schoonjans 2015). For instance, β-catenin cooperates with NR5A2 in the intestinal epithelium to activate the expression of cell cycle genes (Botrugno *et al.*, 2004), while PGC-1α-mediated transactivation of NR5A2 in the liver induces the expression of CYP7A1, a catalytic enzyme involved in bile acid biosynthesis (Shin and Osborne, 2008).

Nuclear receptors, such as the glucocorticoid receptor (Hah *et al.*, 2013), have been found to act as pioneer transcription factors in differentiating tissues, where they interact with close chromatin regions and modulate their accessibility to other factors involved in cell fate specification (Drouin, 2014). Increasing evidence supports a similar role for NR5A2. Chromatin immunoprecipitation analyses performed in a breast cancer cell line revealed that NR5A2 cooperates with FOXA1 - a popular pioneer factor in endodermal tissues - to repress the expression of cell cycle genes. NR5A2 depletion displaced histone deacetylase 2 from the regulatory regions of these genes, promoting histone acetylation and inducing gene expression (Bianco *et al.*, 2015). In addition, NR5A2 co-regulators commonly act through the recruitment of chromatin remodelling complexes. For instance, NR0B2 can inhibit gene expression by localising SIRT1 histone deacetylase on

target gene promoters (Chanda, Xie and Choi, 2010) and interact with histone methyl transferases to silence accessible chromatin regions (Tachibana *et al.*, 2002; Boulias, 2004; Fang *et al.*, 2007). In addition, NR5A2 interacts with the nuclear receptor co-repressor complex containing NCOR and histone deacetylase 3 (HDAC3) NCOR complex to attenuate the expression of inflammatory genes in human hepatocytes (Venteclef *et al.*, 2010).

Apart from modulating chromatin accessibility, the interaction between NR5A2 and other proteins - especially transcription factors - may be crucial to modulate the expression of different regulatory networks under certain physiological conditions. For instance, our laboratory has shown that in the context of a mild AP NR5A2 translocates to the promoters of inflammatory genes through the interaction with the AP-1 transcription factor (Cobo *et al.*, 2018). This will be further discussed in a subsequent section.

### 6.3.3. Post-translational modifications

NR5A2 activity can also be influenced by post-translational modifications, including phosphorylation, SUMOylation and ubiquitination (Fig. I7). Human NR5A2 can be phosphorylated at serine 238 and 243 in response to mitogens by extracellular signal-regulated kinases (ERK), leading to an increase NR5A2 transcriptional activity (Lee *et al.*, 2006). Proteinase kinase A (PKA) can also modulate human NR5A2 activity by phosphorylating serine 469, which affects gene expression by altering its interaction with GATA transcription factors (Bouchard, Taniguchi and Viger, 2005). SUMOylation is one of the best characterised post-translational modifications of NR5A2. It was first identified on lysine 224 in the hinge domain of human NR5A2 (Chalkiadaki and Talianidis, 2005), a residue that was later on found to be conserved in the mouse orthologue (lysine 289) (Stein *et al.*, 2014). SUMOylation at this site has been reported to repress the transcriptional activity of NR5A2 by recruiting co-repressors such as PROX1 (Stein *et al.*, 2014) or the NCOR1/HDAC3 co-repressor complex (Venteclef *et al.*, 2010). Finally, a recent study indicates that NR5A2 protein levels can also be modulated by protein ubiquitination, and subsequent proteasomal degradation (Lai and Hu, 2019).

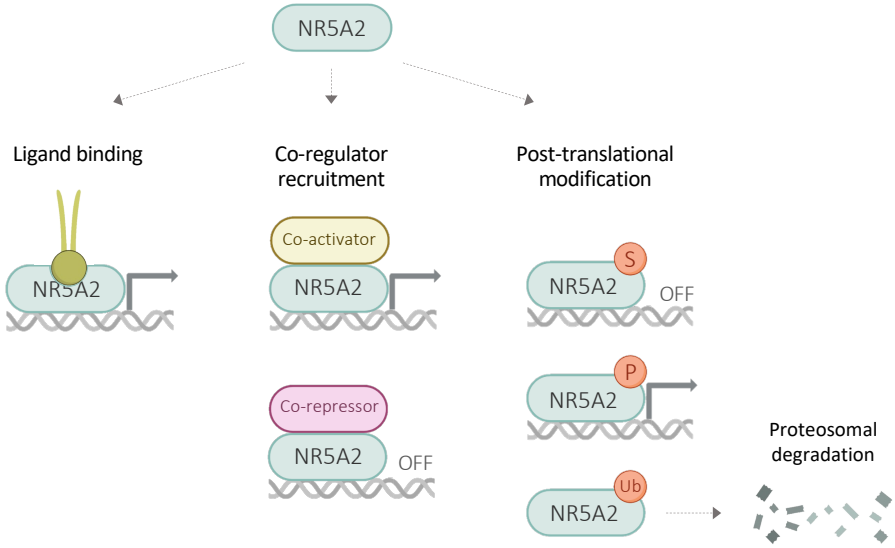


**Figure I7: Mechanisms of regulation of NR5A2 activity.** The transcriptional activity of NR5A2 can be modulated by phospholipid ligand binding, co-regulator recruitment (co-activators and co-repressors) and post translational modifications, such as SUMOylation (S), phosphorylation (P) and ubiquitinization (Ub), which results in proteasomal degradation. These mechanisms can either activate (arrow) or repress (OFF) transcriptional activity.

## 6.4. NR5A2 function

Like many other nuclear receptors, NR5A2 regulates essential functions in development, differentiation and metabolism. NR5A2 is expressed from initial stages of embryonic development and plays a critical role in embryonic stem cells. It directly regulates expression of *Oct4* in the epiblast, thereby maintaining pluripotency prior to gastrulation (Gu *et al.*, 2005) and can replace the latter during reprogramming of murine somatic cells into pluripotent stem cells (Heng *et al.*, 2010). In fact, homozygous *Nr5a2* deletion is associated with embryonic lethality, further supporting its crucial role throughout development (Parét *et al.*, 2001; Schoonjans *et al.*, 2002; Falender *et al.*, 2003). In adult mammals, NR5A2 is mainly expressed in exocrine pancreas, intestine, liver, ovary and brain, although low levels of expression are detected in heart, lungs and immune cells (Fayard, Auwerx and Schoonjans, 2004).

### 6.4.1. NR5A2 in pancreatic development and maintenance of acinar identity

NR5A2 plays a crucial role in pancreatic organogenesis and acinar cell maturation. It is expressed in the pancreatic epithelium at early developmental stages (E9.5) (Rausa *et al.*, 1999). During the secondary transition, NR5A2 becomes expressed at the tips of the branching epithelium, where it controls the generation and expansion of MPC and pre-

acinar cells. *Nr5a2* inactivation in the nascent pre-pancreatic epithelium results in developmental and functional defects in all three pancreatic lineages, although these are more profound in the exocrine compartment. These observations were performed using *Ptf1a*$^{+/Cre}$; *Nr5a2*$^{lox/lox}$, which involves recombination in the pancreatic epithelium at E9.5 (Hale *et al.*, 2014). By contrast, *Nr5a2* ablation at late gestational stages does not affect pancreatic specification, but destabilizes acinar differentiation post weaning. In this case, the authors used the *Pdx-Cre*$^{late}$ driver, which induces recombination in the pancreatic epithelium at E12.5 under the control of the *Pdx1* promoter (Von Figura *et al.*, 2014). In addition, *Nr5a2* inactivation in adult mice - using a ubiquitous tamoxifen-induced *Rosa26-CreER* diver - impairs pancreatic secretion upon hormonal stimulation (Cobo-Vuilleumier, Petra I Lorenzo, *et al.*, 2018). However, the constitutive loss of a single *Nr5a2* allele does not lead to the down-regulation of the acinar program in basal conditions (Cobo *et al.*, 2018).

These studies indicate a crucial role of NR5A2 in acinar identity. Indeed, NR5A2 is expressed at high levels in adult acinar cells (Rausa *et al.*, 1999; Fayard *et al.*, 2003; Flandez *et al.*, 2014), where it has been found to directly regulate the expression of digestive enzymes, as well as transcription, secretion and mitochondrial proteins (Fayard *et al.*, 2003; Cobo-Vuilleumier, Petra I Lorenzo, *et al.*, 2018). This is thought to occur through an interaction with the PTF1 complex (Molero *et al.*, 2012; Cobo-Vuilleumier, Petra I Lorenzo, *et al.*, 2018).

### 6.4.2. NR5A2 during pancreatitis

Acinar dedifferentiation is a crucial step in pancreatic disease. In response to cerulein-induced pancreatitis, acinar cells down-regulate the expression of the acinar program, transiently adopting a duct-like morphology and acquiring the expression of ductal markers. In normal pancreas, dedifferentiation is rapidly resolved and acinar morphology is restored (Jensen *et al.*, 2005; Fendrich *et al.*, 2008; Molero *et al.*, 2012; Flandez *et al.*, 2014). Similar to the acinar transcriptional program, NR5A2 expression is transiently down-regulated in ductal structures during pancreatitis and re-established in regenerated acinar cells, further supporting the role of NR5A2 in the maintenance of acinar identity (Flandez *et al.*, 2014; Von Figura *et al.*, 2014).

Recently, our laboratory described a dual role of NR5A2 in the control of acinar differentiation and pancreatic inflammation. In basal conditions, NR5A2 regulates the expression of acinar genes. However, under certain conditions that result in a down-regulation of *Nr5a2* expression, such as during pancreatitis or in the context of *Nr5a2* constitutive heterozygosity, NR5A2 translocates to the promoters of inflammatory genes, inducing their expression through an interaction with the AP-1 transcriptional complex (Fig. I8) (Cobo *et al.*, 2018). These results indicate an anti-inflammatory role of NR5A2 in the pancreas. In concordance with this, *Nr5a2* inactivation in the pancreas (using the *Pdx-Cre$^{late}$* driver) impairs acinar re-differentiation following pancreatitis induction, leading to persistent acinar atrophy and ductal metaplasia (Von Figura *et al.*, 2014). Similarly, germline *Nr5a2* heterozygous mice (*Nr5a2$^{+/-}$*) experiment an exacerbated response and delayed recovery from cerulein-induced pancreatitis. This is thought to result from NR5A2 haploinsufficiency in pancreatic epithelial cells, since a similar phenotype was observed using *Ptf1a$^{+/Cre}$; Nr5a2$^{+/lox}$* mice (Flandez *et al.*, 2014). Together, these results support the role of NR5A2 in the suppression of pancreatic inflammation.

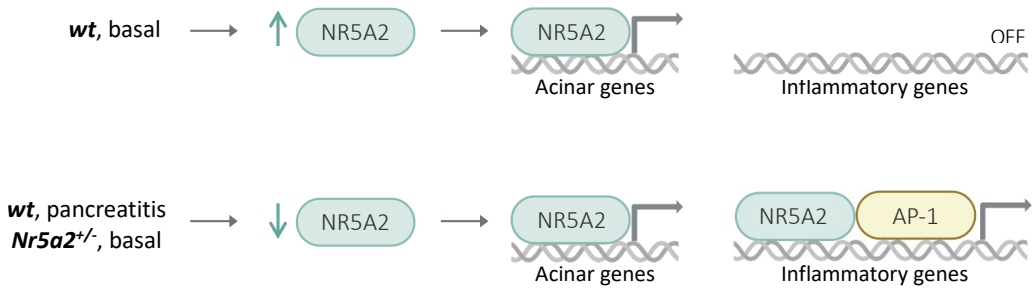


**Figure I8: Mechanism by which NR5A2 regulates acinar and inflammatory gene expression in mice.** In *wt* mice in basal conditions, NR5A2 regulates the expression of acinar genes. In response to cerulein-induced pancreatitis, or in the context of constitutive *Nr5a2* heterozygosity - two conditions that down-regulate *Nr5a2* expression in acinar cells - NR5A2 translocates to the promoters of inflammatory genes, inducing their expression through an interaction with the AP-1 transcriptional complex. Thus, in basal conditions *Nr5a2$^{+/-}$* mice present an inflammatory transcriptome that is reminiscent of early stages of pancreatitis. *Simplified version of the model proposed by Cobo et al. (2018).*

### 6.4.3. NR5A2 in pancreatic oncogenesis

The role of NR5A2 in pancreatic oncogenesis has been explored using mutant *Kras*-driven mouse models, in combination with constitutive *Nr5a2* heterozygosity or pancreatic *Nr5a2* ablation. Von Figura *et al.* (2014) found that, in the context of oncogenic *Kras*, *Nr5a2* inactivation in the pancreas (using *Pdx-Cre$^{late}$* driver) resulted in an almost complete replacement of the pancreatic parenchyma by ductal structures and lesions,

that were also present in *Pdx-Cre$^{late}$; Nr5a2$^{+/lox}$* mice. On the other hand, our laboratory described that constitutive *Nr5a2* heterozygosity cooperates with *Kras*-driven tumorigenesis and pancreatitis to promote neoplastic initiation in the pancreas (Flandez *et al.*, 2014). This acceleration in tumor development has been proposed to occur though NR5A2 haploinsufficiency in pancreatic epithelial cells, since using the Ptf1a-Cre driver to promote recombination in pancreatic epithelial cells in the context of oncogenic *Kras* also led to an increase in the number of neoplastic lesions (Flandez *et al.*, 2014; Von Figura *et al.*, 2014). In addition, genome-wide association studies (GWAS) have revealed an association between pancreatic cancer and single-nucleotide polymorphisms (SNPs) in the vicinity of the *NR5A2* gene (Petersen *et al.*, 2010; Zhang *et al.*, 2016; Chen *et al.*, 2018). Together, these results suggest a tumor suppressive role for NR5A2.

On the other hand, NR5A2 was found to promote – rather than inhibit – proliferation of several human PDAC cell lines *in vitro*, suggesting an oncogenic role for NR5A2 once the tumor has been established (Benod *et al.*, 2011). In concordance with this, NR5A2 overexpression has been associated with a worse clinical outcome in patients with pancreatic cancer (Dong *et al.*, 2011).

### 6.4.4. A close up into the *Nr5a2$^{+/-}$* model

In the last decade, our laboratory has worked under the assumption that the NR5A2 genetic variants that predispose for pancreatic cancer development lead to a partial loss of function, which can be modelled using *Nr5a2$^{+/-}$* mice. Since these mice constitute the model of study of this thesis, the most relevant findings derived from this work – which were published in two independent articles – have been summarised in Boxes 1 and 2.

### 6.4.5. Other roles of NR5A2 in the pancreas

In addition to acinar cells, NR5A2 expression has also been reported in ductal (Benod *et al.*, 2011) and β-cells in adult pancreas (Baquié *et al.*, 2011). While the role of NR5A2 in ductal cells has been poorly characterised, NR5A2 expression in β-cells has been reported to protect them from stress-induced apoptosis (Baquié *et al.*, 2011) and NR5A2 agonism protects against type 1 diabetes (Cobo-Vuilleumier, Petra I. Lorenzo, *et al.*, 2018).

## BOX 1: *Nr5a2* heterozygosity sensitises to, and cooperates with, inflammation in *KRas$^{G12V}$*-driven pancreatic tumorigenesis (Flández *et al.* 2014)

### *Nr5a2* heterozygosity leads to impaired recovery from acute caerulein-induced pancreatitis

NR5A2 is expressed at high levels in the exocrine compartment of the mouse pancreas.

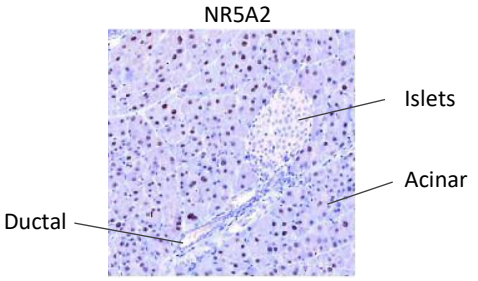


The pancreata of adult *wt* and *Nr5a2$^{+/-}$* mice were histologically undistinguishable.

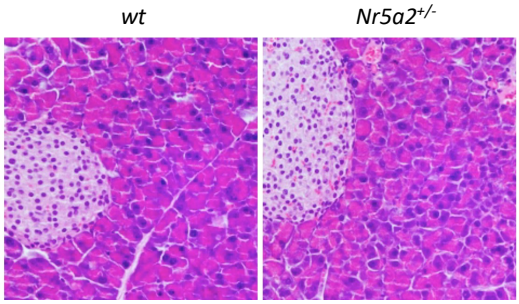


To determine whether *Nr5a2* is involved in pancreatic regeneration following pancreatic injury, we induced a mild acute pancreatitis by administering 7 hourly caerulein doses. Histological analysis showed an exacerbated response in *Nr5a2$^{+/-}$* mice. Although loss of one *Nr5a2* allele is dispensable for basal pancreatic function, these results show that both alleles are required for appropriate recovery from mild acute caerulein-induced damage.

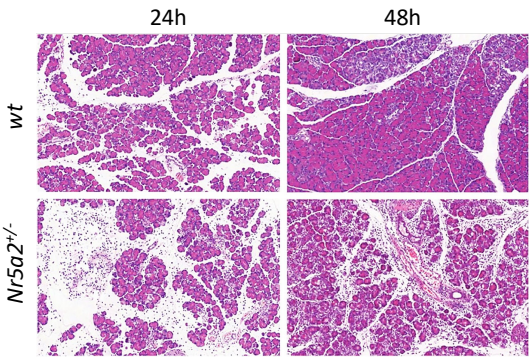


### Epithelial *Nr5a2* is required for appropriate recovery after caerulein-induced pancreatitis

To determine whether the observed phenotype results from *Nr5a2* haploinsufficiency in pancreatic epithelial cells or in other cell types, we generated mice in which one *Nr5a2* allele was selectively inactivated in the pancreas (*Nr5a2$^{lox/+}$;Ptf1a$^{Cre/+}$*). An acute pancreatitis was induced and mice were analysed at 48h. Lack of one *Nr5a2* allele in epithelial cells was sufficient to cause increased inflammation at 48 h to a level comparable with the response observed in *Nr5a2$^{+/-}$* mice. These results show that two *Nr5a2* alleles are required in epithelial cells for proper acinar regeneration upon injury in the pancreas.

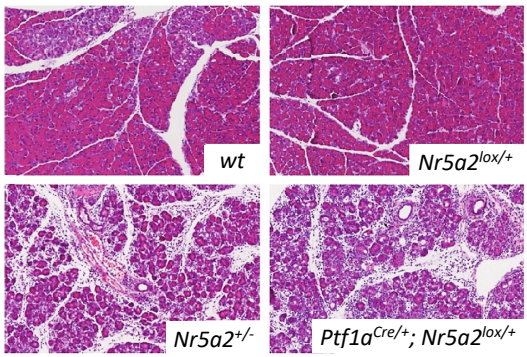


### *Nr5a2* heterozygosity cooperates with pancreatitis in *KRas$^{G12V}$*-driven tumorigenesis

To evaluate whether inactivation of one *Nr5a2* allele contributes to PDAC development, we generated *KRas$^{G12V}$*; *Ptf1a$^{Cre/+}$* mice of either *wt* or *Nr5a2$^{+/-}$* genotype. One month after the induction of a single episode of acute pancreatitis, the pancreatic area affected by preneoplastic lesions was significantly larger in *Nr5a2$^{+/-}$* mice than in controls. These results indicate that, after injury, *Nr5a2* heterozygosity leads to accelerated progression of *KRas$^{G12V}$*-driven tumorigenesis, supporting the notion that loss of *Nr5a2* cooperates with inflammation and *KRas* mutations in the pancreas.

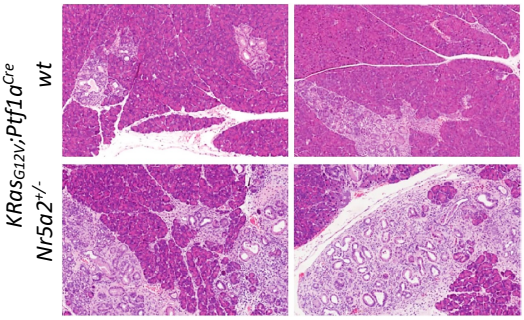

## BOX 2: Transcriptional regulation by NR5A2 links differentiation and inflammation in the pancreas (Cobo *et al.* 2018)

### *Nr5a2* heterozygosity leads to an epithelial-cell autonomous pre-inflammatory state in the pancreas

We used RNA sequencing to compare the transcriptome of *wt* and *Nr5a2*$^{+/-}$ pancreases. Gene set enrichment analysis revealed an upregulation of inflammatory pathways in *Nr5a2*$^{+/-}$ mice, that was not associated to increased abundance of inflammatory cells, based on quantification of CD45 expression.

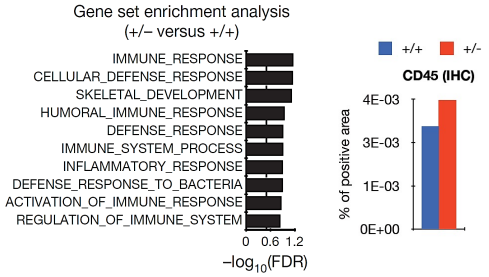


Quantitative reverse transcription PCR analyses confirmed upregulation of inflammatory mediators in isolated acini, suggesting that the defect is specific of acinar cells.

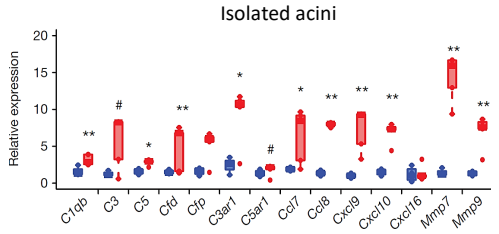


### AP-1 components are upregulated and bind to the promoter of inflammatory genes in *Nr5a2*$^{+/-}$ pancreases

Chromatin immunoprecipitation (ChIP) sequencing analysis revealed that only 7% of the genes that were upregulated in *Nr5a2*$^{+/-}$ mice exhibit NR5A2 binding within their promoter, suggesting the participation of an indirect mechanism. Promoter scanning analysis of upregulated genes revealed an enrichment of AP-1 motifs. In addition, AP-1 proteins were significantly upregulated in *Nr5a2*$^{+/-}$ pancreases.

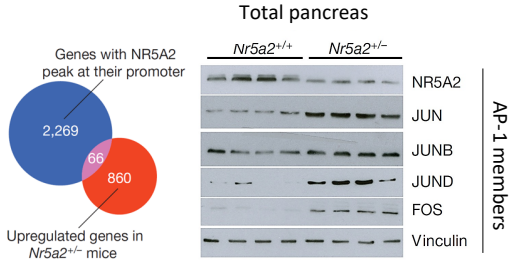


### The NR5A2 transcriptional switch

We performed ChIP followed by qPCR on the promoters of acinar and inflammatory genes. In *wt* mice in basal conditions, NR5A2 bound to the promoters of acinar genes, but transiently translocated to those of inflammatory genes after one dose of caerulein. This transcriptional switch was also observed in untreated *Nr5a2*$^{+/-}$ mice, indicating that *Nr5a2* haploinsufficiency mimics acute pancreatitis at the transcriptome level.

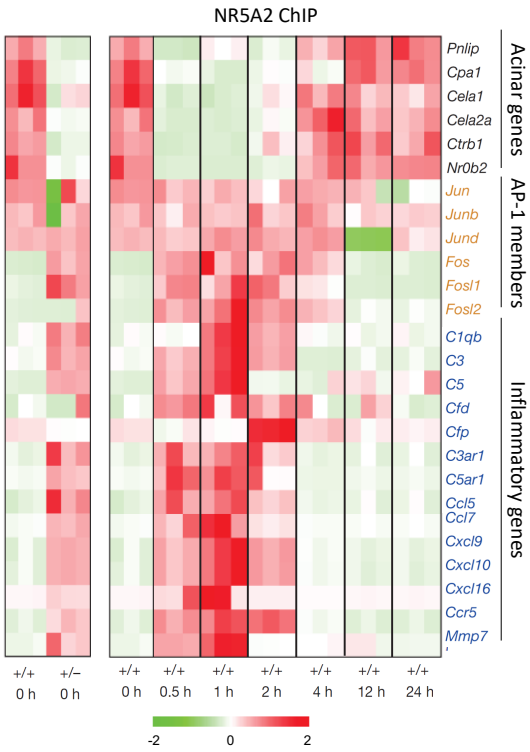


We found that NR5A2 coimmunoprecipitated with the AP-1 member JUN in the pancreas of untreated *Nr5a2*$^{+/-}$ mice and in *wt* mice 1 h after caerulein administration, but not in untreated *wt* mice, supporting the proposition that JUN and AP-1 cooperate in producing the NR5A2 transcriptional switch.

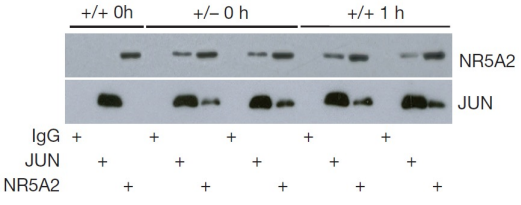


The proposed model of the NR5A2 transcriptional switch further detailed in **Fig. I8**

# OBJECTIVES

Pancreatic inflammation is one of the major risk factors for pancreatic cancer. Our group has shown that germline *Nr5a2* heterozygosity in mice induces pre-inflammation in basal conditions, sensitising the pancreas to inflammation and *Kras*-driven tumorigenesis. Increasing evidence indicates an association between non-genetic risk factors and pancreatic inflammation, including obesity as well as the occurrence and composition of the gut microbiome. These associations are very relevant from the clinical standpoint, since they offer an opportunity to act on modifiable factors to prevent pancreatic disease.

In this context, we aimed to determine the contribution of non-genetic risk factors to pancreatic inflammation in *Nr5a2*$^{+/-}$ mice. We hypothesised that obesity-related disorders could promote pancreatic inflammation in *Nr5a2*$^{+/-}$ mice and that their increased sensitivity to pancreatic inflammation may be modulated by the gut microbiome.

The specific objectives of this thesis were:

1) To investigate the effects of obesity and associated metabolic disorders on pancreatic inflammation in *Nr5a2*$^{+/-}$ mice.
2) To investigate the role of the gut microbiota on pancreatic inflammation in *Nr5a2*$^{+/-}$ mice.

# MATERIALS AND METHODS

## 1. Mouse strains

Mouse strains used for this project had a predominant C57BL/6 background with the following genetic modifications (alone or in combination): *Nr5a2*$^{+/-}$ (Botrugno *et al.*, 2004), *Nr5a2*$^{+/lox}$ (Botrugno *et al.*, 2004); *Villin-CreERT2*$^{+/T}$ (el Marjou *et al.*, 2004; JAX stock #020282) and *Pdx1-CreERT*$^{+/T}$ (Hingorani *et al.*, 2003; JAX stock #014647). Mice were bred to generate: *Nr5a2*$^{+/-}$, *Villin-CreERT2*$^{+/T}$*; Nr5a2*$^{+/lox}$ and *Pdx1-Cre*$^{+/T}$*; Nr5a2*$^{+/lox}$ mice and maintained under standard specific pathogen-free conditions at the animal facility of CNIO. Littermates were used as experimental controls. Experiments were approved by the Animal Ethical Committee of Instituto de Salud Carlos III and performed following guidelines for Ethical Conduct in the Care and Use of Animals. Mice were randomised across experimental conditions. Unless otherwise stated, both males and females mice were used.

## 2. *In vivo* procedures

### 2.1. Tissue collection

Mice were sacrificed by cervical dislocation and the pancreas was quickly collected. A small piece from the tail of the pancreas was flash frozen and stored at -80ºC for subsequent RNA extraction, while the rest was fixed in formalin for histological analysis. For the microbiome-related experiments, bacterial contamination was minimised by cleaning dissection tools with ethanol and sterile PBS prior to pancreas dissection. Tissues used for fluorescence *in situ* hybridisation (FISH) analysis were embedded in optimal cutting temperature compound (OCT), flash frozen and maintained at -80ºC until use. When specified, the spleen was also collected, weighted and fixed in formalin.

### 2.2. Cerulein-induced AP

Mild AP was induced by seven hourly intraperitoneal (i.p.) injections of cerulein (Bachem) at 50 µg/kg. Saline-treated mice were used as experimental controls. Serum was collected at 24 hours (h) for amylase quantification and mice were sacrificed 48 h after the first injection. Severe AP was induced by seven hourly i.p. injections of cerulein (50 µg/kg) for two non-consecutive days, with one day intermission. Serum was collected at 8 h for amylase quantification and mice were sacrificed at 48 h, counting from the first injection of the second day.

### 2.3. Diet intervention

Mice were fed either a control diet (CD; 2018S, Harlan Laboratories) or a high fat diet (HFD; D12451i, Brogaarden) containing 45% of calories from fat. Food and drinking water were provided *ad libitum.* Macronutrient composition of the diets is detailed in Table M1. For the HFD experiments, mice were weighted on a weekly basis. As further detailed in the experimental timelines of each experiments, mice were exposed to different procedures at 8-13 weeks post diet intervention, including the evaluation of glucose tolerance, insulin resistance evaluation, plasma extraction to measure cholesterol and triglyceride levels, cerulein-induced mild AP, and tissue pathological evaluation. These experiments were performed with males and females, although in this thesis we focus on the results obtained in males.

| Macronutrient | CD (3.1 kcal/g) | HFD (4.7 kcal/g) |
|---|---|---|
| Protein | 24% | 20% |
| Carbohydrate | 58% | 35% |
| Fat | 14% | 45% |

**Table M1:** Macronutrient composition of diets (% of calories) used in this thesis. CD: control diet. HFD: High fat diet.

### 2.4. Glucose tolerance test (GTT)

Mice were fasted overnight (for 13h) and basal glycemia was measured from tail blood. Mice were subsequently weighted and administered an i.p. injection of a 20% glucose solution (2 g/kg). Blood glucose levels were measured using a glucometer (Accu-Chek® Aviva) at 15, 30, 60 and 120 minutes.

### 2.5. Antibiotic (ABX) administration protocol

ABX administration was performed following a published protocol (Reikvam *et al.*, 2011) that consists of three days of amphotericin B (amphB; 1 mg/kg) – an antifungal substance used to suppress overgrowth of *Candida* species - followed by five days of an ABX/antifungal concoction composed of vancomycin (50 mg/kg), neomycin (100 mg/kg), metronidazole (100 mg/kg) and amphB (1 mg/kg). Compounds were dissolved in normal drinking water and administered by oral gavage every 12 hours (200 µl/mouse). From day three on, ampicillin (1 mg/ml) was added to drinking water and renewed weekly. Experimental controls were administered normal drinking water.

2.6. Microbiome reconstitution

Microbiome reconstitution was performed through: i) cohousing microbiome-depleted mice with mice reared in conventional conditions, in which case only females were used to facilitate cohousing, or ii) through weekly cage supplementation with fecal pellets from donor mice. In both cases, microbiome reconstitution was coupled with the interruption of ABX treatment.

2.7. Tamoxifen-induced recombination

Recombination in *Villin-CreERT2*$^{+/KI}$; *Nr5a2*$^{+/lox}$ mice was induced in 6-week-old mice by administering tamoxifen-containing food (TAM400/CreER, Harlan) *ad libitum* for 2 weeks. Recombination of the *Nr5a2* floxed allele was verified by standard PCR using published primers (Coste *et al.*, 2007): ACE225 5′ GTCATAGGGAGTCAGGATACCATGG 3′, ACE228 5′ GTTCTGACCACTTTCATCTCCTCACG 3′ and ACE231 5′ GTTAGCAATTTGGCAGATTTACGC 3′ (data not shown).

## 3. Biochemical analysis in plasma/serum

Mouse blood was collected from the submandibular vein in 1.5 ml heparin or EDTA tubes, incubated for 30 min at RT and centrifuged for 10 min at 10000 rpm. The serum/plasma was transferred to a new tube and either immediately processed or stored at -80ºC. For amylase measurements 1.5 ml heparin or EDTA tubes were used indistinctively. For insulin, glucose, triglyceride and cholesterol measurements, mice were fasted for 5 hours and plasma was obtained by collecting blood in heparin tubes.

3.1. Triglyceride and cholesterol quantification in plasma

Triglyceride and total cholesterol determination was performed within 2 h from plasma collection using TG Color GPO/PAP AA (1780107, Wiener lab.) and Colestat enzimático AA (1220110, Weiner lab.) kits, according to manufacturer's instructions.

3.2. Assessment of insulin sensitivity

Plasma insulin and glucose levels were measured using the Ultra Sensitive Mouse Insulin ELISA (90080, Crystal Chem) and Mouse Glucose Assay kits (81692, Crystal Chem) respectively, according to manufacturer's instructions. For insulin detection we followed

the high range assay protocol. HOMA-IR was calculated as previously described (Matthews *et al.*, 1985):

$$\text{HOMA-IR index} = \frac{\text{fasting glucose } \left(\frac{\text{mmol}}{\text{L}}\right) \text{x fasting insulin } \left(\frac{\mu\text{U}}{\text{ml}}\right)}{22.5}$$

A conversion factor of 1 μU = 6.00 pmol/L was used to convert insulin levels from conventional to international units, since it was recently proposed as the optimal conversion factor (Knopp, Holder-Pearson and Chase, 2019).

3.3. Serum/plasma amylase quantification

Serum/plasma samples were diluted 1:50 in distilled water (0123, Braun). Amylase quantification was performed in an ABX Pentra automated clinical chemistry analyser (HORIBA ABX) using Amylase CP diagnostic reagents (A11A01628, HORIBA ABX).

## 4. Histological analysis

4.1. Tissue preparation

Mouse pancreata were fixed overnight in 4% PBS-buffered formaldehyde. After fixation, they were embedded in paraffin and serially sectioned (3 μm) and either stained with hematoxylin and eosin or used for immunohistochemical analysis.

4.2. Histological scoring

Histological scoring was performed in H&E stained sections. Pancreatic inflammation-related histological parameters (edema, leukocyte infiltration and ADM) were scored by adding the grade of severity (0-3) to the extension of the pathological feature (0: absent, 1: focal, 2: multifocal and 3: diffuse). The individual scores were then added into a global histoscore that ranges from 0-18. When specified, lipomatosis was scored based on its severity and extension, as described above (0-6). Pancreas sections were reviewed blindly by F. X. Real and I. Millán. Liver steatosis was scored based on the abundance of micro (0-3) and macrosteatosis (0-3) in periportal, midlobular and pericentral areas separately. Individual scores were then added to obtain a global steatosis score for each liver (0-18). Liver samples were reviewed and scored blindly by a pathologist (E. Caleiras, Histopathology Unit, CNIO), C. Massillo and I. Millán.

### 4.3. Immunohistochemistry analysis

Immunohistochemistry analyses were performed at the Histopathology Unit in the CNIO. The primary antibodies used are listed in Table M2.

| Antibody | Company, reference, clone | Clone |
|---|---|---|
| αF4/80 | ABD Serotec, MCA497 | CI:A3-1 |
| αCD45 | Cell signalling technology, 70257 | D3F8Q |
| αPAX5 | Santa Cruz Biotechnology, sc-1974 | C-20 |

**Table M2:** Antibodies used in immunohistochemistry analyses.

### 4.4. Antigen-specific signal quantification

Slides were digitalised with Axio Scan.z1 (Zeiss) and processed with ZEN 2.3 lite software. Quantification was performed using six randomly selected fields of 5000 x 5000 pixels. Hematoxylin and antigen-specific signals were separated into different channels using the Color Deconvolution plugin of Image J software, and the pixel area of each individual channel was quantified using the same software. The antigen-specific signal was then normalised to the hematoxylin area.

## 5. Fluorescence *in situ* hybridization

Fluorescence *in situ* hybridization (FISH) analyses were performed at the Molelular Cytogenetics Unit in the CNIO using probes specifically designed to a complementary 16S rRNA sequence unique to eubacteria. Sections of 5 µm of OCT-preserved pancreata were mounted on positively charged slides (SuperFrost, Thermo Scientific). Briefly, tissues were postfixed in freshly prepared 4% paraformaldehyde. After enhancement of the bacteria wall permeabilization by lysozyme treatment (10g/L Tris HCl 6.5M), the samples were incubated for 1 hour at 45°C in the presence of the specific probe in a hybridizer machine (Dako). This was performed in 20 µl of hybridization buffer (20 nM Tris, pH 8.0. 0.9 M NaCl, 0.02% SDS, 30% formamide) containing 100 ng of the probe. Finally, tissues were washed in washing solution (70% formamide, 10mM Tris pH7.2 and 01% BSA), dehydrated in a series of ethanol, air-dried and stained with 0.5 µg/ml DAPI/Antifade solution (Palex Medical). FISH images were captured using a Leica DM5500B microscope with a CCD camera (Photometrics SenSys) connected to a PC running the CytoVision

software 7.2 image analysis system (Applied Imaging). Images were blinded analyzed to score for the number of FISH signals.

## 6. RNA analysis

6.1. RNA isolation from total pancreas

Pieces of mouse pancreas were homogenised using ULTRA-TURRAX T10 homogeniser (IKA) in cold GTC buffer (4M guanidine thiocyanate, 0.1M Tris-HCl pH 7.5 prepared in DEPC treated water) to which 1% 2-mercaptoethanol was added immediately before use and total RNA was isolated using the phenol-chloroform method (Chirgwin *et al.*, 1979). Total RNA was then treated with DNase I (DNA-free DNase Treatment & Removal Reagents, Ambion) according to manufacturer's instructions.

6.2. RNA-sequencing (RNA-seq) analysis of mouse pancreata

RNA quality was determined with the RNA Integrity Number (RIN) using an Agilent 2100 Bioanalyzer. Gender and RIN-matched samples with RIN values ranging from 6.9 to 9 were sent to the Genomics Unit at the CNIO for library preparation and sequencing. Total number of reads per sample ranged from 18 to 24 million. RNA-seq data was processed using Nextpresso v1.9.2.4 (Graña *et al.*, 2018) using default parameters. This software enables us to evaluate read quality, align reads to a mouse reference genome (mm10), and perform differential expression analysis using DEseq to obtain a list of deregulated genes between samples. Statistical significance was set at p-adj < 0.05. Ranked gene lists generated by DEseq (in which genes are ranked based on log2-fold change) were subjected to GSEAPreranked v6.0.12 using the GO biological processes, REACTOME and KEGG libraries. This analysis was performed using the GenePattern platform (Reich *et al.*, 2006). A highly restrictive threshold of FWER p-val < 0.05 was used to establish significance, unless otherwise stated.

Genes/pathways that overlap across conditions were identified using Venny 2.1 online software and represented using the Eulerr R package. Heatmaps were generated using the online Morpheus software (https://software.broadinstitute.org/morpheus/).

Mouse MCP-counter (mMCP-counter) was used to estimate the immune and stromal composition in pancreas samples using transcriptomic data (Petitprez *et al.*, 2020).

To explore immune gene set enrichment across comparisons, pathways that contained one of these terms within their names were selected: immune, inflammatory, B cell, T cell, cytokine, antigen, interleukin, IL, interferon, chemokine, leukocyte, neutrophil, defense, myeloid and tumor necrosis factor.

6.3. RNA-seq analysis of published transcriptomic data from intestine

Published transcriptomic data from duodenum and ileum of mice reared in germ-free (GF) and conventional conditions (CV) was downloaded from GEO (GEO accession: GSE114399). Read counts were normalised using DESeq2 (Love, Huber and Anders, 2014), in the R v4.0.3 framework or higher using RStudio. The enrichment of ABX-related signatures was assessed using single sample GSEA (ssGSEA) 10.6 from the GenePattern platform (Reich *et al.*, 2006).

6.4. Transcriptomic analysis of human pancreas

Transcriptomic data of 328 human pancreas samples from the Genotype-Tissue Expression (GTEx) project were used (Consortium, 2017). The enrichment of ABX-related signatures was assessed using single sample GSEA (ssGSEA) 10.6 from the GenePattern platform (Reich *et al.*, 2006).

## 7. Microbiome analysis

7.1. Feces collection and DNA isolation

To minimise bacterial contamination, fresh fecal pellets were collected directly from mice into 1.5 ml tubes and stored at -80ºC. Total DNA extraction was performed using the QIAamp® Fast DNA Stool Mini Kit (51604, Quiagen) according to manufacturer's instructions, increasing the lysis temperature to 95ºC as recommended for Gram-positive bacterial detection.

7.2. Bacterial DNA quantification

Bacterial DNA quantification was performed by quantitative PCR (qPCR), as previously described (Reikvam *et al.*, 2011). Degenerate primers were used to amplify the V2 and V6 regions of the 16S rDNA gene. The number of 16S copies was normalised to mouse genomic DNA, quantified using primers for mouse poly immunoglobulin receptor (mpIgR). Primers used for this analysis are listed in Table M3. Reactions were carried out

with 5 ng of DNA using SYBR® Green PCR Master Mix in the QuantStudio 6 Flex system (Thermofisher).

| Target | Primer name | Sequence (5'-3') |
|---|---|---|
| 16S V2 region | 16S-V2-101F | AGYGGCGIACGGGTGAGTAA |
| | 16S-V2-361R | CYIACTGCTGCCTCCCGTAG |
| 16S V6 region | 16S-V6-784F | AGGATTAGATACCCTGGTA |
| | 16S-V6-1061R | CRRCACGAGCTGACGAC |
| Mouse pIgR genomic region | mpIgRgenomic.for | TTTGCTCCTGGGCCTCCAAGTT |
| | mpIgRgenomic.rev | AGCCCGTGACTGCCACAAATCA |

**Table M3:** Target region, name and sequence of primers used for amplification of bacterial 16S and mouse genomic DNA. The matching forward and reverse primers targeted to mouse cDNA lie in separate exons. Primers extracted from Reikvam *et al.* (2011).

## 7.3. 16S rDNA sequencing, library preparation and data processing

### Library preparation and DNA sequencing

Fecal DNA from 6-8 week old cohoused *Nr5a2*$^{+/-}$ and *wt* mice was isolated as described above. Libraries were prepared by the Genomics Unit at Complutense University of Madrid (UCM) according to Illumina's 16S Metagenomic Sequencing Library Preparation protocol. Samples were indexed with the Nextera XT Index Kit v2 Set D (FC-131-2004, Illumina). The individual libraries were pooled in equimolecular concentrations and sequenced by the Sequencing and Bioinformatic Service at FISABIO (Valencia) in a MiSEq sequencer using paired 300 bp reads. Sequencing depth ranged from 16953-59609 reads per sample.

### Amplicon sequence variant (ASV) construction and taxonomy assignment

Amplicon sequence variant (ASV) construction was performed in collaboration with M. D. Alonso and N. Malats (Genetics and Molecular Epidemiology Group, CNIO) using the DADA2 pipeline according to developers' instructions (DADA2 Pipeline Tutorial 1.16). Upon read quality inspection, reads were trimmed to 245 bp and error models were performed using all sequences. Paired-end reads were then merged according to their ≈ 30 bp overlap and filtered by length, keeping sequences ranging from 438-469 bp. Finally, taxonomies were assigned using Silva NR 99 138.1 species training set.

Taxonomic diversity analysis

ASVs were normalised to median sequencing depth using phyloseq R package. To evaluate microbial diversity within each sample (alpha diversity), we computed observed ASV numbers as well Shannon and Simpson indices accounting for both microbial richness and evenness. Microbial diversity across samples (beta diversity) was visualised via non-metric multidimensional scaling plots (NMDS) based on Bray-Curtis dissimilarity matrices. The significance of differences between *Nr5a2*$^{+/-}$ and *wt* mice was tested using permutational multivariate analysis of variance (PERMANOVA) with 999 permutations, using vegan R package. Microbiome diversity plots were depicted using ggplot2 R package. Confidence interval ellipses were represented using the stat_ellipse function. Alpha and beta diversity was also computed on data that was agglomerated at different taxonomic levels (i.e. phylum, class, order, family, genus, species) using the phyloseq R package.

Differential taxonomic abundance analysis

Differential taxonomic abundance analysis was performed using DESeq2 R package (Love, Huber and Anders, 2014) by comparing i) *Nr5a2*$^{+/-}$ versus *wt* samples and ii) *wt* or *Nr5a2*$^{+/-}$ samples with highest histopathological scores during pancreatitis vs those with lowest scores, at different taxonomic levels - phylum, class, order, family, genus, species, and ASV. The significance threshold was set at p-adj < 0.05.

All analyses were conducted in the R v4.0.3 framework or higher using RStudio. Unless otherwise indicated, analyses in the main text were performed using ASVs, rather agglomerated data.

## 8. Flow cytometry analysis of immune cells

8.1. Immune cell isolation

Mouse blood (~ 300 µl) was collected from the submandibular vein in EDTA tubes and kept at RT until used. Blood samples were transferred to 15 ml tubes, incubated with 5ml of EL Erythrocyte lysis buffer (79217, Quiagen) for 10 min at RT and subsequently diluted with 10 ml of PBS. After centrifugation at 1600 rpm for 3 min at RT, the supernatant was carefully aspirated (leaving ~ 200 µl) and transferred to 96 well V-bottom plates. Cells

were then centrifuged at 1600 rpm for 3 min at RT, washed with 200 µl of PBS and centrifuged again at the same speed prior to resuspension in viability marker (described in 8.2).

Mouse spleens were collected in cold PBS and kept on ice until processing. Tissues were disaggregated by pressing the spleen with the plunger head of a 1 ml syringe through a 40 µm cell strainer placed on a 50 ml tube. To maximise cell collection, strainers were washed with 10 ml of cold PBS. Cell suspensions were centrifuged at 1600 rpm for 3 min at 4ºC, resuspended in cold PBS and counted in a Countess 3 Automated Cell Counter (Invitrogen). Next, 2 x $10^6$ cells from each sample were transferred to 96 well V-bottom plates.

8.2. Cell staining with surface markers

Once tissue suspensions were placed in 96-well V-bottom plates, cells were pelleted by centrifugation. Unless specified, all centrifugations were performed at 1600 rpm for 3 min at 4ºC. Cells were resuspended in 200 µl of a 1:200 dilution of the viability marker LIFE/Dead™ Fixable Aqua (L34965, Invitrogen) and incubated for 30 min at RT. Cells were then centrifuged, washed with 200 µl of PBS and centrifuged again for subsequent resuspension in 100 µl of cold blocking buffer, consisting on a 1:200 dilution of Mouse Fc Block™ (553142, BD Biosciences) in PBS staining (1% BSA, 0.05% sodium azide in PBS). After a 15 min incubation at 4ºC, cells were centrifuged, resuspended in 50 µl of fluorescently labelled antibodies prepared in PBS staining and incubated for 30 min at 4ºC in the dark. A list of the antibodies used for flow cytometry is provided in Table M4.

Next, cells were washed by adding 150 µl of cold PBS staining and centrifuging. A final fixing step was performed by resuspension in 100 µl of 4% PFA in PBS and incubation in the dark for 10 min on ice, followed by centrifugation at 1600 rpm for 5 min at 4ºC. To avoid tandem dye degradation, fixing time never exceeded 15 min (including centrifugation). The fixing solution was meticulously removed after centrifugation, by pressing the plate against filter paper prior to resuspension in 100 µl of cold PBS staining and storage at 4ºC in the dark.

Cell suspensions were processed within 24 h with an LSRFortessa™ X-20 cell analyser (BD Biosciences) and analysed with FlowJo v10 sotfware. UltraComb eBeads™ Compensation

Beads (01-222-42, Invitrogen) were used as compensation controls. Cell populations were gated after excluding doublets (discriminated by FSC-A and FSC-W), non-viable cells and cell debris (discriminated by FSC-A and SSC-A) using the combinations of markers listed in Table M5.

| Target | Fluorophore | Clone | Company, reference | Dilution |
|---|---|---|---|---|
| B220 | PECy5 | RA3-6B2 | Biolegend, 103222 | 1:100 |
| CD3 | APC | 145-2C11 | Biolegend, 100312 | 1:50 - 1:100 |
| CD3 | PE CF594 | 145-2C11 | Bioscience, 562332 | 1:200 |
| CD4 | APC eF780 | RM4.5 | eBioscience, 17-0042-83 | 1:100-1:200 |
| Ly6G | PE | 1A8 | Pharmingen, 551461 | 1:100 - 1:200 |
| Ly6C | FITC | HK1.4 | Biolegend, 128006 | 1:100 |
| CD11b | BV570 | M1/70 | Biologend, 101233 | 1:50 - 1:100 |
| CD8 | FITC | 53-6.7 | Beckman, 733264 | 1:200 |
| NK1.1 | BV421 | PK136 | BD Pharmigen, 562921 | 1:100 |
| CD25 | PerCP Cy5.5 | PC61.5 | eBioscience, 45-0251-82 | 1:100 |

**Table M4:** List of antibodies used for flow cytometry analyses.

| Source | Population | Markers |
|---|---|---|
| Blood | B cells | CD3- B220+ |
| | T cells | CD3+ B220- |
| | $CD4^+$ T cells | CD3+ B220- CD4+ |
| | $CD8^+$ T cels | CD3+ B220- CD8+ |
| | Monocytes/macrophages | CD3- B220- CD11B+ Ly6G- |
| | Neutrophils | CD3- B220- CD11B+ Ly6G+ Ly6C+ |
| Spleen | NK cells | CD3- NK1.1+ |
| | B cells | CD3- B220+ |
| | T cells | CD3+ B220- |
| | $CD4^+$ T cells | CD3+ B220- CD8- CD4+ |
| | $CD8^+$ T cells | CD3+ B220- CD4- CD8+ |

**Table M5:** Markers used to identify the immune populations immunoprofiled in this thesis.

## 9. Statistical analysis

Statistical analysis of the 16S rDNA sequencing experiment was performed using the R v4.0.3 software. Significance of the RNA-seq experiments was calculated by the Nextpresso v1.9.2.4 pipeline, with the exception of the statistical analysis of the overlap

between two groups of genes or pathways, which was performed using an online tool (http://nemates.org/MA/progs/overlap_stats.html). The remaining statistical analyses were performed using the software GraphPad PRISM v8.0.1. The type of statistical test used is specified in the figure legends. In all cases, $P < 0.05$ was considered significant. Exact P values were reported when $P < 0.01$, while $P > 0.01$ were reported as ns.

# RESULTS

# CHAPTER I

# Effects of high fat diet on pancreatic inflammation in *Nr5a2*$^{+/-}$ mice

To investigate the effects of obesity in the context of *Nr5a2* heterozygosity, adult *wt* and *Nr5a2*$^{+/-}$ mice were fed a HFD and their response was compared in basal conditions and upon induction of a mild AP. Mice fed a CD were used as experimental controls. The experiments described in this chapter were performed with mice of both sexes, but only the results obtained in males have been included in this report, since the metabolic effects of HFD feeding were more evident in these mice.

## 1.1. *Nr5a2* heterozygosity has no major effects on HFD-induced alterations in glucose metabolism and plasma lipid content

To determine whether *Nr5a2* heterozygosity sensitises mice to the development of obesity-associated disorders, we explored the effects of HFD feeding on multiple parameters that are well known to be affected in obese individuals, including: body weight, insulin resistance, glucose metabolism and plasma lipid concentrations. The timeline of this experiment is depicted in Fig. R1A.

*Wt* and *Nr5a2*$^{+/-}$ male mice were fed either with a CD or a HFD and their weekly weight was compared over a period of ten weeks. We did not detect significant differences in body weight between genotypes at the start of diet intervention (Fig. R1B). At the end of the ten weeks, HFD-fed mice displayed significantly higher body weight compared to CD controls regardless of genotype ($P_{wt} < 0.001$, $P_{Nr5a2+/-} < 0.001$). However, there were no significant differences in body weight increase across genotypes for either of the diets administered (Fig. R1C). The same observations were made for gonadal white adipose tissue weight (data not shown). These results indicate that *Nr5a2* heterozygosity does not have a major impact on HFD-induced alterations in body weight or adipose tissue accumulation.

To assess insulin resistance, we measured fasting plasma glucose and insulin levels and calculated HOMA-IR at week eight of diet intervention. HFD feeding led to an increase in fasting glucose (Fig. R1D), insulin (Fig. R1E), and HOMA-IR both in control and *Nr5a2*$^{+/-}$ mice (Fig. R1F). However, no significant differences were detected across genotypes in either of the dietary conditions, indicating that *Nr5a2* heterozygosity does not affect insulin sensitivity (Figs. R1D, R1E, R1F).

To assess glucose homeostasis, we performed a GTT at week nine of diet intervention. HFD feeding resulted in impaired glucose tolerance in mice of both genotypes, as reflected by the significant increase detected in the area under blood glucose curve (AUC) (Fig. R1H). However, no major differences were detected across genotypes upon both dietary interventions (Figs. R1G and R1), indicating that *Nr5a2* heterozygosity does not affect glucose tolerance.

We also evaluated the effects of HFD feeding on plasma lipid content at week eight of diet intervention. HFD-fed mice displayed increased total plasma cholesterol levels compared to CD mice regardless of genotype (Fig. R1I), while plasma triglyceride levels remained unaffected upon HFD feeding (Fig. R1J). No differences were observed across genotypes in any experimental condition analysed, indicating that *Nr5a2* heterozygosity does not affect plasma levels of the lipids analysed.

**Figure R1** (see on next page)**: *Nr5a2* heterozygosity has no major effects on HFD-induced alterations in glucose metabolism and plasma lipid content. (A)** Experimental timeline: *wt* and *Nr5a2*$^{+/-}$ mice were fed a HFD or a CD for 10 weeks and the incidence of multiple obesity-associated metabolic disorders was assessed through plasma measurements and GTT. **(B)** Baseline body weight. Significance was calculated using unpaired two-tailed t test, assuming a consistent SD (n = 12-13/group). **(C)** Weekly body weight gain, shown as a percentage of weight increase from baseline value. **(D)** Fasting plasma glucose levels. **(E)** Fasting plasma insulin levels. **(F)** HOMA-IR index. **(G)** GTT. **(H)** Area under glucose tolerance curve (AUC). **(I)** Fasting total plasma cholesterol. **(J)** Fasting plasma triglyceride levels. For C, G, data show mean ± SEM and significance was calculated using two-way ANOVA on repeated measures and Sidak's multiple comparison test (n = 6-7/group). For D, E, F, H, I, J data show mean ± SD and significance was calculated using two-way ANOVA on repeated measures (n = 6-7/group)**.** HFD, high fat diet; CD, control diet; GTT, glucose tolerance test.

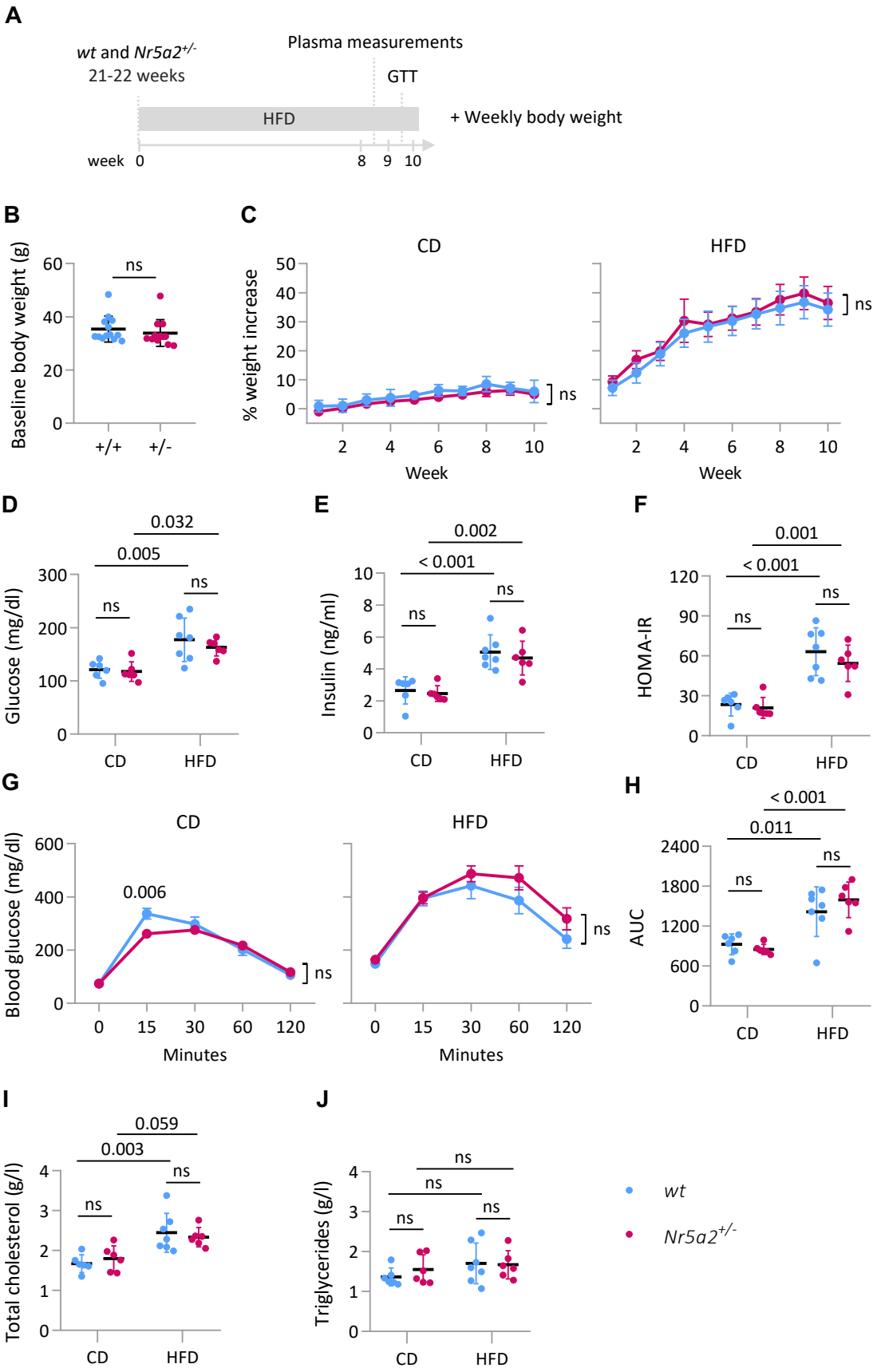
A
wt and Nr5a2+/-
21-22 weeks
Plasma measurements
GTT
HFD
+ Weekly body weight
week 0
8 9 10
B
Baseline body weight (g)
ns
+/+ +/-
C
CD
HFD
% weight increase
Week
ns
D
Glucose (mg/dl)
0.032
0.005
ns
CD HFD
E
Insulin (ng/ml)
0.002
< 0.001
ns
F
HOMA-IR
0.001
< 0.001
G
Blood glucose (mg/dl)
0.006
Minutes
H
AUC
< 0.001
0.011
I
Total cholesterol (g/l)
0.059
0.003
J
Triglycerides (g/l)
wt
Nr5a2+/-

## 1.2. *Nr5a2* heterozygosity may attenuate HFD-induced hepatic steatosis

HFD feeding has been reported to alter pancreatic histology (Rouse *et al.*, 2014) and induce hepatic steatosis (Tsuru *et al.*, 2020). In this context, we aimed to determine whether *Nr5a2*$^{+/-}$ mice were more sensitive to HFD feeding. For this, we evaluated pancreas and liver sections from HFD- and CD-fed *wt* and *Nr5a2*$^{+/-}$ male mice at 13 weeks of diet intervention (Fig. R2A). Representative images of pancreas and liver sections are shown in Fig. R2B and R2C.

Pancreatic histology scores were determined based on the presence of edema, leukocyte infiltration, and ADM. We also evaluated pancreatic lipomatosis. We did not detect major alterations in the histology and lipomatosis scores across groups but there was a tendency for a non-significant increase in lipomatosis in HFD-fed *wt* mice compared to CD controls (P = 0.100, Fig. R2D and R2E). Hepatic steatosis scores were determined based on the abundance of micro- and macro-steatosis in the periportal, mid-lobular, and pericentral zones. We found increased steatosis scores in HFD-fed mice compared to CD controls (Fig. R2F), although this was only significant in *Nr5a2*$^{+/-}$ mice, possibly due to the limited number of *wt* mice used ($P_{wt}$ = 0.100, $P_{Nr5a2+/-}$ = 0.024). Interestingly, we also detected a non-significant reduction in steatosis in HFD-fed *Nr5a2*$^{+/-}$ males compared to *wt* controls (Fig. R2F).

These analyses suggest that: i) HFD administration does not induce major alterations in pancreatic histology but causes liver steatosis in mice of both genotypes, ii) *Nr5a2* heterozygosity has no major effect on basal pancreas histology, and iii) *Nr5a2* heterozygosity may protect from HFD-induced hepatic steatosis. Due to the limited number of mice used for these analyses, a more in-depth analysis using a higher number of mice is warranted.

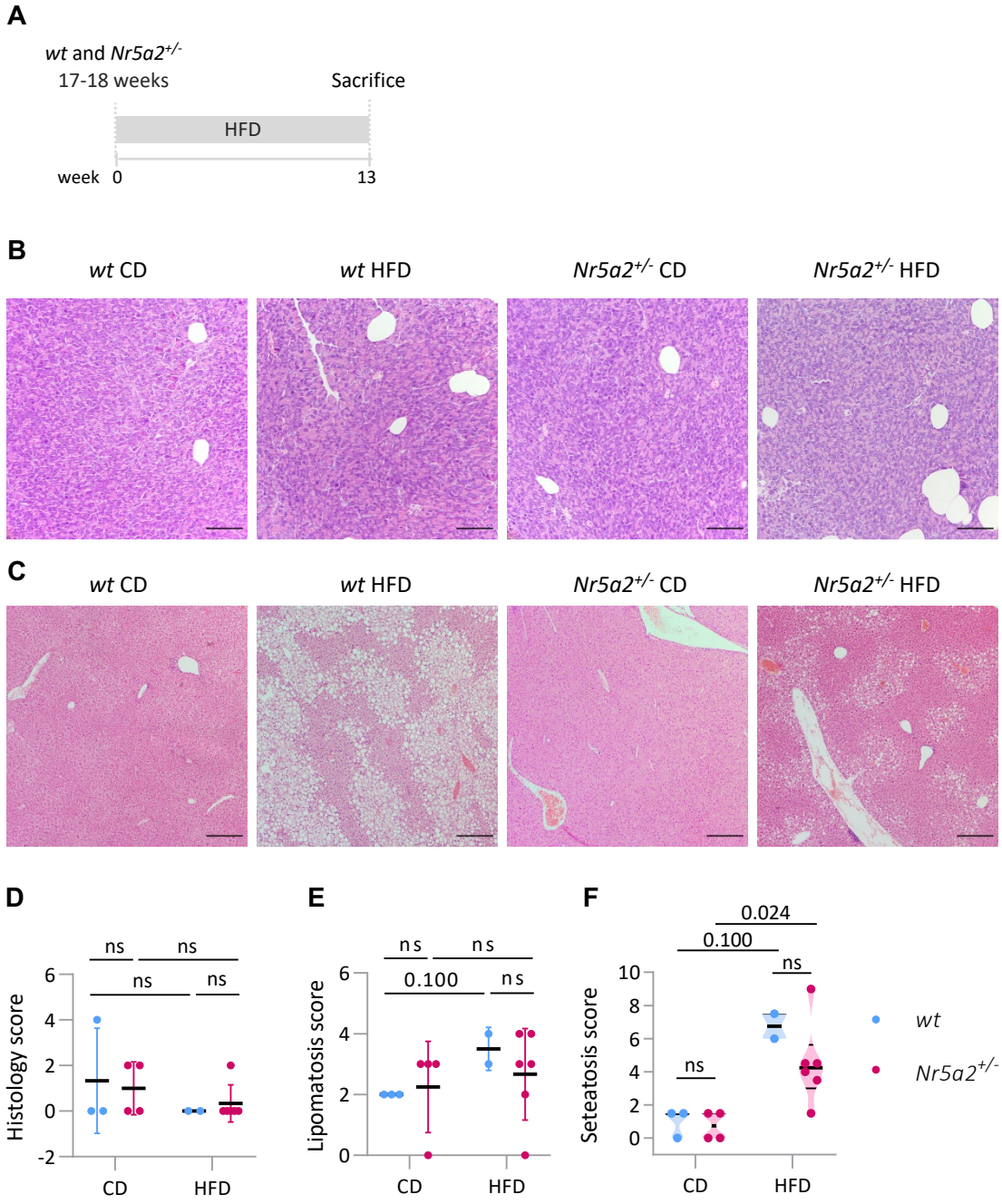


**Figure R2: *Nr5a2* heterozygosity may attenuate HFD-induced liver steatosis. (A)** Experimental timeline: *wt* and *Nr5a2*$^{+/-}$ mice were fed a HFD or a control diet CD and sacrificed at week 13. **(B)** Representative images of pancreas sections. Scale bar: 200 µm. **(C)** Representative images of liver sections. Scale bar: 500 µm **(D)** Histological scores (0-18) of pancreas sections, as described in methods. Data is presented as mean ± SD. **(E)** Pancreatic lipomatosis score (0-6). **(F)** Violin plot showing liver steatosis scores based on the abundance of micro- and macro-steatosis, as described in methods. Statistical significance was calculated using Mann Whitney test (n = 2-6/group). HFD, high fat diet; CD, control diet.

### 1.3. *Nr5a2* heterozygosity does not cooperate with HFD-induced pancreatic inflammation

To investigate whether HFD feeding modulates the effects of cerulein administration in the context of a mild AP in *Nr5a2*$^{+/-}$ mice, HFD- and CD-fed *wt* and *Nr5a2*$^{+/-}$ mice were given seven hourly injections of cerulein at week 10 of diet intervention (Fig. R3A).

To evaluate pancreatic exocrine damage, plasma amylase levels were measured at 24 hours post pancreatitis induction. Mice were sacrificed at 48 h and their pancreata were collected for histologic analysis. CD-fed *Nr5a2*$^{+/-}$ males displayed higher pancreatic histopathological scores (Fig. R3C) and plasma amylase levels (Fig. R3D) compared to *wt* controls, confirming our previous reports that *Nr5a2* heterozygosity sensitises to pancreatic inflammation (Flandez *et al.*, 2014; Cobo *et al.*, 2018). As expected, HFD-fed *wt* mice presented increased histopathological scores (Fig. R3C) and plasma amylase concentration (Fig. R3D) compared to CD controls, confirming previous reports indicating that HFD-induced obesity induces pancreatic injury (Rouse *et al.*, 2014). However, such increase was not observed in *Nr5a2*$^{+/-}$ mice, indicating that *Nr5a2* heterozygosity does not cooperate with HFD to induce pancreatic inflammation. Representative images of pancreas sections are shown in Fig. R3B.

We took advantage of these experiments to replicate the protective effect of *Nr5a2* heterozygosity on hepatic steatosis. In agreement with the observations described above, we found an increase in steatosis scores in HFD-fed mice compared to CD controls, regardless of genotype (Fig. R3E). In addition, HFD-fed *Nr5a2*$^{+/-}$ mice displayed lower steatosis scores than their *wt* counterparts, supporting the notion that *Nr5a2* heterozygosity attenuates HFD-induced liver steatosis.

These results indicate that HFD-induced obesity increase the severity of pancreatitis in *wt*, but not in *Nr5a2*$^{+/-}$ males, suggesting that *Nr5a2* heterozygosity protects from HFD-induced pancreatic damage in males.

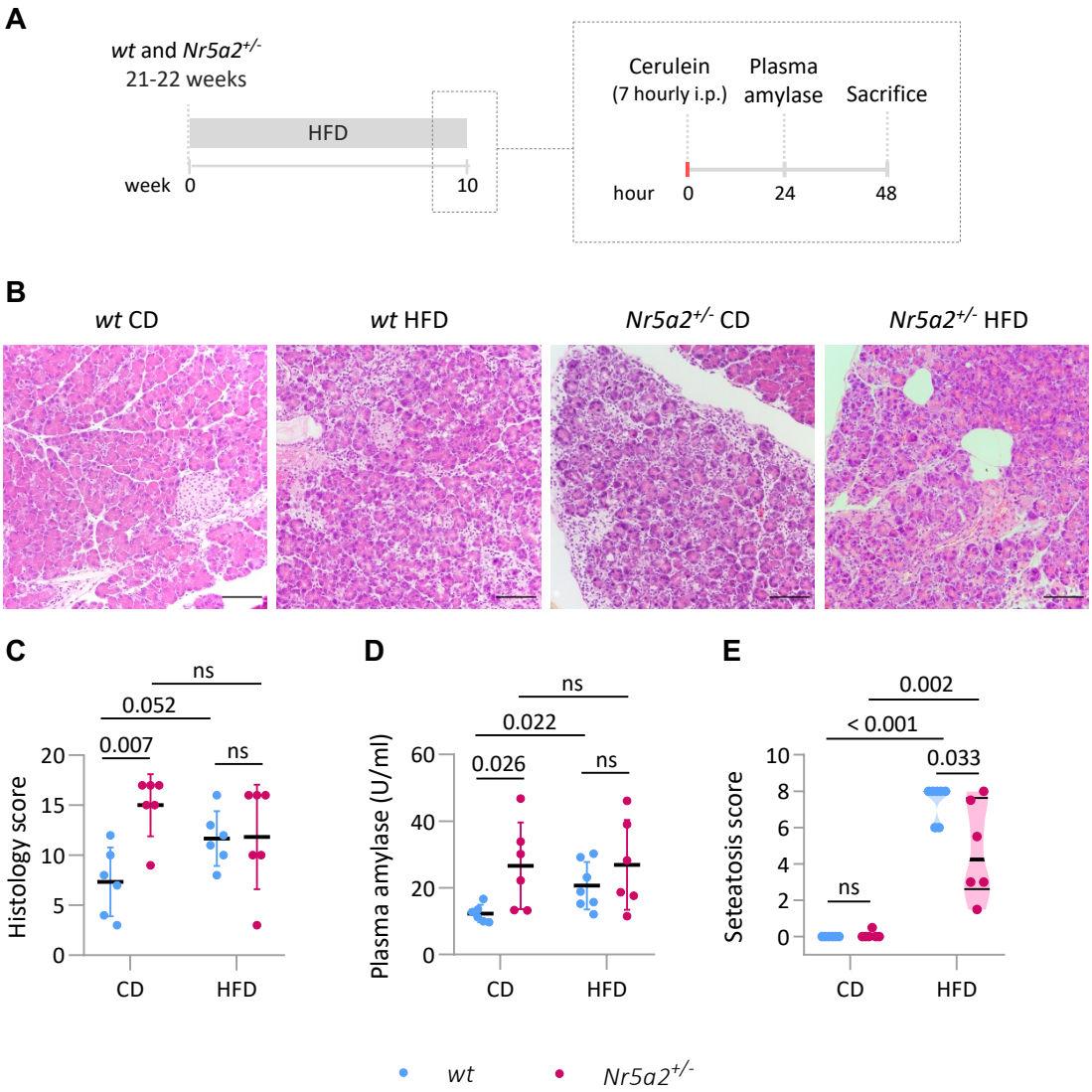


**Figure R3: *Nr5a2* heterozygosity does not cooperate with HFD-induced pancreatic inflammation. (A)** Experimental timeline: *wt* and *Nr5a2*$^{+/-}$ mice were fed a HFD or a CD and exposed to seven hourly injections of cerulein (50 µg/kg) at week 10. **(B)** Representative images of pancreas sections, 48 h post-pancreatitis induction. Scale bar: 200 µm. **(C)** Histological scores (0-18) of pancreas sections, as described in methods. Data is presented as mean ± SD. **(D)** Plasma amylase levels, 24 h post-pancreatitis induction. **(E)** Violin plot showing liver steatosis scores based on the abundance of micro- and macro-steatosis, as described in methods. Statistical significance was calculated using Mann Whitney test (n = 6-7/group). P-values > 0.100 are reported as ns. HFD, high fat diet; CD, control diet.

.

# CHAPTER II

# Role of the gut microbiome in pancreatic inflammation in *Nr5a2*$^{+/-}$ mice

## 2.1. ABX-mediated gut microbiome depletion protects *Nr5a2*$^{+/-}$ mice from cerulein-induced pancreatic damage

To determine whether the gut microbiome contributes to the pancreatic inflammatory phenotype of *Nr5a2*$^{+/-}$ mice, we assessed the effect of inducing a mild AP in mice that received an ABX cocktail known to deplete the gut microbial flora (Fig. 9A). The gut microbiome regulates inflammation in multiple tissues (Al Bander *et al.*, 2020). Since *Nr5a2*$^{+/-}$ mice are sensitised to the effects of cerulein administration, we aimed at identifying whether their exacerbated response to cerulein-induced AP was dependent on the presence of the gut microbiome.

We depleted the gut flora by oral administration of broad-spectrum ABX using a published protocol (Reikvam *et al.*, 2011). This consisted of three days of oral gavage with amphB – an antifungal substance used to suppress overgrowth of *Candida* species - followed by five days of oral gavage with an ABX/antifungal concoction composed of vancomycin, neomycin, metronidazole and amphB. From day three on, ampicillin was added to drinking water. Mice that followed this procedure will be referred to as ABX-treated mice. Experimental controls were administered normal drinking water ($H_2O$). As expected, ABX treatment led to successful and sustained depletion of gut bacteria, as indicated by 16S DNA quantification in feces at day 24 (Fig. R4B).

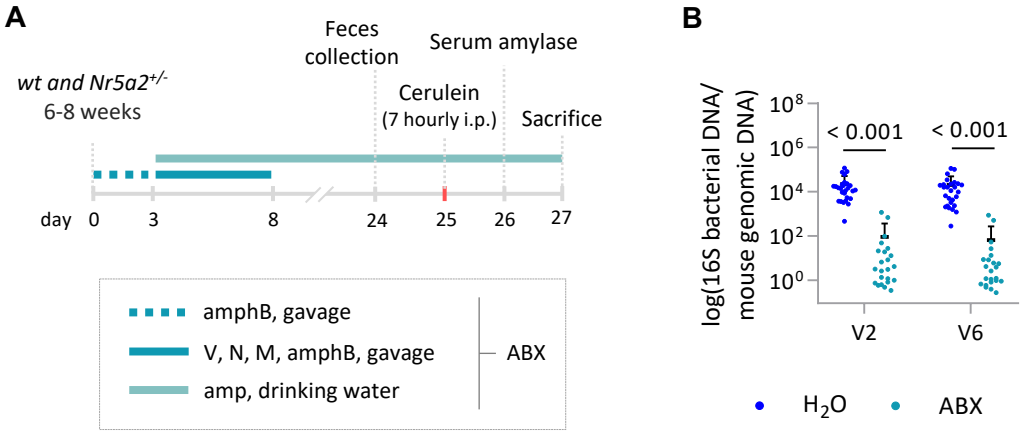


**Figure R4: Exploring the role of the gut microbiome in cerulein-induced pancreatic damage using broad-spectrum ABX. (A)** Experimental timeline: 6-8 week old *wt* and *Nr5a2*$^{+/-}$ mice received ABX and were exposed to seven hourly injections of cerulein (50 µg/kg). Effects on exocrine pancreas were assessed by measuring serum amylase levels at 24 h and through histologic analysis of the pancreas at 48 h. Controls received $H_2O$. **(B)** Bacterial DNA load in fecal pellets: 16S ribosomal DNA was determined by quantitative PCR amplification of the V2 and V6 regions, normalised to mouse genomic DNA. Graph shows log-transformed means ± SD. Statistical significance was calculated using Mann Whitney test (n = 23-27/group). V, vancomycin; N, neomycin; M, metronidazole; amphB, amphotericin B; amp, ampicillin; ABX, antibiotics.

Prior to exploring the effects of ABX treatment upon AP induction in cerulein-treated mice, saline controls were used to determine the effects of the ABX cocktail on the pancreas in basal conditions. Histological analysis of the pancreas did not reveal any alterations upon ABX treatment in mice of either genotype (Figs. R5A, R5B, R5C). Serum amylase levels were not significantly different in ABX-treated *wt* mice compared to untreated controls ($P_{wt}$ = 0.126), while a mild - but significant - increase was detected in *Nr5a2*$^{+/-}$ mice (Fig. R5D). These results indicate that ABX-mediated gut microbiome depletion does not cause major alterations on the exocrine pancreas in basal conditions. Representative images of pancreas sections are shown in Fig. R5A. We then assessed the effects of AP induction in ABX-treated and control mice of both genotypes. Cerulein administration to *wt* and *Nr5a2*$^{+/-}$ mice not treated with ABX resulted in a significant increase in histopathological scores (Figs. R6B and R6D) and serum amylase levels (Fig. R6E). Both pancreatic damage (Figs. R6B and R6D) and serum amylase levels (Fig. R6E) were significantly higher in *Nr5a2*$^{+/-}$ mice compared to their *wt* counterparts, confirming that *Nr5a2* heterozygosity sensitises to pancreatic inflammation.

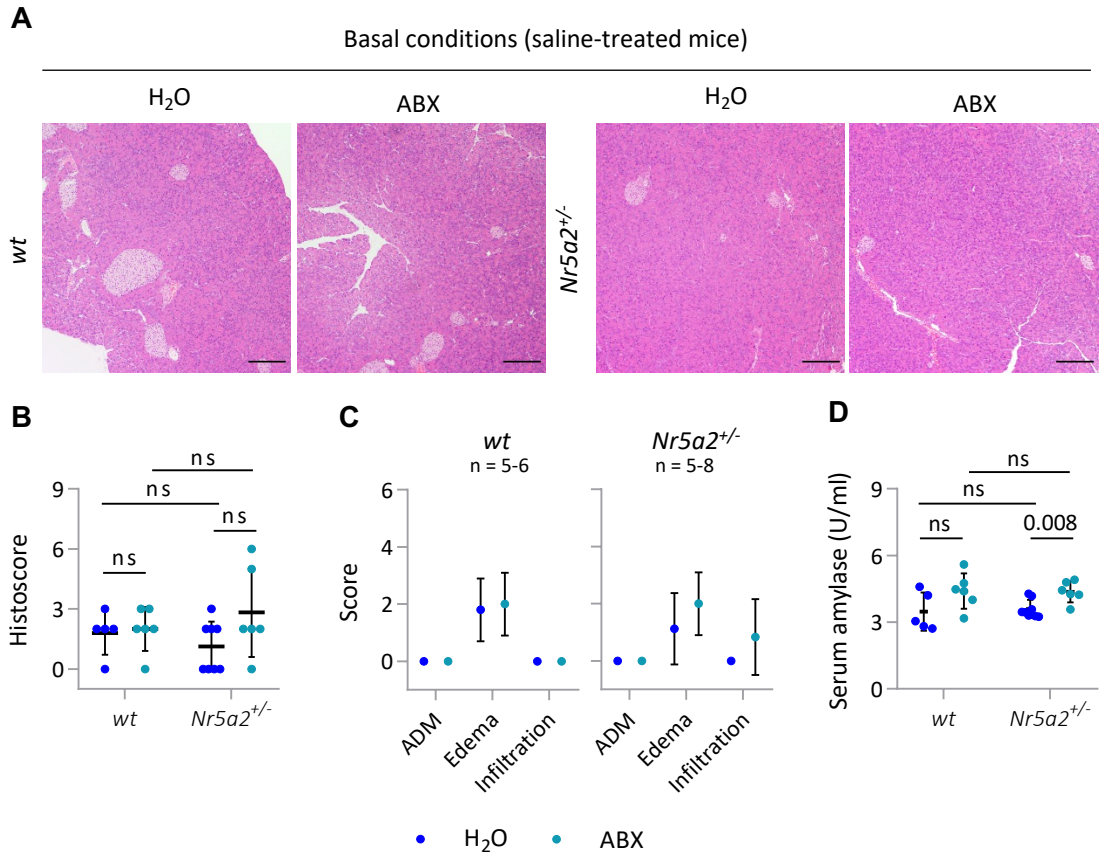


**Figure R5: ABX administration has no major effects on pancreas histology and basal serum amylase levels.** Effects of ABX administration on the histology of the pancreas (see timeline in Fig. R4A). **(A)** Representative images of pancreas sections showing no alterations. **(B)** Histological scores (0-18) of pancreas sections, as described in methods. Scale bar: 200 µm. **(C)** ADM, edema and leukocyte infiltration individual scores (0-6). **(D)** Serum amylase levels. B, C, D show means ± SD (n = 5-8 mice/group). Statistical significance was calculated using Mann Whitney test. P-values > 0.100 are reported as ns. V, vancomycin; N, neomycin; M, metronidazole; amphB, amphotericin B; amp, ampicillin; ABX, antibiotics.

Next, we evaluated the effect of AP induction in ABX-treated mice. In *wt* mice that were exposed to cerulein-induced AP, the histopathological scores were significantly higher than in saline-treated mice (Figs. R6C and R6D), but serum amylase levels were not significantly increased (Fig. R6F). In contrast, in *Nr5a2*$^{+/-}$ mice that had received ABX prior to AP induction, neither histopathological scores (Figs. R6C and R6D) nor serum amylase levels (Fig. R6F) were significantly different than in saline controls. These results indicate that ABX-mediated gut microbiome depletion protects *Nr5a2*$^{+/-}$ mice from cerulein-induced damage. Representative images of pancreas sections are shown in Fig. R6A.

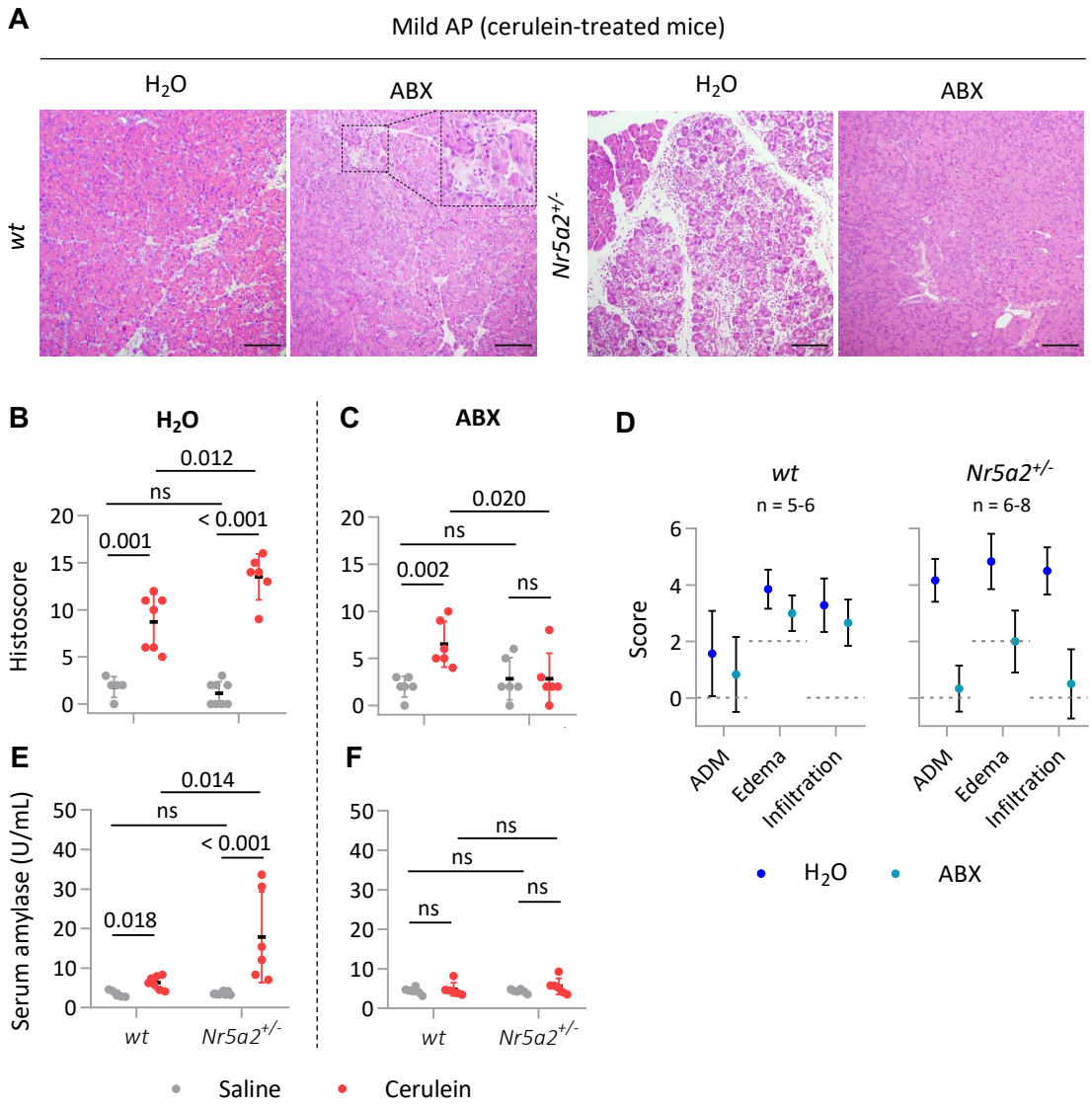


**Figure R6: ABX-mediated gut microbiome depletion protects *Nr5a2*$^{+/-}$ mice from cerulein-induced mild acute pancreatic damage.** Effects of ABX administration on exocrine pancreas during mild AP (see timeline in Fig. R4A). **(A)** Representative images of pancreas sections at 48 h post AP induction: a noticeable reduction in histologic damage is observed in ABX-treated *Nr5a2*$^{+/-}$ mice compared to controls. Zoomed section shows a cell-infiltrated area. Scale bar: 200 µm. **(B, C)** Histological scores (0-18) of pancreas sections, as described in methods. **(D)** ADM, edema and leukocyte infiltration individual scores (0-6). Dashed line shows representative basal histoscore. **(E, F)** Serum amylase levels at 24 h post AP induction. Data is presented as mean ± SD. Statistical significance was calculated using Mann Whitney test (n = 5-8/group). P-values > 0.100 are reported as ns. AP, acute pancreatitis; ABX, antibiotics.

To determine whether ABX treatment also rescued mice from a more severe pancreatitis, mice were exposed to seven hourly cerulein injections on two non-consecutive days (Fig R7A). I confirmed that ABX treatment led to successful microbiome depletion (Fig. R7B). Mice of both genotypes that were administered ABX and then exposed to severe AP, displayed a non-significant reduction in histopathological scores, but these did not reach the scores expected for mice in basal conditions (Fig. R7C). These results suggest that

ABX-mediated microbiome depletion only leads to partial protection from cerulein-induced severe AP.

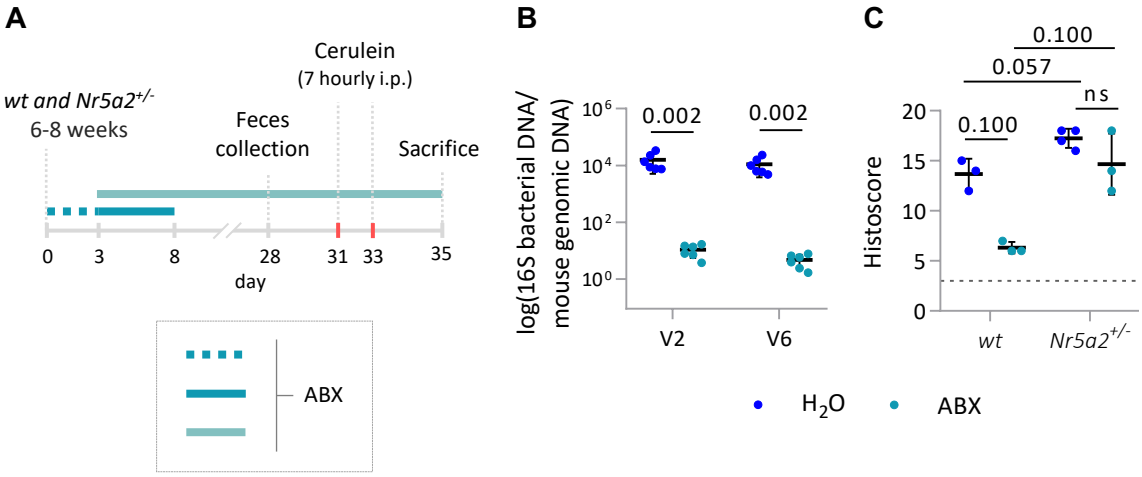


**Figure R7: ABX treatment results in partial protection from severe cerulein-induced damage. (A)** Experimental timeline: A severe AP was induced in ABX-treated (ABX) and control mice ($H_2O$) by seven hourly injections of cerulein (50 µg/kg) on days 0 and 2. Mice were sacrificed at 48 h. **(B)** Bacterial DNA load in fecal pellets. 16S ribosomal DNA was determined by quantitative PCR amplification of the V2 and V6 regions, **(Fig. R7 cont.)** normalised to mouse genomic DNA. Graph shows log-transformed means ± SD, n = 6/group. **(C)** Histological scores (0-18) for pancreas sections at 48 hours post induction, as described in methods. Dashed line shows representative basal histoscore. Graph shows means ± SD (n = 3-4/group). Statistical significance was calculated using Mann Whitney test. P-values > 0.100 are reported as ns. AP; acute pancreatitis.

To demonstrate that the protective effects described above were indeed mediated by gut microbiome depletion, we evaluated the effects of cerulein on ABX-treated *Nr5a2*$^{+/-}$ mice upon gut microbiome reconstitution (Fig. R8A). This was achieved by administering ABX for eight days, followed by three weeks of cohousing with mice reared in conventional conditions. This approach has been consistently reported as a successful method for rapid microbiome reconstitution (Liang *et al.*, 2020). Given that we did not find major differences among male and female mice in the experiments described above (data not shown), and to facilitate cohousing, only *Nr5a2*$^{+/-}$ females were used. Consistent with the above-mentioned results, *Nr5a2*$^{+/-}$ mice that had received ABX prior to AP induction displayed reduced histopathological scores (Fig. R8C) and plasma amylase levels (Fig. R8D) compared to untreated controls. In contrast, *Nr5a2*$^{+/-}$ mice in which the gut microbiome had been reconstituted after ABX treatment, cerulein administration led to an increase in both the histopathological scores (Fig. R8C) and plasma amylase concentration (Fig. R8D). Microbiome reconstitution required interruption of the ampicillin treatment (from day eight onwards, Fig. R8A); therefore, the

ABX-treated and reconstituted groups did not receive the exact same ABX treatment regimen. To control for this difference, I also evaluated the effects of mild AP in mice that received only maintenance ampicillin treatment. No significant differences were detected between cerulein-induced untreated, ampicillin-treated and reconstituted mice. These results provide strong evidence that the effect of ABX on the severity of pancreatitis is mediated by gut microbiome depletion. Representative images of pancreas sections are shown in Fig. R8B.

Together, the results described above indicate that ABX-mediated gut microbiome depletion protects *Nr5a2*$^{+/-}$ mice from cerulein-induced pancreatic damage.

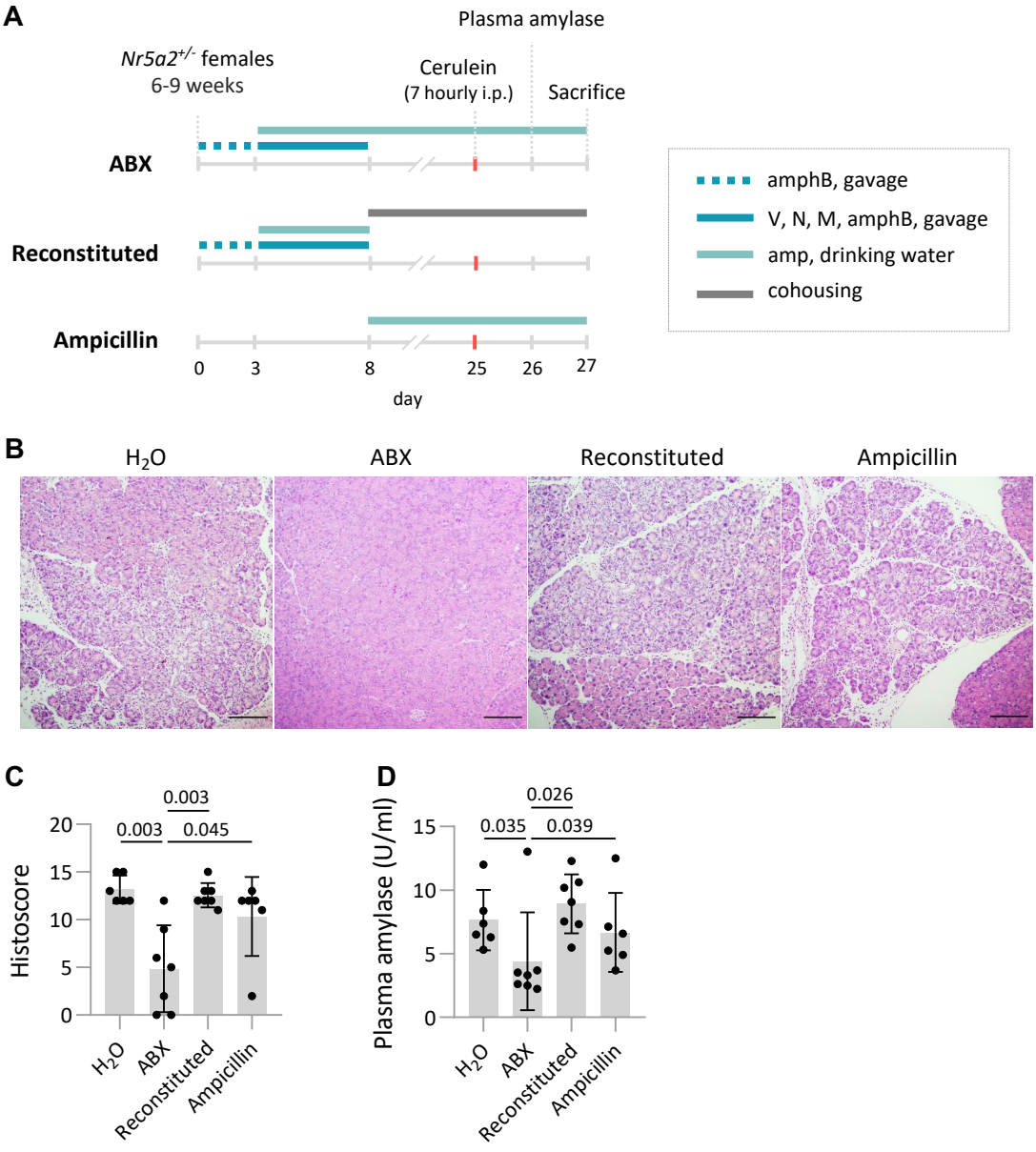

**Figure R8** (see on previous page)**: Gut microbiome reconstitution restores the sensitivity of *Nr5a2*$^{+/-}$ mice to cerulein-induced pancreatic damage. (A)** Experimental timeline: *Nr5a2*$^{+/-}$ females were subjected to tree different procedures: ABX administration (ABX), ABX administration and microbiome reconstitution by cohousing with untreated *Nr5a2*$^{+/-}$ mice (reconstituted) or ampicillin administration (ampicillin). Mice were subjected to seven hourly injections of cerulein (50 µg/kg) and their response was compared to that of $H_2O$ treated mice. **(B)** Representative images of pancreas sections show a notorious increase in tissue damage upon microbiome reconstitution. **(C)** Serum amylase levels at 24 h post induction. Scale bar: 200µm. **(D)** Histological scores (0-18) of pancreas sections at 48 h post-induction, as described in methods. Data is presented as mean ± SD. Statistical significance is calculated using Mann Whitney test, n = 6-7/group. P-values > 0.100 are not reported. V, vancomycin; N, neomycin; M, metronidazole; amphB, amphotericin B; amp, ampicillin.

## 2.2. *Nr5a2* heterozygosity does not promote pancreatic inflammation by increasing the abundance of intrapancreatic bacteria

Intestinal bacteria have been reported to contribute to pancreatic disease by translocating to the pancreas and directly influencing the pancreatic microenvironment (Pushalkar *et al.*, 2018; Aykut *et al.*, 2019; Riquelme *et al.*, 2019). Intestinal barrier dysfunction has been proposed as the initial phenomenon responsible for this process. Since NR5A2 is expressed in intestinal epithelial cells and participates in intestinal homeostasis (Fernandez-Marcos, Auwerx and Schoonjans, 2011; Bayrer *et al.*, 2018), and our experiments were conducted on mice that had germline heterozygosity, we hypothesised that intestinal haploinsufficiency could contribute to pancreatic inflammation in *Nr5a2*$^{+/-}$ mice by increasing the permeability of the gut epithelium and bacterial migration to the pancreas.

To determine whether germline *Nr5a2* heterozygosity compromises the intestinal barrier, we evaluated gut permeability to FITC-dextran in basal conditions and during mild AP, as depicted in Fig. R9A. Four hours after oral administration, plasma FITC dextran levels were comparable across genotypes and conditions (i.e. mice in basal conditions vs AP, Fig. R9B), supporting the notion that neither *Nr5a2* heterozygosity nor our model of pancreatitis induction compromise the permeability of the gut epithelium. In line with these results, no changes in bacterial abundance – quantified by FISH using a 16S rRNA probe – were detected across groups (Figs. R9C and R9D), suggesting that the higher pancreatic damage observed in *Nr5a2*$^{+/-}$ mice does not result from an increased bacterial translocation to the pancreas.

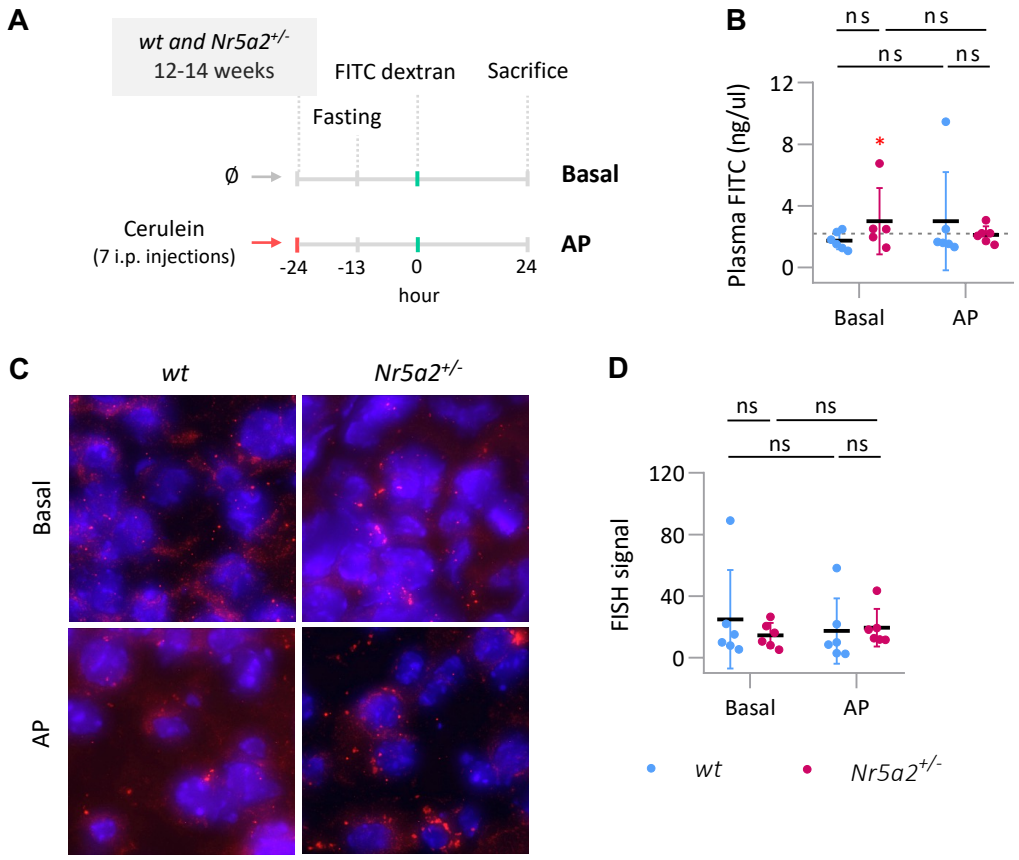


**Figure R9: *Nr5a2*$^{+/-}$ mice display a functional intestinal barrier and normal bacterial abundance in the pancreas. (A)** Experimental timeline to evaluate gut permeability in *wt* and *Nr5a2*$^{+/-}$ mice in basal conditions and during a mild AP, assessed through the administration of FITC dextran (440 mg/kg) by oral gavage, followed by FITC quantification in plasma at 4 h. Data in basal conditions and pancreatitis correspond to two independent experiments. **(B)** Plasma FITC dextran levels 4 h after oral administration. **(C)** Representative FISH images of pancreas sections using a 16S ribosomal RNA fluorescent probe. **(D)** Quantification of FISH signal. Data is presented as mean ± SD. Statistical significance is calculated using Mann Whitney test (n = 6/group). P-values > 0.100 are reported as ns. * = Outlier removed since value > 3xSD.

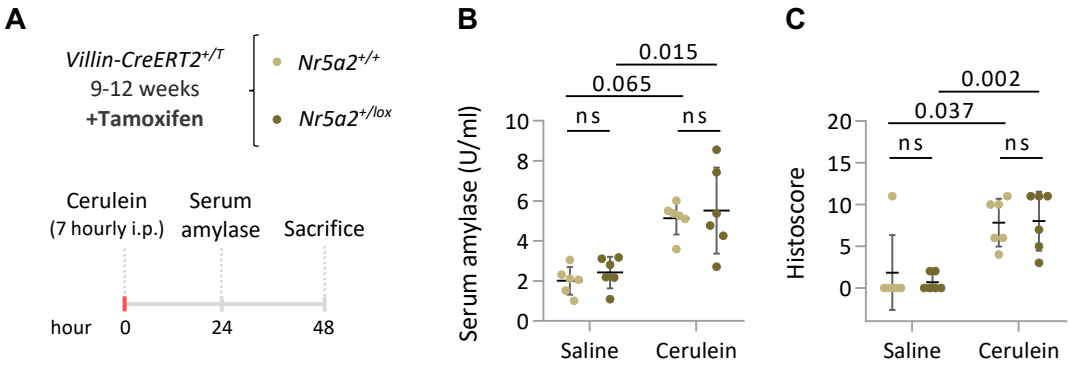


**Figure R10: *Nr5a2* heterozygosity in the gut epithelium does not sensitise mice to the effects of cerulein-induced damage. (A)** Experimental timeline: Tamoxifen treated *Villin-CreERT*$^{+/T}$*; Nr5a2*$^{+/+}$ or *Villin-CreERT*$^{+/T}$*; Nr5a2*$^{+/-}$ were exposed to mild AP by seven hourly injections of cerulein (50 µg/kg). **(B)** Serum amylase levels at 24 h. **(C)** Histological scores (0-18) for pancreas sections at 48 h, as described in methods. Data is presented as mean ± SD. Statistical significance was calculated using Mann Whitney test (n = 6/group=. P-values > 0.100 are reported as ns. AP; acute pancreatitis.

## 2.3. *Nr5a2*$^{+/-}$ mice display a normal fecal microbiome composition and diversity

The above-mentioned experiments were performed with cohoused *wt* and *Nr5a2*$^{+/-}$ littermates, a practice that is well known to homogenise the gut microbiota (Liang *et al.*, 2020). However, since our results indicate that cerulein-induced pancreatic damage in *Nr5a2*$^{+/-}$ mice relies on the presence of the gut microbiome and an association between certain gut microbiome signatures and pancreatic disease has been reported (Riquelme *et al.*, 2019; Kartal *et al.*, 2022), we aimed at identifying whether *Nr5a2*$^{+/-}$ mice had a distinct microbiome composition that could explain their increased sensitivity to pancreatic inflammation.

We profiled fecal microbiomes from cohoused *wt* (n = 10) and *Nr5a2*$^{+/-}$ (n = 10) mice by 16S ribosomal DNA gene (16S rDNA) sequencing. Reads were used to construct unique "amplicon sequence variants" (ASVs). After normalization to median sequencing depth, we did not detect significant differences in alpha (within sample) and beta (across sample) diversity between genotypes (Fig. R11A and R11B). After correcting for multiple testing, differential abundance analysis using DEseq2 led to the identification of a single ASV that was overrepresented in the *wt* microbiota (ASV1) and two ASVs that were overrepresented in the *Nr5a2*$^{+/-}$ microbiome (ASV2 and ASV3) (Fig. 11C). None of these ASVs was resolved at the species level. ASV1 and ASV2 belonged to the *Muribaculaceae* family and differed in a single nucleotide, while ASV3 belonged to the *Rikenella* genus.

To further compare the fecal microbiome composition of *wt* and *Nr5a2*$^{+/-}$ mice, I also computed alpha and beta diversity measures and performed differential abundance analysis at different taxonomic levels (i.e. species, genus, family, order, class and phylum). There were no significant differences in microbial diversity and taxon abundance between genotypes at any taxonomic resolution.

These results indicate that the composition of the fecal microbiome is comparable across genotypes, suggesting that the increased sensitivity of *Nr5a2*$^{+/-}$ mice to pancreatic inflammation does not result from the presence of a pro-inflammatory microbiome.

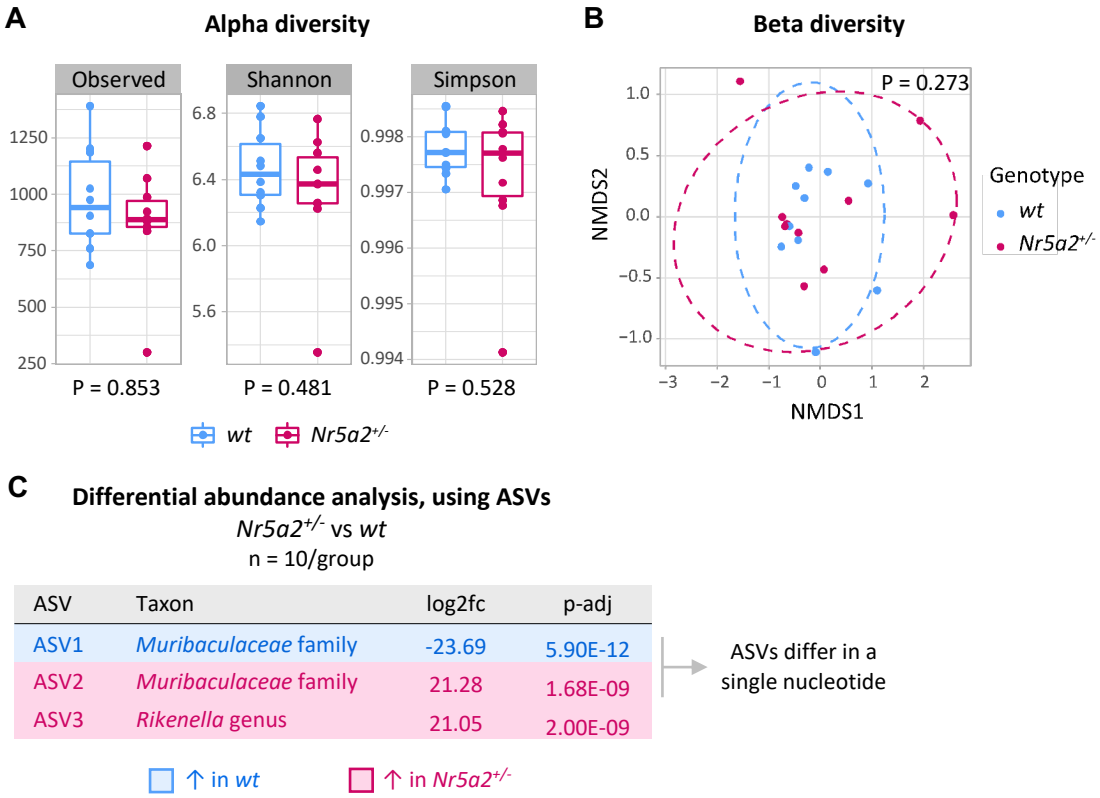


**Figure R11: *Nr5a2*$^{+/-}$ mice display a normal fecal microbiome composition and diversity.** The microbiota from *wt* (n = 10) and *Nr5a2*$^{+/-}$ mice (n = 10) mice in basal conditions was profiled by 16S rDNA sequencing of fecal samples. **(A)** Alpha diversity analysis (i.e. within sample diversity based on species richness and evenness) with the most common indices. Boxplots represent median, first and third quartile. Whiskers show minimum and maximum spread. Significance was calculated using Mann Whitney test. **(B)** Beta diversity analysis (i.e. between sample diversity) with Bray non-metric multidimensional scaling (NMDS). Statistical significance was calculated using PERMANOVA with 999 permutations. Ellipses represent 95% confidence interval. **(C)** DESeq2 differential abundance analysis of ASVs in *Nr5a2*$^{+/-}$ vs *wt* mice resulted in the identification of one ASV that was significantly overrepresented in *wt* mice (blue) and two that were significantly overrepresented in *Nr5a2*$^{+/-}$ mice (purple), using a significance threshold of p-adj < 0.05. No differentially abundant taxa were found upon agglomeration of ASVs by species, genus, family, order, class or phylum (data not shown).

## 2.4. Horizontal transmission factors are not responsible for the *Nr5a2*$^{+/-}$ phenotype

To obtain additional evidence for the absence of a distinct pro-inflammatory microbiota in *Nr5a2*$^{+/-}$ mice, we compared the effects of inducing a pancreatitis in *Nr5a2*$^{+/-}$ and *wt* mice that had been either cohoused or separated by genotype for three months (Fig. R12A). While cohousing homogenises the gut microbiomes, separate breeding was reported to result in progressive divergence in bacterial composition (Liang *et al.*, 2020). I did not find significant differences in the severity of cerulein-induced pancreatitis between cohoused and separately bred mice regardless of genotype, strongly suggesting that the *Nr5a2*$^{+/-}$ phenotype is not transferred to *wt* mice upon cohousing

(Fig. R12B). These results further support the notion that horizontal transmission factors (i.e. microbes) are not responsible for the increased sensitivity to pancreatic damage observed in *Nr5a2*$^{+/-}$ mice.

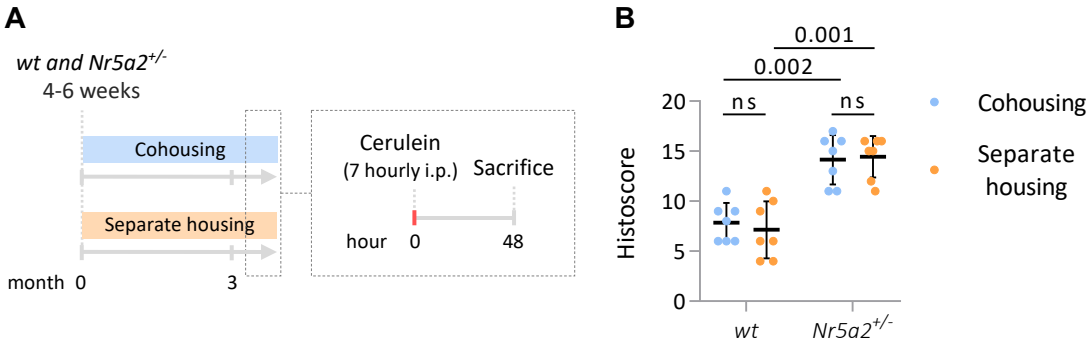


**Figure R12: Microbiome homogenization through cohousing of *Nr5a2*$^{+/-}$ and *wt* mice does not modulate the severity of a mild AP. (A)** Experimental timeline: *Nr5a2*$^{+/-}$ and *wt* mice were cohoused or separated by genotypes for three months. Mice underwent a mild acute pancreatitis with seven hourly injections of cerulein (50 µg/kg). **(B)** Histological scores (0-18) for pancreas sections at 48 hours, as described in methods. Data is presented as mean ± SD. Statistical significance is calculated using Mann Whitney test (n = 7/group). AP; acute pancreatitis.

## 2.5. An exploratory analysis identifies bacterial taxa that may predispose to cerulein-induced pancreatic damage in *wt* and *Nr5a2*$^{+/-}$ mice

To identify bacterial taxa that may predispose *wt* and *Nr5a2*$^{+/-}$ to increasing levels of pancreatic damage, I took advantage of the fact that some of the mice used to analyse the gut microbiome were later used for the experiment depicted in Fig. R4A. I compared the gut microbiome from *wt* mice that experienced higher damage (n=3) to those with lower damage (n=3), as determined from the histological damage scores. Differential abundance analysis revealed a predominance of phyla *Deferribacterota* and *Desulfobacterota*, classes *Desulfovibrionia* and *Deferribacteres*, family *Deferribacteracea* and genus *Lachnospiraceae*, *Bilophila* and *Mucispirillum* in high-damage *wt* mice, while low-damage mice were enriched in phyla *Proteobacteria* and *Verrucomicrobiota*, class *Verrucomicrobiae* and genus *[Eubacterium] ventriosum* group (Fig. R13A). On the other hand, differential abundance analysis at different taxonomic levels between high damage (n = 2) and low damage (n = 2) *Nr5a2*$^{+/-}$ mice revealed a predominance of *Acholaplasmataceae* and *Turicibacter* at the family and genus level, in high damage *Nr5a2*$^{+/-}$ mice (Fig. R13B). A taxonomic tree of differentially abundant taxa is depicted in Fig. R13C.

**A**

**Differential abundance analysis**
*wt* high (n = 3) vs *wt* low (n = 3)

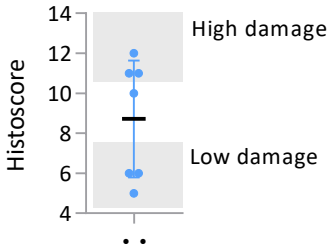


| Level | Taxon | log2fc | p-adj |
|---|---|---|---|
| Phylum | *Proteobacteria* | -2.6 | 0.012 |
| Phylum | *Verrucomicrobiota* | -1.9 | 0.026 |
| Class | *Verrucomicrobiae* | -1.8 | 0.018 |
| Genus | *[Eubacterium] ventriosum group* | -21.1 | 3.540E-06 |
| Phylum | *Desulfobacterota* | 1.2 | 0.003 |
| Phylum | *Deferribacterota* | 2.7 | 0.012 |
| Family | *Deferribacteraceae* | 3.3 | 0.005 |
| Class | *Desulfovibrionia* | 1.5 | 0.001 |
| Class | *Deferribacteres* | 3.0 | 0.006 |
| Genus | *Lachnospiraceae A2* | 21.0 | 3.540E-06 |
| Genus | *Bilophila* | 7.0 | 0.003 |
| Genus | *Mucispirillum* | 3.0 | 0.043 |

↑ in *wt* high ↑ in *wt* low

**B**

**Differential abundance analysis**
*Nr5a2*$^{+/-}$ high (n = 2) vs *Nr5a2*$^{+/-}$ low (n = 2)

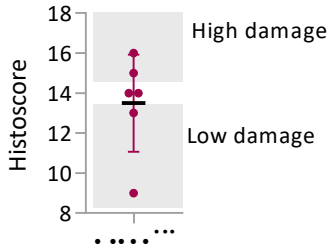


| Level | Taxon | log2fc | p-adj |
|---|---|---|---|
| Family | *Acholeplasmataceae* | 7.5 | 0.048 |
| Genus | *Turicibacter* | 9.5 | 0.008 |

↑ in *Nr5a2*$^{+/-}$ high

**C**

**Phylogenetic tree of the identified taxa**

| Phylum | Class | Order | Family | Genus |
|---|---|---|---|---|
| *Firmicutes* | *Bacilli* | *Erysipelotrichales* | *Erysipelotrichaceae* | *Turicibacter* |
| | | *Acholeplasmatales* | *Acholeplasmataceae* | |
| | *Clostridia* | *Lachnospirales* | *Lachnospiraceae* | *A2* |
| | | | | *[Eubacterium] ventriosum group* |
| *Desulfobacterota* | *Desulfovibrionia* | *Desulfovibrionales* | *Desulfovibrionaceae* | *Bilophila* |
| *Deferribacterota* | *Deferribacteres* | *Deferribacterales* | *Deferribacteraceae* | *Mucispirillum* |
| *Proteobacteria* | | | | |
| *Verrucomicrobiota* | *Verrucomicrobiae* | | | |

↑ in *wt* high ↑ in *wt* low ↑ in *Nr5a2*$^{+/-}$ high

**Figure R13: An exploratory analysis identifies bacterial taxa that may predispose to cerulein-induced pancreatic damage in *wt* and *Nr5a2*$^{+/-}$ mice.** Following gut microbiome profiling, *wt* and *Nr5a2*$^{+/-}$ mice were exposed to cerulein-induced mild AP, meaning that the microbial composition could be associated to their response to pancreatic damage**.** Differential abundance analysis with DESeq2 was performed to compare mice of either genotype displaying the highest pancreatic histoscores (high damage) with those that displayed the lowest histoscores (low damage). Differential abundance analysis were performed at each taxonomic level. Tables display taxa that were found to be differentially abundant at p-adj < 0.05 in **(A)** *wt* **(Fig. R13 cont.)** (n = 3/group) and **(B)** *Nr5a2*$^{+/-}$ mice (n = 2/group). **(C)** Phylogenetic tree of the identified taxa. Log2FC: $\log_2$ fold-change. AP; acute pancreatitis.

To investigate whether the identified taxa associated with high pancreatic damage were consistent across genotypes, we explored the enrichment of differentially abundant taxa in *wt* and *Nr5a2*$^{+/-}$ mice. These analysis revealed an inconsistency between genotypes: taxa that were significantly enriched in one direction (i.e. high or low damage) in *wt* mice displayed a non-significant trend in the opposite direction in *Nr5a2*$^{+/-}$ mice (Fig. R14). The only exception was the family *Acholeplasmataceae*, which was significantly enriched in high damage *Nr5a2*$^{+/-}$ ($log_2$ fold-change = 7.47; p-adj = 0.048) and displayed the same trend in high damage *wt* mice ($log_2$ fold-change = 1.88; p-adj = 0.844) (Fig. R14).

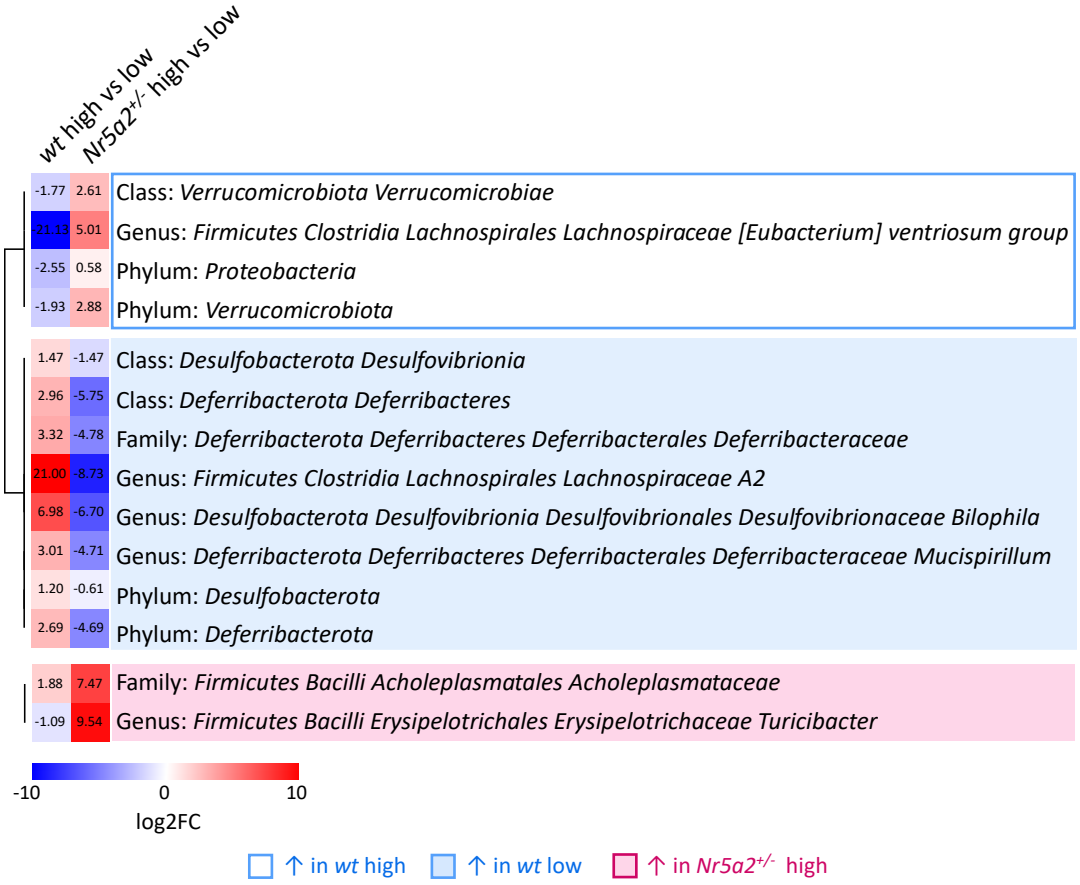


**Figure R14: Enrichment of differentially abundant taxa across genotype.** Heatmap of the log2 fold changes obtained in DESeq2 differential abundance analyses from high vs low damage *wt* and high vs low damage *Nr5a2*$^{+/-}$ mice. Graph shows taxa whose abundance was significantly different (p-adj < 0.05) in at least one comparison.

While exploratory, these analyses suggest that specific bacterial taxa may predispose *wt* and *Nr5a2*$^{+/-}$ to cerulein-induced pancreatic damage. In addition, these results suggest that *wt* and *Nr5a2*$^{+/-}$ may differ in their sensitivity to bacterial taxa. However, these findings need to be replicated in independent experiments and with increased sample size.

## 2.6. Transcriptomic effects of ABX-mediated gut microbiome depletion in mouse pancreas

To dissect the molecular mechanisms through which ABX-mediated microbiome depletion protects *Nr5a2*$^{+/-}$ mice from cerulein-induced pancreatic damage, we performed a comprehensive RNA-seq analysis on total pancreas from *wt* and *Nr5a2*$^{+/-}$ mice, receiving either ABX or $H_2O$, in basal conditions and during AP (n = 3/group; Fig. R15A). $H_2O$-treated mice were used as controls to explore the transcriptomic effects of ABX administration, and mice in basal conditions were used as experimental controls to assess the effects of AP induction. To assess intra and intergroup variability and to detect possible outliers, we performed a correlation analysis across samples. This revealed Pearson correlation coefficients (r) values above 0.99 between replicates, with the exception a sample from the *Nr5a2*$^{+/-}$ ABX basal group, which was considered an outlier and excluded from the dataset (Fig. R15B). Principal component analysis (PCA) representation of the remaining samples is shown in Fig. R15C.

Global transcriptomic changes across conditions were evaluated by performing differential gene expression and GSEA using the Gene Ontology Biological Processes, KEGG and Reactome databases. To overcome the limitations derived from the low number of differentially expressed genes (DEGs) detected in some comparisons, GSEA was performed using pre-ranked gene lists, in which genes are ranked based on log2-fold change rather than significance. Due to the large number of deregulated pathways detected, a highly restrictive threshold of FWER p-val < 0.05 was used to establish significance, unless otherwise stated.

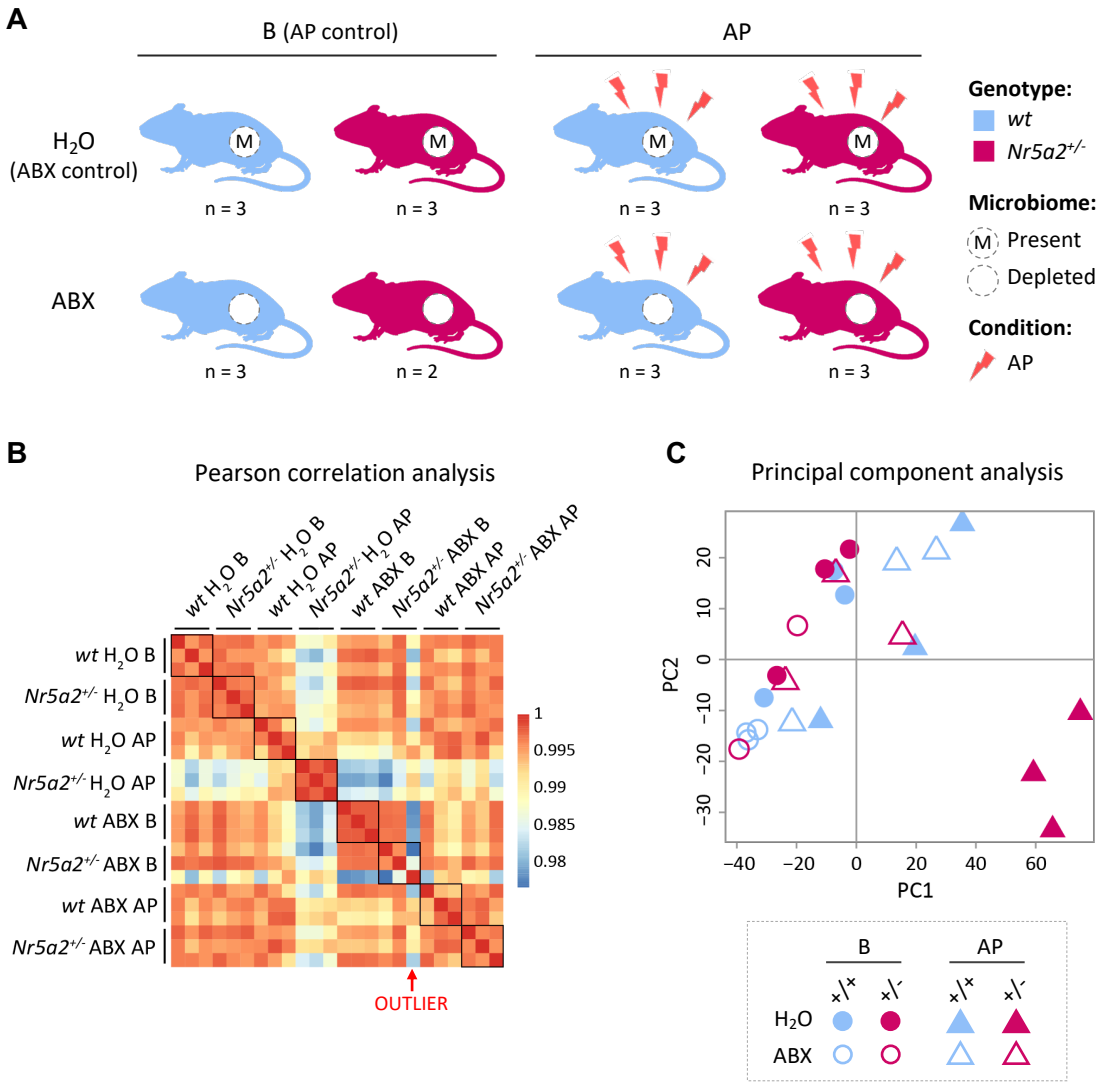


**Figure R15: Overview of the RNA-sequencing experiment performed to assess the transcriptomic effects of ABX-mediated gut microbiome depletion in basal conditions and during pancreatitis**. **(A)** Experimental conditions used to assess the transcriptomic effects of ABX-mediated gut microbiome depletion in basal conditions and upon induction of a cerulein mild AP (see timeline on Fig. R4A). **(B)** Heatmap representing Pearson correlation coefficients between samples; an outlier belonging to the *Nr5a2*$^{+/-}$ ABX B group can be pointed out. Scale bar represents the range of the correlations (r) of rlog-transformed normalised counts with DESeq. **(C)** Principal component analysis, excluding the outlier. B, basal; AP, acute pancreatitis; ABX, antibiotics.

Through the analysis of these data we aimed to answer the following questions: 1) what are the transcriptomic effects of depleting the gut microbiome in basal conditions?, 2) what are the transcriptomic effects of inducing a mild AP in the presence of the gut microbiome?, 3) what are the transcriptomic effects of inducing a mild AP in the absence of the gut microbiome?, and 4) are pancreata from ABX and control mice transcriptomically different during AP?

### *What are the transcriptomic effects of depleting the gut microbiome in basal conditions?*

To explore the transcriptomic effects of depleting the gut microbiome in basal conditions, I performed differential expression and GSEA by comparing the transcriptome of ABX-treated vs. control mice of both genotypes (Fig R16A). Treatment with ABX induced transcriptomic alterations both in *wt* and *Nr5a2*$^{+/-}$ mice, although the effects were stronger in *wt* mice, possibly due to differences in the number of biological replicas: we found 400 DEGs and 252 enriched pathways in the pancreas of ABX-treated *wt* mice, while there were only 7 DEGs and 159 enriched pathways in ABX-treated *Nr5a2*$^{+/-}$ pancreata (Fig. R16B and R16C). At the gene level, a single gene was found to be up-regulated in mice of both genotypes (*Clec11a*), while no overlap in down-regulated genes was detected (Fig. R16D).

To assess whether gene set enrichment was consistent across genotypes, I represented the normalised enrichment scores (NES) of all pathways in each comparison (Fig. R16E). Eighty-two percent of the pathways analysed displayed the same directionality of regulation – either positive (12.1 %) or negative (69.4%) NES - in mice of both genotypes (Fig. R16E, see Q2 and Q3). In addition, all terms that were significantly deregulated in one of the two comparisons displayed the same directionality in the opposite one (Fig. 16E), indicating a high consistency in the transcriptomic effects of ABX treatment in *wt* and *Nr5a2*$^{+/-}$ mice. This was further confirmed using Cytoscape (Shannon *et al.*, 2003; data not shown), a platform that enables pathway enrichment analysis visualization and annotation: pathways that were deregulated by ABX treatment in *wt* and *Nr5a2*$^{+/-}$ mice referred to the same biological processes, as summarised in Fig. R16F. In short, treatment with ABX resulted in the up-regulation of pathways related to mitochondrial function, protein synthesis, and RNA metabolism and in the down-regulation of pathways related

**Figure R16** (see on next page)**: Transcriptomic effects of ABX-mediated gut microbiome depletion in basal conditions. (A)** Representation of the RNA-seq comparisons performed to explore the transcriptomic effects of depleting the gut microbiome in basal conditions. **(B)** Number of differentially expressed genes (DEGs) detected at p-adj < 0.05. **(C)** Number of enriched pathways detected at FWER pval < 0.05. **(D)** Venn diagram representing the overlap of up-regulated and down-regulated genes in *wt* and *Nr5a2*$^{+/-}$ pancreata. **(E)** Representation of normalised enrichment scores (NES) of all pathways in each comparison. **(F)** Representative pathways that were enriched in both *wt* and *Nr5a2*$^{+/-}$ pancreata. B, basal; AP, acute pancreatitis; ABX, antibiotics.

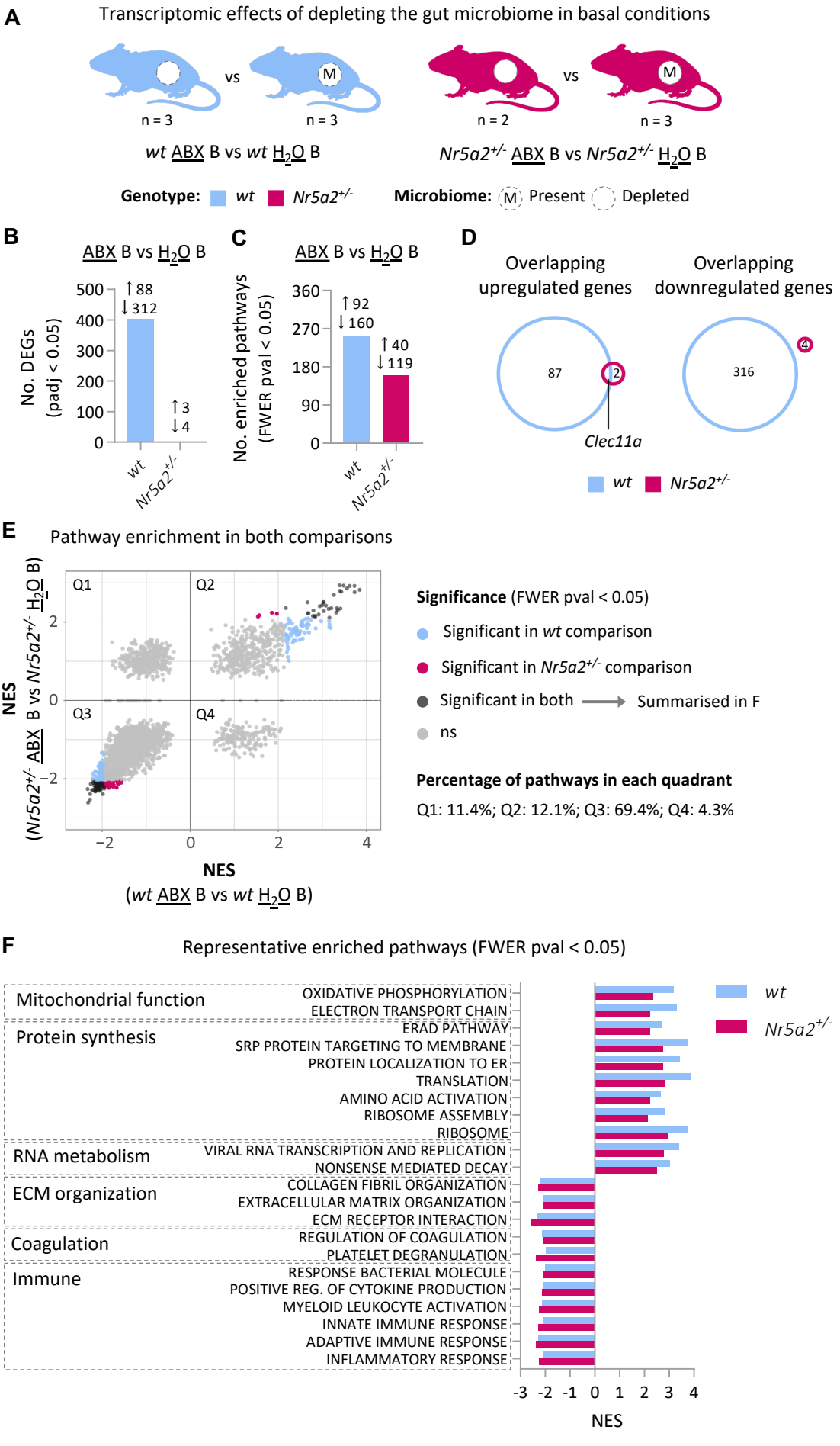
A
Transcriptomic effects of depleting the gut microbiome in basal conditions
vs
n = 3
n = 3
wt ABX B vs wt H2O B
vs
n = 2
n = 3
Nr5a2+/- ABX B vs Nr5a2+/- H2O B
Genotype: wt Nr5a2+/-
Microbiome: Present Depleted
B
ABX B vs H2O B
No. DEGs (padj < 0.05)
↑88 ↓312
↑3 ↓4
wt
Nr5a2+/-
C
ABX B vs H2O B
No. enriched pathways (FWER pval < 0.05)
↑92 ↓160
↑40 ↓119
wt
Nr5a2+/-
D
Overlapping upregulated genes
Overlapping downregulated genes
87
2
316
4
Clec11a
wt
Nr5a2+/-
E
Pathway enrichment in both comparisons
NES (Nr5a2+/- ABX B vs Nr5a2+/- H2O B)
Q1
Q2
Q3
Q4
NES (wt ABX B vs wt H2O B)
Significance (FWER pval < 0.05)
Significant in wt comparison
Significant in Nr5a2+/- comparison
Significant in both → Summarised in F
ns
Percentage of pathways in each quadrant
Q1: 11.4%; Q2: 12.1%; Q3: 69.4%; Q4: 4.3%
F
Representative enriched pathways (FWER pval < 0.05)
Mitochondrial function
OXIDATIVE PHOSPHORYLATION
ELECTRON TRANSPORT CHAIN
Protein synthesis
ERAD PATHWAY
SRP PROTEIN TARGETING TO MEMBRANE
PROTEIN LOCALIZATION TO ER
TRANSLATION
AMINO ACID ACTIVATION
RIBOSOME ASSEMBLY
RIBOSOME
RNA metabolism
VIRAL RNA TRANSCRIPTION AND REPLICATION
NONSENSE MEDIATED DECAY
ECM organization
COLLAGEN FIBRIL ORGANIZATION
EXTRACELLULAR MATRIX ORGANIZATION
ECM RECEPTOR INTERACTION
Coagulation
REGULATION OF COAGULATION
PLATELET DEGRANULATION
Immune
RESPONSE BACTERIAL MOLECULE
POSITIVE REG. OF CYTOKINE PRODUCTION
MYELOID LEUKOCYTE ACTIVATION
INNATE IMMUNE RESPONSE
ADAPTIVE IMMUNE RESPONSE
INFLAMMATORY RESPONSE
NES
wt
Nr5a2+/-

to extracellular matrix (ECM) organization, coagulation and – importantly - immune response. In addition, ABX administration led to the up-regulation of acinar signatures in both *wt* and *Nr5a2*$^{+/-}$ mice (data not shown).

Together, these results indicate that, at the transcriptomic level, ABX-mediated gut microbiome depletion has comparable anti-inflammatory effects both in *wt* and *Nr5a2*$^{+/-}$ mice.

### *What are the transcriptomic effects of inducing a mild AP in the presence of the gut microbiome?*

I then explored the transcriptomic effects of inducing a mild AP in the presence of the gut microbiome in mice of both genotypes (Fig. R17A, upper diagram). The transcriptomic changes resulting from cerulein administration were more profound in *Nr5a2*$^{+/-}$ mice, as expected from our previous work (Flandez *et al.*, 2014; Cobo *et al.*, 2018): 630 DEGs and 47 enriched pathways were identified in *wt* mice, compared with 6529 DEGs and 168 enriched pathways in *Nr5a2*$^{+/-}$ mice (Fig. R17B and R17C, see $H_2O$). In line with these findings, the transcriptome of pancreata from *Nr5a2*$^{+/-}$ mice upon AP displayed the lowest intergroup correlation coefficients (Fig. R14B) and clustered apart from all other samples in the PCA (Fig. R14C).

To explore the differences resulting from inducing a pancreatitis in *wt* and *Nr5a2*$^{+/-}$ mice, we represented gene set enrichment in both comparisons (Fig R17D). Seventy-six percent of the pathways displayed the same directionality of regulation in mice of the two genotypes, indicating an overall consistency in the transcriptomic changes (Fig. R17D, see Q2 and Q3). Accordingly, there was an up-regulation of immune pathways and down-regulation of amino acid metabolism independently of the genotype (Fig. R17D, see 2-7). In *Nr5a2*$^{+/-}$ pancreata, this was accompanied by the up-regulation of cell cycle pathways (Fig. R17D, see collapsed pathway curation 2). Interestingly, pancreatitis also had some opposite effects across genotypes: the pathways related to protein synthesis and mitochondrial function were significantly down-regulated in *Nr5a2*$^{+/-}$ AP pancreata

while they were up-regulated in *wt* AP pancreata (Fig. R17D, see collapsed pathway curation 8-10).

Together, these results indicate that: i) AP induction promotes an inflammatory transcriptome independently of the genotype, ii) the transcriptomic effects of inducing an AP are more profound in *Nr5a2*$^{+/-}$ than in *wt* mice, and iii) in *Nr5a2*$^{+/-}$ mice, AP induction is accompanied by the up-regulation of cell cycle pathways and the down-regulation of protein synthesis and mitochondrial function gene sets.

### *What are the transcriptomic effects of inducing a mild AP in the absence of the gut microbiome?*

In this analysis, I aimed at acquiring a deeper insight into how the ABX-mediated gut microbiome depletion protects *Nr5a2*$^{+/-}$ mice from a mild AP. I compared the transcriptome of mice, *wt* and *Nr5a2*$^{+/-}$, that had undergone an AP after ABX administration (Fig. R17A, lower diagram). I also compared the number of DEGs and de-regulated pathways in these conditions to those detected upon pancreatitis induction in control mice (reported above). A similar number of genes and pathways was deregulated in control and ABX-treated *wt* mice upon AP induction: 1622 genes and 178 pathways were deregulated in ABX-treated *wt* mice undergoing an AP vs. 630 genes and 47 pathways deregulated in control pancreata (Fig. R17B and R17C). By contrast, 17 genes and 95 pathways were deregulated in ABX-treated *Nr5a2*$^{+/-}$ mice and 6529 genes and 168 pathways were deregulated in control *Nr5a2*$^{+/-}$ pancreata, indicating that the transcriptomic effects associated with AP are attenuated in *Nr5a2*$^{+/-}$ mice that had undergone ABX-mediated microbiome depletion (Fig. R17B and R17C).

Overall, these results indicate that ABX administration effectively diminish the transcriptomic effects of cerulein in *Nr5a2*$^{+/-}$ mice, but not in *wt*, mice.

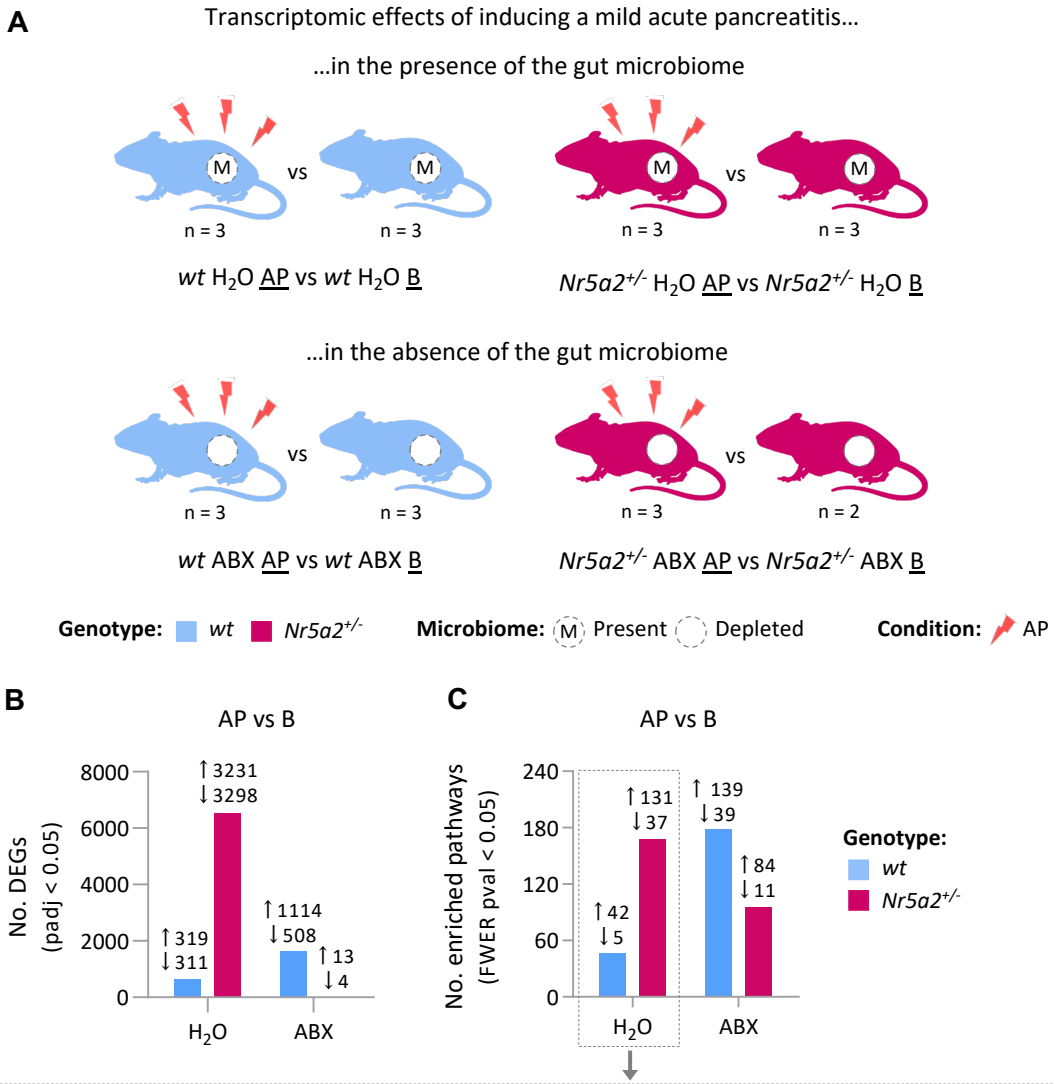
A
Transcriptomic effects of inducing a mild acute pancreatitis…
…in the presence of the gut microbiome
M
vs
n = 3
wt H2O AP vs wt H2O B
Nr5a2+/- H2O AP vs Nr5a2+/- H2O B
…in the absence of the gut microbiome
n = 2
wt ABX AP vs wt ABX B
Nr5a2+/- ABX AP vs Nr5a2+/- ABX B
Genotype: wt Nr5a2+/-
Microbiome: Present Depleted
Condition: AP
B
AP vs B
No. DEGs (padj < 0.05)
↑3231 ↓3298
↑319 ↓311
↑1114 ↓508
↑13 ↓4
H2O
ABX
C
AP vs B
No. enriched pathways (FWER pval < 0.05)
↑131 ↓37
↑42 ↓5
↑139 ↓39
↑84 ↓11
Genotype:
wt
Nr5a2+/-
D
Comparison of pathway enrichment
NES (Nr5a2+/- H2O AP vs Nr5a2+/- H2O B)
NES (wt H2O AP vs wt H2O B)
Q1
Q2
Q3
Q4
Significance (FWER pval < 0.05)
Significant in wt
Significant in Nr5a2+/-
Significant in both
ns
Collapsed pathway curation
1 CELL CYCLE
2 CELL CYCLE, IMMUNE RESPONSE
3 IMMUNE RESPONSE
4 IMMUNE RESPONSE
5 AMINO ACID METAB.
6 AMINO ACID METAB.
7 AMINO ACID METAB., MITOCHONDRIAL FUNCTION
8 PROTEIN SYNTHESIS, MITOCHONDRIAL FUNCTION
9 RNA METABOLISM
10 PROTEIN SYNTHESIS
Percentage of pathways in each quadrant
Q1: 8.2%; Q2: 53.8%; Q3: 22.1%; Q4: 13.4%

**Figure R17** (see on previous page)**: Transcriptomic effects of inducing a mild AP in ABX-treated and control mice. (A)** Representation of the RNA-seq comparisons performed to explore the effect of inducing a mild AP in the presence and absence of gut microbiome. **(B)** Number of differentially expressed genes (DEGs) detected at p-adj < 0.05. **(C)** Number of enriched pathways detected at FWER pval < 0.05. **(D)** Representation of normalised enrichment scores (NES) of all pathways in each comparison with manual pathway curation. B, basal; AP, acute pancreatitis; ABX, antibiotics.

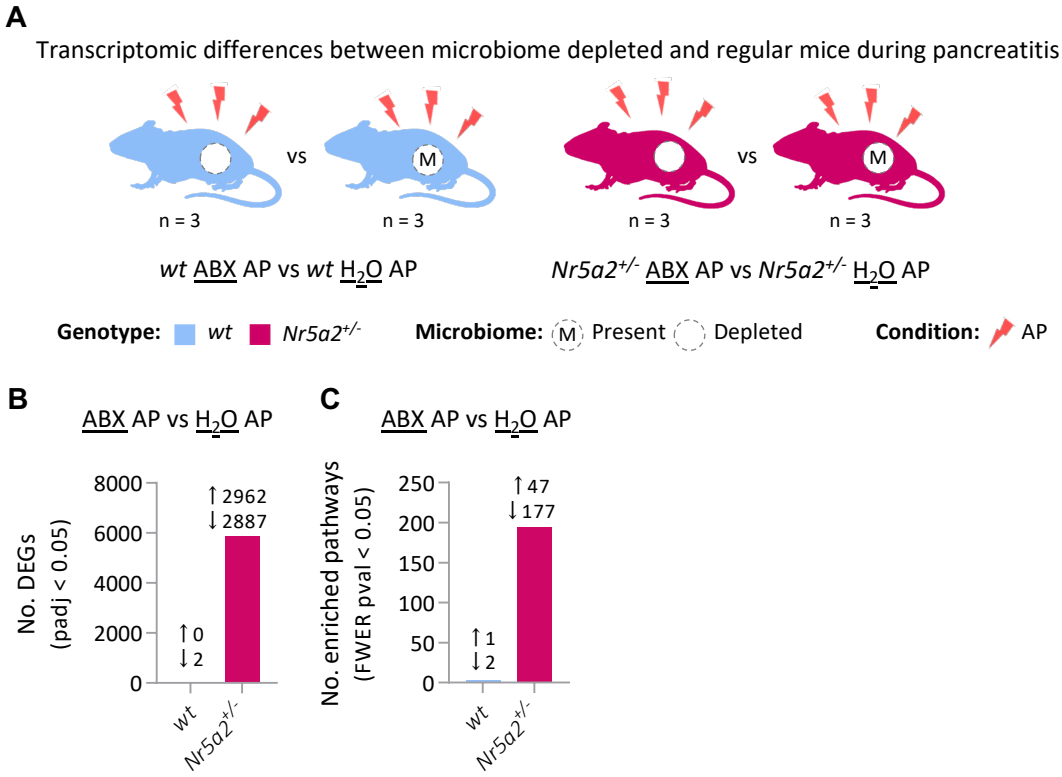


**Figure R18: ABX treatment has a major impact on the transcriptomic effects of pancreatitis in *Nr5a2*$^{+/-}$ mice. (A)** Representation of the RNA-seq comparisons performed to identify the transcriptomic differences between microbiome-depleted and conventional mice during pancreatitis. **(B)** Number of DEGs detected at p-adj < 0.05. **(C)** Number of enriched pathways detected at FWER pval < 0.05. B, basal; AP, acute pancreatitis; ABX, antibiotics, DEGs, differentially expressed genes.

## *ABX administration induces a sub-inflammatory state in basal conditions that rescues pre-inflammation in Nr5a2*$^{+/-}$ *mice*

To further explore the anti-inflammatory effect of ABX, we represented the enrichment of immune-related pathways across conditions using control mice as reference (mice that had received regular water and had not undergone a pancreatitis) (Fig. R19). This graph enables visualising the pre-inflammatory phenotype present in *Nr5a2*$^{+/-}$ mice, which is characterised by the enrichment of immune pathways in basal conditions (Fig. R19, see 2). To allow comparison with the transcriptomic analyses that led to the characterization of this phenotype (Cobo *et al.*, 2018), these observations were done using a more relaxed

false discovery rate (FDR) of 25%. This representation revealed that ABX administration induces a sub-inflammatory state in *wt* and *Nr5a2*$^{+/-}$ mice in basal conditions, thus rescuing pre-inflammation in *Nr5a2*$^{+/-}$ mice (Fig. R19A, see 2 and 3). The induction of a mild AP resulted in the up-regulation of immune-related pathways, both in *wt* and – more predominantly – in *Nr5a2*$^{+/-}$ mice (Fig. R19A, see 5 and 6). Administration of ABX prior to pancreatitis induction attenuated the up-regulation of immune pathways only in *Nr5a2*$^{+/-}$ mice (Fig. R19A, see 7 and 8). Importantly, upon pancreatitis induction, ABX-treated *Nr5a2*$^{+/-}$ mice return to their basal pre-inflammatory state (Fig. R19A, see 2 and 8).

These results indicate that i) treatment with ABX induces a sub-inflammatory state in basal conditions that rescues pre-inflammation in *Nr5a2*$^{+/-}$ mice, ii) in *wt* mice pancreatitis induction up-regulates the immune response both in $H_2O$ and ABX treated mice, iii) while pancreatitis induction profoundly up-regulates immune terms in $H_2O$ treated *Nr5a2*$^{+/-}$ mice, ABX treated *Nr5a2*$^{+/-}$ transition from the sub-inflammatory state to their basal pre-inflammatory state upon pancreatitis induction.

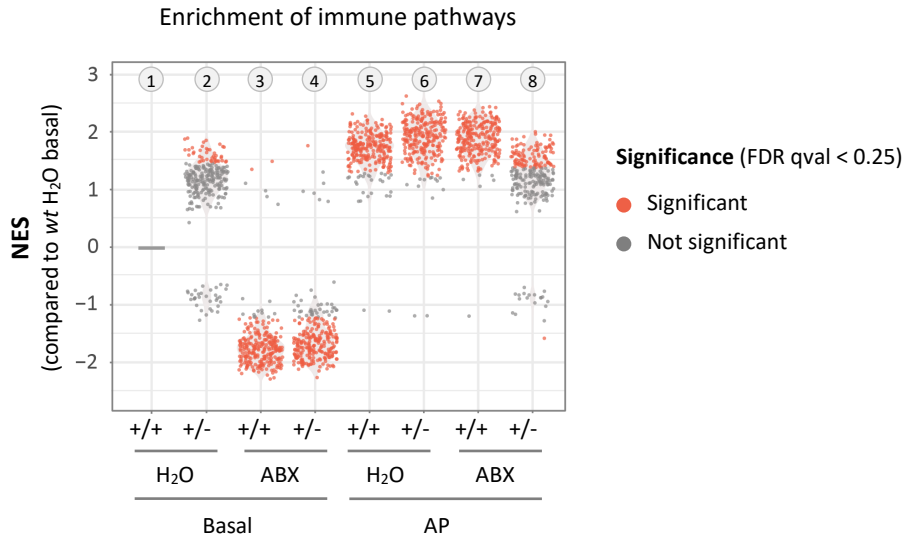


**Fig R19: ABX administration induces a sub-inflammatory state in basal conditions that rescues pre-inflammation in *Nr5a2*$^{+/-}$ mice.** Normalised enrichment scores (NES) of immune-related pathways, taking control *wt* mice in basal conditions as a reference. Color represents significance using a permissive threshold of FDR qval < 0.05. Graph shows that: i) *Nr5a2*$^{+/-}$ mice display a basal pre-inflammatory phenotype (see 1 and 2), ii) ABX administration results in down-regulation of immune signatures in basal conditions, rescuing

pre-inflammation in *Nr5a2*$^{+/-}$ mice (see 3 and 4), iii) pancreatitis results in up-regulation of immune **(Fig. R19 cont.)** pathways, especially in *Nr5a2*$^{+/-}$ mice (see 5 and 6) and iv) ABX administration attenuates immune pathway up-regulation only in *Nr5a2*$^{+/-}$ mice (see 7 and 8). AP, acute pancreatitis.

### *Treatment with ABX and pancreatitis induction modulate the same transcriptional pathways in an opposite manner in Nr5a2*$^{+/-}$ *mice and, to a lesser extent, in wt mice*

The above-mentioned results suggest that ABX administration and cerulein have opposite transcriptomic effects on the activity of immune-related pathways and protein synthesis/mitochondrial pathways in *Nr5a2*$^{+/-}$ mice. To further explore this notion, we represented the overlap between pathways that were enriched during pancreatitis in mice harbouring gut microbiota ($H_2O$ AP vs $H_2O$ B) and those enriched upon ABX administration in basal conditions (ABX B vs $H_2O$ B). In *wt* mice, 24 of the 42 pathways up-regulated during AP (57%, involved in immune response) were regulated in the opposite direction by ABX. However, 8 (19%, involved in protein synthesis) were regulated in the same direction. Regarding the pancreatitis down-regulated pathways, the overlap did not reach the significance threshold (P = 0.109). These results indicate that, in *wt* mice, pancreatitis and ABX modulate the expression of immune pathways in an opposite manner, but modulate the enrichment of protein synthesis pathways in the same direction (Fig. R20A).

In *Nr5a2*$^{+/-}$ mice, out of the 131 pancreatitis up-regulated pathways, 31 (27%, involved in immune response) were regulated in the opposite direction by ABX. Regarding the pancreatitis down-regulated pathways, out of the 37 pathways, 22 (59%, involved in protein synthesis, mitochondrial function and amino acid metabolism) were regulated in the opposite direction by ABX. No pathways were regulated in the same direction in any case. These results indicate that, in *Nr5a2*$^{+/-}$ mice, pancreatitis and ABX modulate the expression of immune pathways, protein synthesis, mitochondrial metabolism and amino acid metabolism in opposite manners (Fig. R20A).

Together, these results indicate that the transcriptomic effects of ABX administration partially counteract those of pancreatitis induction, especially in *Nr5a2*$^{+/-}$ mice, suggesting a possible mechanism for the protective effects of ABX.

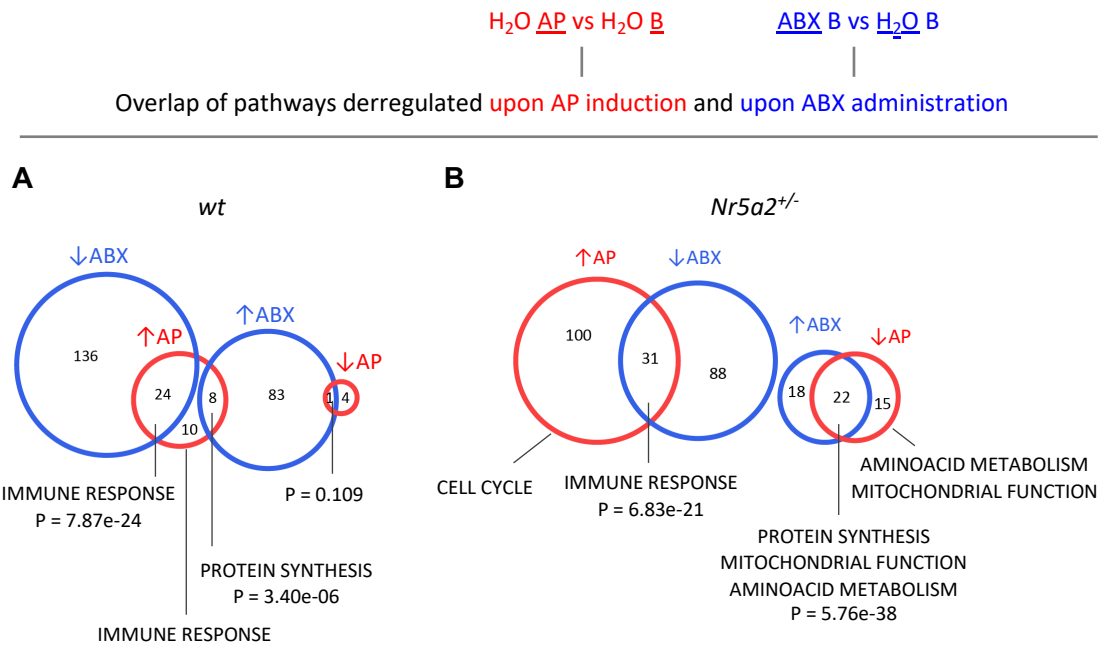


**Fig R20: Treatment with ABX and pancreatitis induction modulate the same transcriptional pathways in an opposite manner in *Nr5a2*$^{+/-}$ mice and, to a lesser extent, in *wt* mice. (A)** Venn diagram representing overlap between pathways deregulated during pancreatitis in *wt* mice harbouring microbiota (↑AP and ↓AP) and those deregulated upon ABX administration in basal conditions (↑ABX and ↓ABX) at FWER pval < 0.05, showing that pancreatitis and ABX regulate the expression of immune pathways in an opposite manner, but affect protein synthesis pathways in the same direction. **(B)** Venn diagram representing overlap between pathways deregulated during pancreatitis in *wt* mice harbouring microbiota (↑AP and ↓AP) and those deregulated upon ABX administration in basal conditions (↑ABX and ↓ABX) at FWER pval < 0.05, showing that pancreatitis and ABX modulate the expression immune pathways, protein synthesis, mitochondrial metabolism and aminoacid metabolism in opposite manners. P values represent the significance of the overlap. B, basal; ABX, antibiotics; AP, acute pancreatitis.

## 2.7. Identification of potential modulators of the anti-inflammatory effect of ABX

The results presented in the previous section suggest that the protective effects of ABX in *Nr5a2*$^{+/-}$ mice could result – at least partially – from inhibition of the immune response in basal conditions. In this context, we aimed to determine whether the effect of ABX was mediated by specific TFs. We postulated that such TFs should meet two requirements: i) their DNA-binding motif should be enriched in regulatory regions of ABX down-regulated genes, and ii) ABX administration should affect their expression levels in mouse pancreas.

First, I generated two signatures using the leading edge of the top ten most significantly down-regulated pathways in ABX-treated mice of both genotypes compared to untreated controls (Fig. R21A). The resulting "↓ **ABX +/+**" and "↓ **ABX +/-**" signatures

contained 274 and 511 genes, respectively, and overlapped in 218 of them (Fig. R21A). Next, I performed motif enrichment analysis on the promoters (-300 +50 bp around the transcriptional start site, TSS) of the genes included in these two signatures using HOMER. A single motif was found to be significantly enriched in "↓ **ABX +/+**" genes at qval < 0.05, while 29 were detected in "↓ **ABX +/-**" genes, possibly due to differences in the number of genes in the signatures (data not shown). The most significantly enriched motifs are represented in Fig. R21B. Genes included in the "↓ **ABX +/+**" signature were enriched in the DNA binding motifs for SMAD4, PU.1, KLF14, SPIB, IRF8, SMAD2 and CEBPB, while genes included in the "↓ **ABX +/-**" signature were enriched in IRF8, ELF3, PU.1, ETV2, ERG and ETS1 motifs (Fig. R21B).

Analysis of the normalised expression values of these TFs across our RNA-seq data in basal conditions revealed that ABX administration was associated with a down-regulation of the expression of most of these TFs: CEBPB, ELF3, PU.1 (encoded by the *Spi1* gene), KLF14, IRF8, ETS1 and ERG (Fig. R21C). Interestingly, these TFs were also up-regulated in *Nr5a2*$^{+/-}$ mice compared to *wt* mice (Fig. R21C).

Together, these results point to a putative role of CEBPB, ELF3, PU.1, KLF14, IRF8, ETS1 and ERG as potential modulators of the anti-inflammatory effect of ABX.

To validate potential modulators of ABX down-regulated genes in human pancreas, I analysed the transcriptomic data of 328 human pancreas samples from the GTEx project (Consortium, 2017). We postulated that the expression of putative modulators of the anti-inflammatory effect of ABX should correlate with the enrichment "↓ **ABX +/+**" and "↓ **ABX +/-**" signatures in human pancreas. The RNA expression of all these TFs, except for KLF14, was correlated with the enrichment of these signatures across all samples using ssGSEA. Notably, PU.1 (encoded by the *SPI1* gene) was the TF with the highest correlation, followed by ETS1 and ERG (Fig. R22). These results further suggest a putative role of CEBPB, ELF3, PU.1, IRF8, ETS1 and ERG, but not KLF14, as potential modulators of the anti-inflammatory effect of ABX.

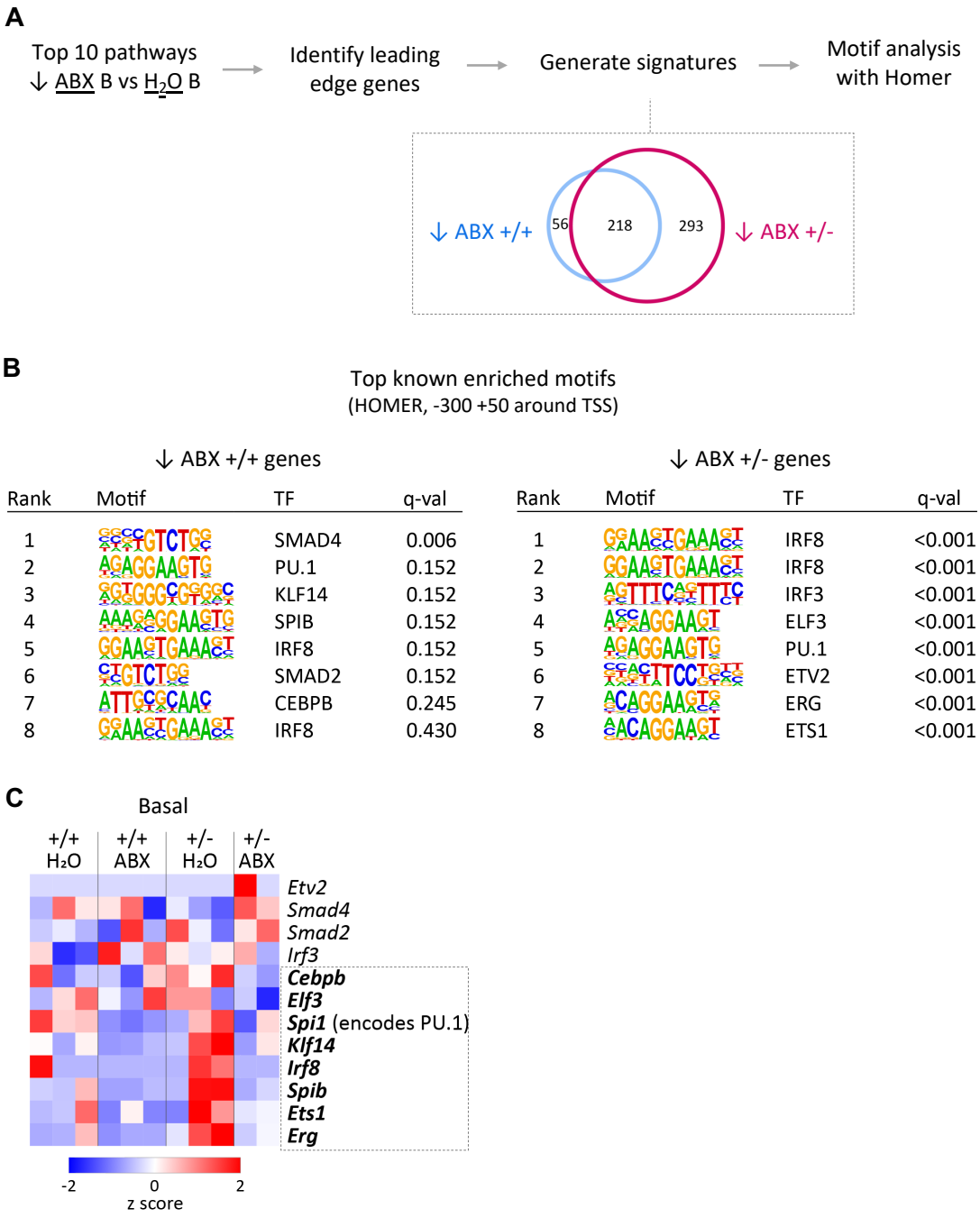


**Figure R21: Motif analysis identifies potential transcription factors involved in the anti-inflammatory effect of ABX. (A)** Strategy used to identify potential transcription factors involved in the anti-inflammatory effect of ABX in basal conditions: Motif analysis was performed in signatures obtained by combining the leading-edge genes of the top ten most significant pathways down-regulated by ABX treatment in *Nr5a2*$^{+/-}$ and *wt* mice in basal conditions. The resulting "↓ ABX +/+" (274 genes) and "↓ ABX +/-" (511 genes) signatures overlapped in 218 genes**. (B)** Motif analysis in the promoters (-300 + 500 around transcriptional start site, TSS) of genes in the gene sets, showing the most significantly enriched motifs identified using HOMER software. **(C)** RNA expression of TFs identified through motif analysis; data correspond to normalised count expression in basal conditions, represented as z-scores. Dashed line shows a group of TFs whose expression is regulated upon ABX administration in basal conditions. B, basal; ABX, antibiotics.

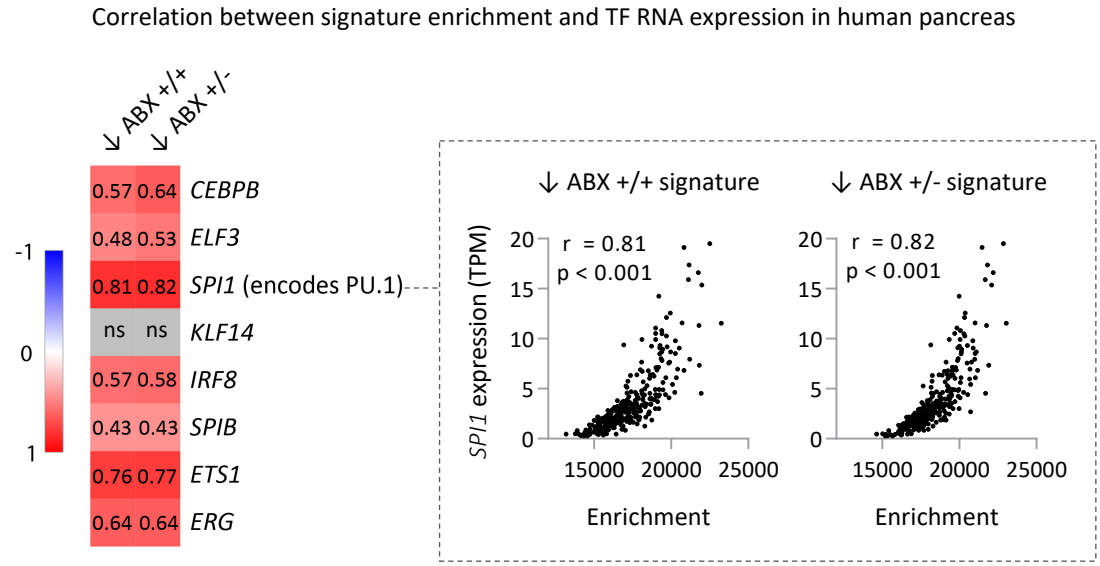


**Figure R22: The expression of putative modulators of the anti-inflammatory effect of ABX correlates with the enrichment of ABX-related signatures in human pancreas.** Correlation between the enrichment of the ABX-related signatures "↓ ABX +/+" and "↓ ABX +/-" and expression of selected TFs in human pancreas samples from GTEx. RNA-seq expression is expressed as transcripts per million (TPM). Enrichment is expressed in ssGSEA arbitrary units. Heatmap shows Pearson correlation coefficients (r) for cases in which the enrichment was significant, at $p < 0.05$. Not significant (ns) enrichments are shown in grey. ABX, antibiotics.

## 2.8. The transcriptomic effects of gut microbiome depletion in the pancreas are reminiscent of those distinguishing the intestine of germ-free (GF) vs conventionally (CV) reared mice

The above-mentioned results suggest that gut microbiome depletion down-regulates the expression of putative modulators of the immune response in the pancreas. However, additional effects of the ABX administered could not be ruled out. To acquire further evidence for an involvement of the gut microbiome, I explored published transcriptomic data from duodenum and ileum of mice reared in GF and CV conditions (Weger *et al.*, 2019). This revealed a down-regulation of *Spi1* (encodes PU.1), *Ets1* and *Irf8* transcripts in GF mice compared to CV controls in both tissues (Fig. R23A). Using ssGSEA, we also detected a down-regulation of the "↓ **ABX +/+**" and "↓ **ABX +/-**" signatures in GF mice compared to CV controls, both in duodenum and ileum (Fig. R23B). This indicates gut microbiome depletion has similar transcriptomic effects in the pancreas and in the small intestine.

Together, these results indicate that: i) we have identified a set of TFs that are down-regulated upon gut microbiome depletion both in the pancreas and in the intestine and could act as potential modulators of the anti-inflammatory effect of ABX, ii) the expression of these TFs correlates with enrichment of ABX-related signatures in human pancreas, and iii) the effects of gut microbiome depletion in the pancreas are comparable to those in the intestine.

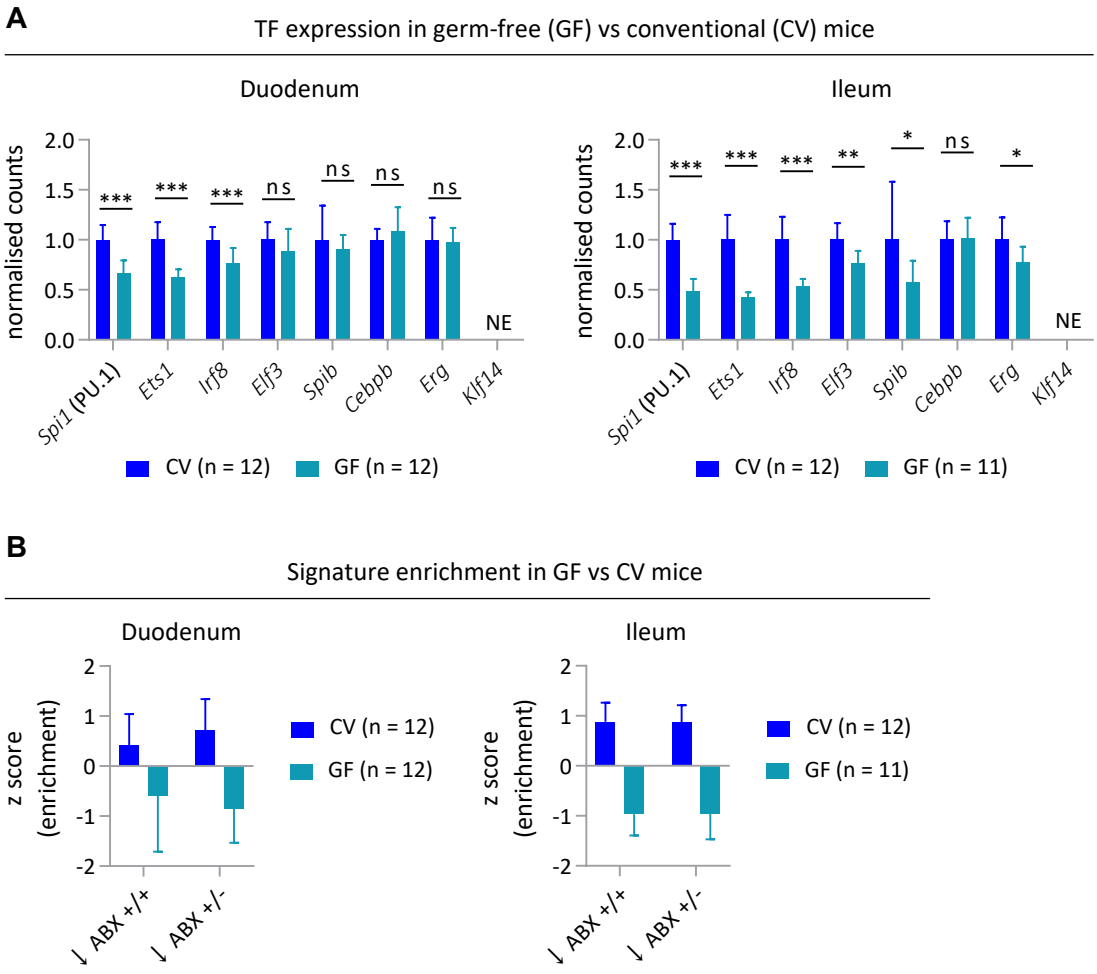


**Figure R23: The transcriptomic effects of gut microbiome depletion in the pancreas are reminiscent of those distinguishing the intestine of germ-free (GF) vs conventionally (CV) reared mice** Analysis of published transcriptomic data of duodenum and ileum from mice reared in germ-free (GF) and conventional (CV) conditions. **(A)** DEseq2 normalised counts from the RNA-seq analysis, normalised to the mean of CV values. Statistical significance was calculated using unpaired two-tailed t test with Holm-Sidak correction for multiple testing, without assuming a consistent SD. P > 0.05 ns, P < 0.05 (*), P < 0.01 (**), P < 0.001 (***). **(B)** Z-score normalised expression of ssGSEA enrichment of the ABX-related "↓ ABX +/+" and "↓ ABX +/-" signatures in duodenum and ileum from GF and CV mice. NE: not expressed.

## 2.9. *Nr5a2*$^{+/-}$ mice have elevated levels of T and CD4+ cells, that are normalised upon ABX administration

To assess whether the sub-inflammatory state was accompanied by changes in the abundance of immune cell populations, I used mMPC-counter (Petitprez *et al.*, 2020) to estimate the immune and stromal composition in mouse pancreas. This analysis revealed a reduction in the scores of T cells, B derived cells, memory B cells and monocyte/macrophages in ABX-treated mice, independently of the genotype (Fig. R24A). Interestingly, the scores obtained for these immune populations were higher in *Nr5a2*$^{+/-}$ mice, suggesting that their increased sensitivity to pancreatic inflammation may have an immune component (Fig. R24A). I then stained for CD45, F4/80, and PAX5 to quantify leukocytes, macrophages, and B cells, respectively, in pancreas tissue but did not detect any significant differences across conditions, possibly due to the very low number of inflammatory cells present in basal conditions in this tissue (Fig. R24B and not shown).

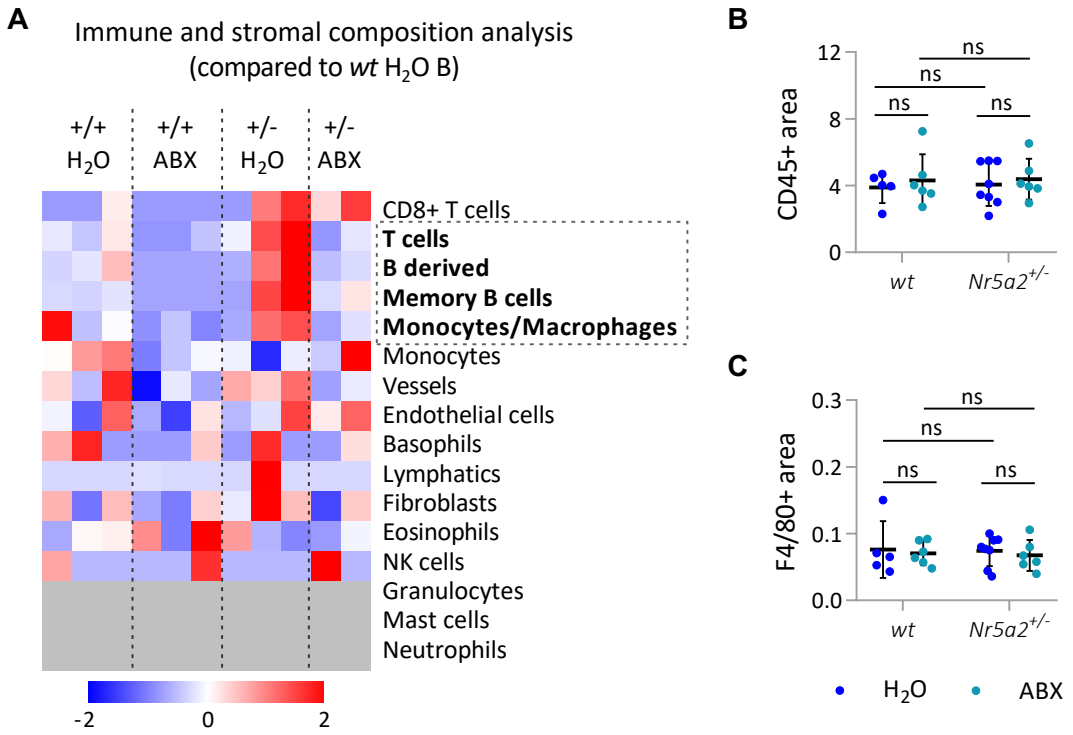


**Figure R24: Immune and stromal composition analysis reveals that the effects of ABX and *Nr5a2* heterozygosity may have an immune component. (A)** Mouse MCP-counter estimates of immune and stromal composition in ABX and $H_2O$ treated mouse pancreas, represented in a heatmap as z-scores of MCP-counter arbitrary units, showing a group of immune populations whose MCP-counter estimated abundance is modulated upon ABX administration in basal conditions. Grey indicates no expression was detected. **(B)** CD45+ area quantification, normalised to hematoxylin area. **(C)** F4/80+ area quantification, normalised to hematoxylin area.. Data is presented as mean ± SD. Statistical significance is calculated using Mann Whitney test (n = 5-8/group).

To asses whether ABX administration had in systemic effects on immune cell populations, I immunoprofiled peripheral blood from *wt* and *Nr5a2*$^{+/-}$ mice under three different conditions: basal, post-ABX administration, and upon gut microbiome reconstitution (Fig. R25A). Following the gating strategy depicted in Fig. R25B, I quantified the abundance of B cells (CD3- B220+), T cells (CD3+ B220-), CD4+ T cells (CD3+ B220- CD4+), monocytes/macrophages (CD3- B220- CD11B+ Ly6G-), and neutrophils (CD3- B220- CD11B+ Ly6G+ Ly6C+). ABX administration led to a significant decrease in the abundance of total T and CD4+ T cells that was rescued upon gut microbiome reconstitution. Interestingly, these populations were also increased in basal conditions and microbiome-reconstituted *Nr5a2*$^{+/-}$ mice, but not in microbiome-depleted mice (Fig. R25C). Gut microbiome depletion was also found to affect the abundance of monocytes/macrophages and neutrophils in *wt* an *Nr5a2*$^{+/-}$ mice respectively, although these were not rescued upon microbiome reconstitution (Fig. R25C).

Activation of splenic CD4+ T cells was recently reported to correlate with the severity of AP in mice (Glaubitz *et al.*, 2020). To determine wether gut microbiome depletion and/or *Nr5a2* heterozygosity also had an impact on this population, I immunoprofiled control and ABX-treated *wt* and *Nr5a2*$^{+/-}$ mice (Fig. R26A). Following the gating strategy depicted in Fig. R26B, I quantified the abundance of B (CD3- B220+), T (CD3+ B220-), CD4+ T (CD3+ B220- CD4+), CD8+ T (CD3+ B220- CD4+), and NK cells (CD3- NK1.1+). I did not find statistically significant differences in the abundance of any of these cell types. However, consistent with the above-mentioned results, there was a borderline significant increase in the percentage of T cells ($P = 0.078$) and CD4+ T cells ($P = 0.056$) in *Nr5a2*$^{+/-}$ mice, compared to *wt* mice, and this difference was not observed in ABX-treated mice.

Together, these results indicate an association between the abundance of T and CD4+ T cells and pancreatic susceptibility to inflammation, suggesting a mechanism through which *Nr5a2* heterozygosity may sensitise the pancreas to inflammation and a cellular explanation for how gut microbiome depletion could protect *Nr5a2*$^{+/-}$ mice from the effects of pancreatic inflammation.

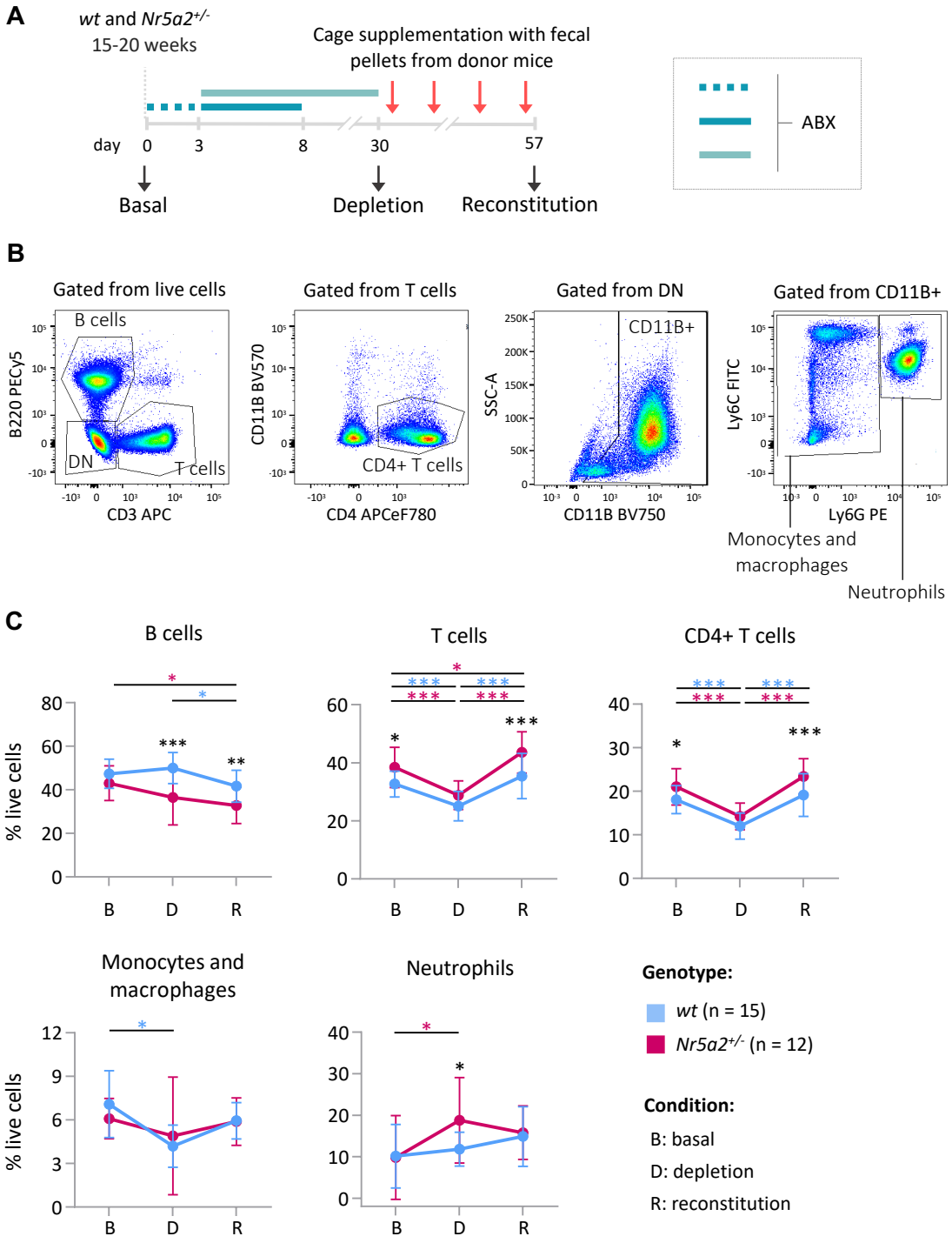


**Figure R25: *Nr5a2*$^{+/-}$ mice have elevated levels of circulating CD4+ T cells that are normalised upon ABX administration. (A)** Experimental setup: immune cell populations in blood were examined in *wt* and *Nr5a2*$^{+/-}$ mice in basal conditions, after ABX-mediated gut microbiome depletion, and upon gut microbiome reconstitution through exposure to fecal pellets from donor mice. **(B)** Gating strategy on live blood cells. **(C)** Graphs representing % of live cells of the following immune populations: B cells (CD3- B220+), T cells (CD3+ B220-), CD4+ T cells (CD3+ B220- CD4+), monocytes and macrophages (CD3- B220- CD11B+ Ly6G-) and neutrophils (CD3- B220- CD11B+ Ly6G+ Ly6C+). Data is presented as mean ± SD. Significance across conditions is calculated using two-way ANOVA with Sidak's multiple comparison test, and represented for wt (blue) and *Nr5a2*$^{+/-}$ (purple). Significance between genotypes is calculated using unpaired two-tailed t-test for each condition and represented in black. P > 0.05 not shown, P < 0.05 (*), P < 0.01 (**), P < 0.001 (***).

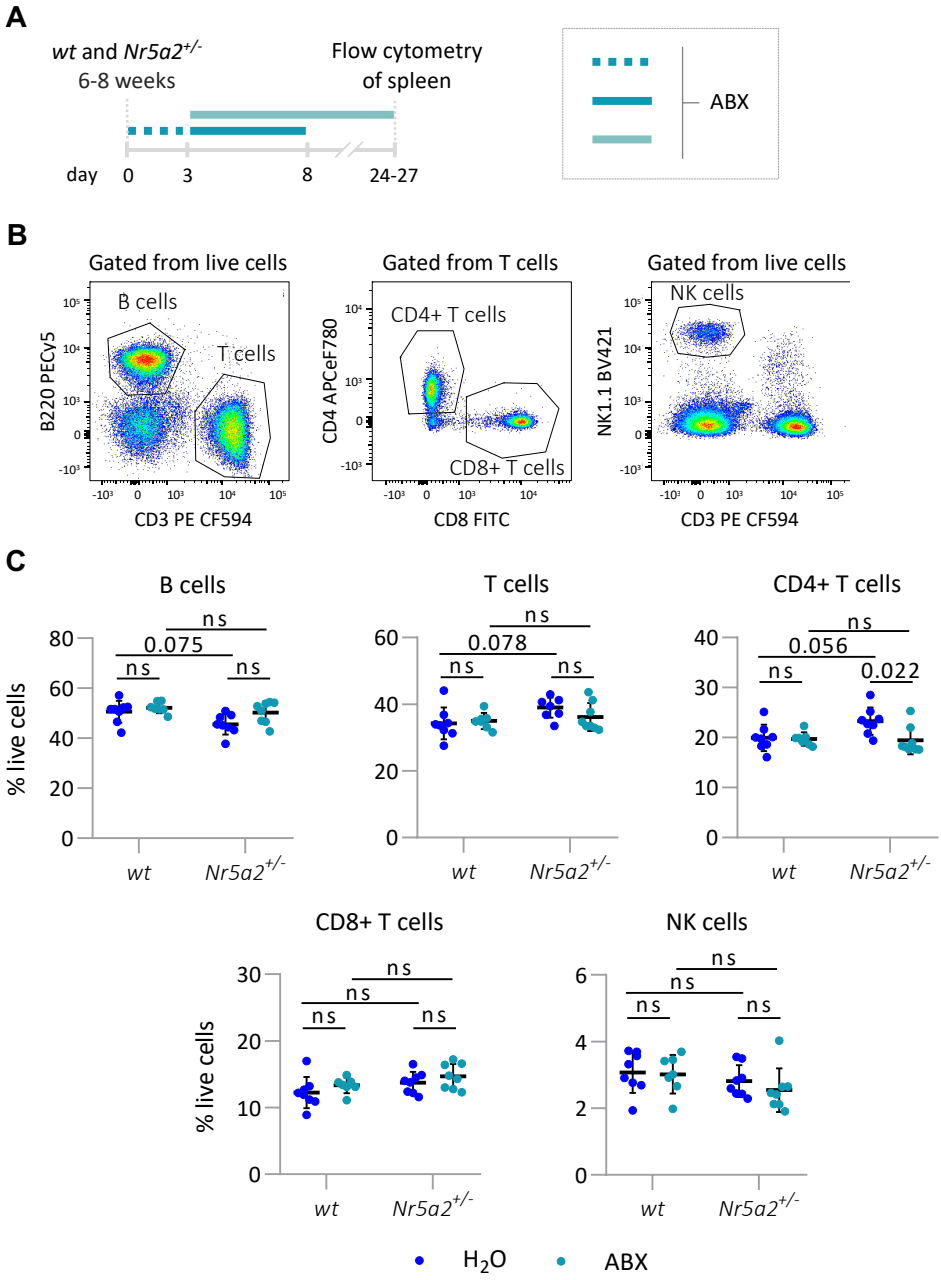


**Figure R26: ABX administration reduces the levels of splenic CD4+ T cells selectively in *Nr5a2*$^{+/-}$ mice.** **(A)** Experimental setup: ABX- and $H_2O$-treated *wt* and *Nr5a2*$^{+/-}$ mice was extracted in basal conditions, after ABX-mediated gut microbiome depletion and upon reconstitution of the gut microbiome through cage supplementation with fecal pellets from donor mice. **(B)** Gating strategy on live cells from blood. **(C)** Graphs representing % of live cells of the following immune populations: B cells (CD3- B220+), T cells (CD3+ B220-), CD4+ T cells (CD3+ B220- CD4+), CD8+ T cells (CD3+ B220- CD8+) and NK cells (CD3- NK1.1+). Data is presented as mean ± SD. Significance across conditions is calculated using two way ANOVA with Tukey's multiple comparison test (n = 7-8/group).

## 2.10. *Nr5a2* heterozygosity in the pancreas is not sufficient to elicit an inflammatory response as intense as the one observed in *Nr5a2*$^{+/-}$ mice upon AP induction

Our results suggest that the increased pancreatic damage observed in *Nr5a2*$^{+/-}$ mice may have an immune component, rather than being completely dependent on NR5A2 haploinsufficiency in pancreatic epithelial cells. In this context we aimed to determine whether NR5A2 haploinsufficiency in the pancreatic epithelium was sufficient to elicit an inflammatory response as intense as the one observed in *Nr5a2*$^{+/-}$ mice upon pancreatitis induction. For this, we induced an AP with cerulein in *Pdx1-Cre*$^{+/T}$; *Nr5a2*$^{+/lox}$, in which one *Nr5a2* allele is constitutively deleted in the pancreatic epithelium (Fig. R27A). *Pdx1-Cre*$^{+/T}$; *Nr5a2*$^{+/lox}$ mice displayed increased histopathological scores and serum amylase levels compared to *Pdx1-Cre*$^{+/T}$; *Nr5a2*$^{+/+}$ controls during pancreatitis (Fig. R27B and R27C). However, these were lower to those observed cerulein-treated *Nr5a2*$^{+/-}$ mice, suggesting that NR5A2 haploinsufficiency in the pancreas does not elicit an inflammatory response as intense as the one observed in *Nr5a2*$^{+/-}$ mice (Fig. R27B and R27C).

The *Pdx1-Cre* allele has been reported to generate mosaic recombination in the pancreas (Hingorani *et al.*, 2003). To investigate whether the reduced sensitivity to pancreatic inflammation observed in *Pdx1-Cre*$^{+/T}$; *Nr5a2*$^{+/lox}$ mice resulted from incomplete recombination, we assessed *Nr5a2* recombination in the pancreas by qPCR (Fig. R27D). Unexpectedly, no recombination was detected in pancreata from cerulein-induced *Pdx1-Cre*$^{+/T}$; *Nr5a2*$^{+/lox}$ mice, possibly resulting from an increased proliferation of unrecombined cells post pancreatitis induction.

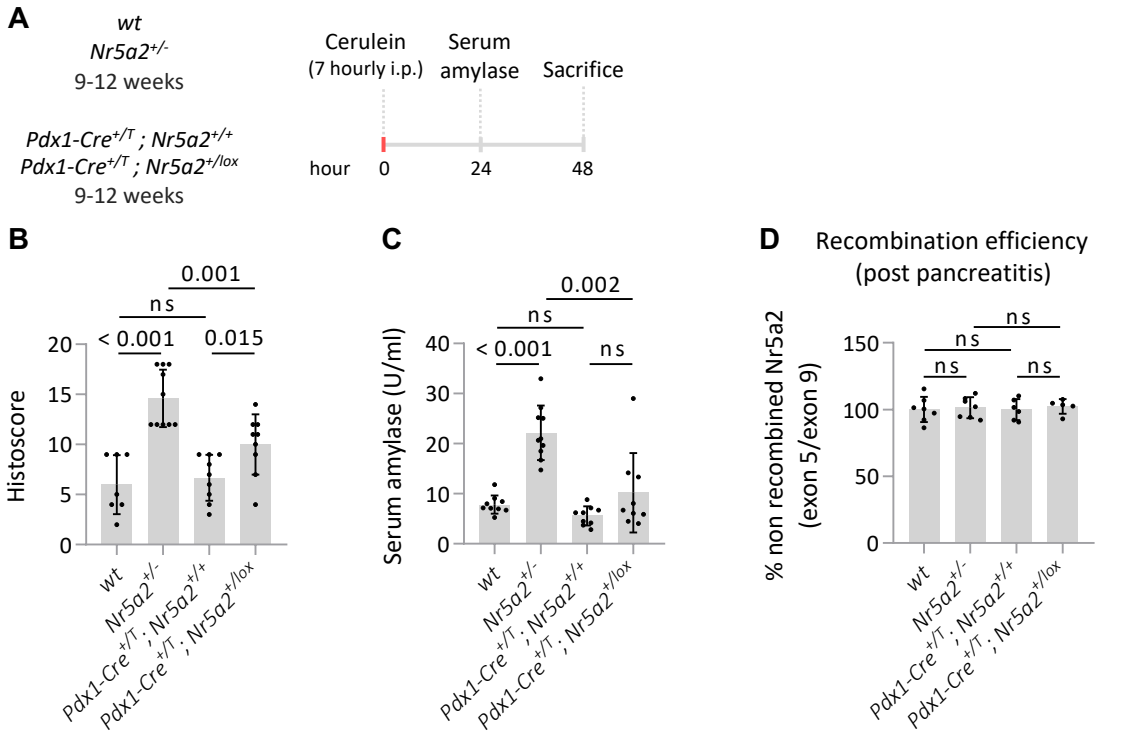


**Figure R27: *Nr5a2* heterozygosity in the pancreas is not sufficient to elicit an inflammatory response as intense as the one observed in *Nr5a2*$^{+/-}$ mice upon AP induction. (A)** Experimental timeline: *Pdx1-CreERT*$^{+/T}$*; Nr5a2*$^{+/lox}$ and *Pdx1-CreERT*$^{+/T}$*; Nr5a2*$^{+/+}$ mice were exposed to mild AP with seven hourly injections of cerulein (50 µg/kg) and their response was compared to that in *Nr5a2*$^{+/-}$ and *wt* mice. **(B)** Histological scores (0-18) for pancreas sections at 48 hours, as described in methods (n = 7-10/group). **(C)** Serum amylase levels at 24 hours (n = 9-10/group). **(D)** Recombination efficiency of the *Nr5a2* gene in the pancreas 48 hours after pancreatitis induction, based on qPCR amplification of exon 5 normalised against exon 9 (n = 5-7/group). Data is presented as mean ± SD. Statistical significance is calculated using Mann Whitney test. AP; acute pancreatitis. AP; acute pancreatitis.

# DISCUSSION

## 1. *Nr5a2* haploinsufficiency reduces the sensitivity to obesity-induced pancreatic inflammation

Animal studies have supported the association between obesity and exocrine pancreatic disease: HFD-induced obesity in rodents causes mild defects in the exocrine pancreas (Rouse *et al.*, 2014), cooperates with pancreatic inflammation (Rouse *et al.*, 2014; Hong *et al.*, 2020; Xu *et al.*, 2021), and increases the incidence of neoplasia in mouse models of *Kras*-driven pancreatic cancer (Dawson *et al.*, 2013; Philip *et al.*, 2013).

*Nr5a2* haploinsufficiency also increases susceptibility to pancreatic disease in mice. In basal conditions, it promotes an inflammatory transcriptome in the absence of histological alterations (Cobo *et al.*, 2018). In this context, we hypothesised that *Nr5a2* heterozygosity could sensitise mice to obesity-induced pancreatic injury. Contrary to what we expected, HFD administration did not cause major alterations in pancreatic histology in basal conditions neither in *wt* nor in *Nr5a2*$^{+/-}$ mice (Fig. R2B). The interpretation of these results is limited by the fact that a low number of mice was used for these analyses. In addition, we cannot rule out that a more thorough evaluation of pancreatic injury might reveal subtle changes in pancreatic features that have been reported to be altered in HFD-fed mice but that were not evaluated (e.g. apoptosis, ductal changes, acinar hypertrophy, necrosis and vascular injury) (Rouse *et al.*, 2014).

Since *Nr5a2* haploinsufficiency sensitises the pancreas to inflammation and *Kras*-driven tumorigenesis (Flandez *et al.*, 2014; Von Figura *et al.*, 2014; Cobo *et al.*, 2018), we also hypothesised that obesity could further exacerbate pancreatitis in *Nr5a2*$^{+/-}$ mice. Our experiments confirm, as previously reported, that HFD-induced obesity exacerbates pancreatitis in *wt* mice (Rouse *et al.*, 2014; Xu *et al.*, 2021). However, *Nr5a2*$^{+/-}$ mice were protected from obesity-induced pancreatic inflammation (Figs. R3B, R3C and R3D). While this may reflect functional redundancy between haploinsufficiency and obesity, an analysis of transcriptomic data from the normal human pancreas GTEx dataset revealed a modest positive correlation between NR5A2 expression and the activity of an obesity signature (containing the most significant genes enriched in the pancreas from BMI-high vs -low individuals) ($r = 0.20$, $P < 0.001$, data not shown), indicating that the effects of obesity in human pancreas do not converge with those of low NR5A2 expression.

Obesity is a complex disease, in which excess body weight co-exists with other conditions, such as type 2 diabetes, hyperlipidemia, hepatic steatosis, and systemic inflammation. This intricate scenario complicates the identification of the exact mechanisms through which obesity promotes pancreatic disease. Several obesity-related metabolic conditions – such as type 2 diabetes (Solanki, Barreto and Saccone, 2012; Goodger *et al.*, 2016), hypertriglyceridemia (Albai, Roman and Frandes, 2017) and hepatic steatosis (Yoon *et al.*, 2017) – are independent risk factors for acute pancreatitis. Thus, obesity is thought to contribute to pancreatic inflammation through these intermediate conditions (Fig. D1A) (Khatua, El-Kurdi and Singh, 2017). This idea is supported by some experiments that were not included in this thesis, in which I compared the effects of HFD-induced obesity in *wt* males and females. While HFD-induced obesity was comparable across sexes, an exacerbation of pancreatitis was observed only in *wt* males. Importantly, only *wt* males - but not females - displayed insulin resistance, glucose intolerance, and severe hepatic steatosis upon HFD feeding, supporting that the effects of obesity on pancreatic inflammation are mediated through intermediate pathologies (Fig. D1A). In this context, I postulate two different mechanisms through which *Nr5a2* haploinsufficiency may be associated with reduced obesity-induced pancreatic damage. First, it may protect from obesity-associated intermediate conditions, thereby resulting in reduced pancreatic inflammation. Second, it may reduce the effect of these intermediate conditions that promote pancreatic disease (Fig. D1B).

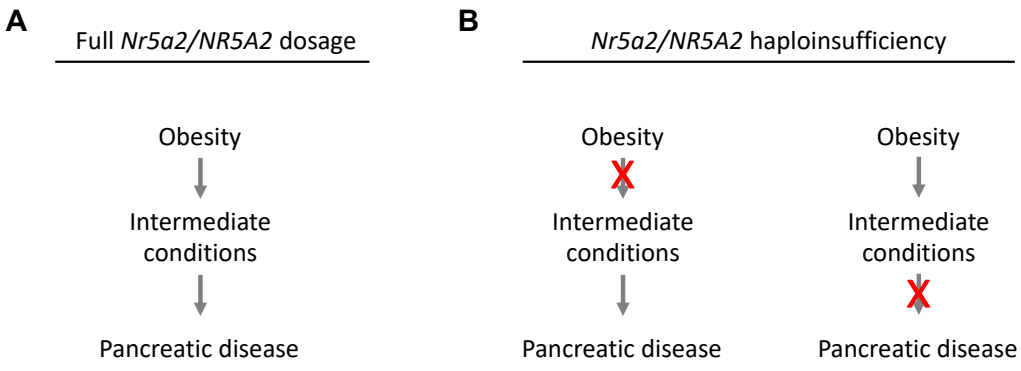


**Figure D1: Mechanisms through which *Nr5a2/NR5A2* haploinsufficiency may protect from obesity-induced pancreatic inflammation. (A)** The literature suggests that obesity promotes pancreatic disease through the development of intermediate conditions that predispose for pancreatic disease. **(B)** In this thesis, I found that *Nr5a2* haploinsufficiency protects from obesity-induced pancreatic inflammation. Our results indicate that this may occur through two different mechanisms: by protecting from obesity associated intermediate conditions and/or by reducing the sensitivity to these intermediate conditions that promote pancreatic disease.

### *Does Nr5a2/NR5A2 haploinsufficiency protect from obesity-associated intermediate conditions?*

To date, GWAS studies have not reported any associations between *NR5A2* variability and obesity-associated metabolic conditions, such as diabetes, hyperlipidemia, and hepatic steatosis (GWAS Catalog and PheGenI databases, accessed on 14/05/2022). However, multiple studies have reported an association between SNPs in the vicinity of *NR5A2* and anthropometric measurements, such as BMI (Fox *et al.*, 2007), waist-to-hip ratio (Kichaev *et al.*, 2019; Pulit *et al.*, 2019), BMI-adjusted waist-to-hip ratio (Lotta *et al.*, 2018; Zhu *et al.*, 2020), and height (Yengo *et al.*, 2018).

Our model of HFD-induced obesity caused insulin resistance, glucose intolerance, and hypercholesterolemia (Fig. R1). Our results indicate that *Nr5a2* haploinsufficiency does not predispose to any of these obesity-associated alterations. In line with this, feeding a HFD was reported to have similar effects on glucose tolerance and insulin resistance in *Nr5a2*$^{+/-}$ and *wt* mice (Hattori *et al.*, 2014). These observations support that *Nr5a2* haploinsufficiency does not affect HFD-induced glucose intolerance, insulin resistance, and hyperlipidemia. To validate these observations, in collaboration with M.E. López de Maturana and N. Malats (Genetic and Molecular Epidemiology Group, CNIO), we have performed preliminary analyses to explore the association between obesity and diabetes in humans (not shown). First, we generated a *NR5A2* genetic risk score based on 13 SNPs that reflects the risk of developing pancreatic cancer. The *NR5A2* gene score was not associated with the risk of type 2 diabetes, further supporting the observations we made in mice. In contrast, *NR5A2* was reported to be associated with a reduced risk of type 1 diabetes - an autoimmune disease caused by autoimmune destruction of pancreatic β cells - through the induction of self-tolerance, increased β-cell survival and regeneration (Baquié *et al.*, 2011; Cobo-Vuilleumier, Petra I Lorenzo, *et al.*, 2018; Cobo-Vuilleumier and Gauthier, 2020). While our results do not support a major impact of *NR5A2* haploinsufficiency on glucose homeostasis, NR5A2 agonistic activation was found to improve glucose tolerance and insulin sensitivity in *wt* mice (Lee *et al.*, 2011).

On the other hand, our experiments indicate that *Nr5a2* heterozygosity attenuates HFD-induced hepatic steatosis (Figs. R2C, R2F and R3E). This could be mediated through a modulation of lipid absorption. NR5A2 is a major regulator of bile acid metabolism

(Mataki *et al.*, 2007; Lee *et al.*, 2008) and its loss in hepatocytes was reported to reduce bile acid levels in the liver, gallbladder, and intestine, thereby compromising intestinal lipid absorption (Mataki *et al.*, 2007). In addition, changes in bile acid composition – induced by chemical inhibition of intestinal bile acid uptake – were reported to protect from HFD-induced non-alcoholic fatty liver disease and to improve glucose tolerance (Rao *et al.*, 2016). This offers a possible mechanism through which *Nr5a2* haploinsufficiency in hepatocytes could protect from HFD-induced liver steatosis (Fig. D2). In addition, NR5A2 activation decreased liver steatosis in HFD-fed mice (Lee *et al.*, 2011). *NRH-25*, the *NR5A2 C. elegans* homolog, was also found to regulate lipid metabolism in response to dietary components (Lin and Wang, 2017). Interestingly, the protective effects of *Nr5a2* haploinsufficiency in the liver may not influence glucose tolerance, since liver-specific *Nr5a2* ablation has no effects in glucose homeostasis (Lee *et al.*, 2011).

The validation of these findings/hypothesis in humans is complicated by the fact that epidemiological studies rarely include information on whether subjects present hepatic steatosis. To overcome this limitation, we plan to explore the association between the *NR5A2* genetic risk score and transcriptomic steatosis signatures in the GTEx dataset.

Importantly, hepatic steatosis has been proposed as a prognostic factor for AP, even after adjusting for BMI (Reddy, 2013; Xu *et al.*, 2015; Yoon *et al.*, 2017). These findings suggest that *Nr5a2/NR5A2* haploinsufficiency could protect from obesity-associated pancreatic damage through the attenuation of hepatic steatosis (Fig. 2D).

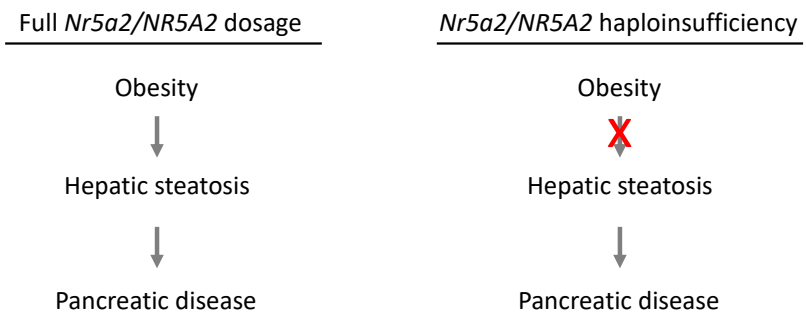


**Figure D2: *Nr5a2/NR5A2* haploinsufficiency may protect from obesity-induced pancreatic inflammation through the attenuation of hepatic steatosis.** Hepatic steatosis is one of the mechanisms through which obesity may promote pancreatic disease. Our results indicate that *Nr5a2* haploinsufficiency attenuates obesity-induced hepatic steatosis, thereby suggesting a possible mechanism through which *Nr5a2/NR5A2* haploinsufficiency may protect from obesity-induced pancreatic damage.

*Does Nr5a2/NR5A2 haploinsufficiency reduce the sensitivity to intermediate conditions that promote pancreatic disease?*

*Nr5a2/NR5A2* haploinsufficiency may also reduce the sensitivity to the effects of intermediate conditions that promote pancreatic disease, such as diabetes (Fig. D1C). To test this hypothesis using human data, we have stratified individuals based on the *NR5A2* genetic risk score into WT-like (those harbouring NR5A2 variants not predisposing to PDAC development) and HET-like (those whose *NR5A2* variants predispose for PDAC development). Our preliminary data indicate that, while diabetes is associated to PDAC development in WT-like controls, this is not the case in HET-like individuals (data not shown). This suggests that *NR5A2* haploinsufficiency may indeed reduce the sensitivity to intermediate conditions that promote pancreatic disease. Further analyses will explore the association with pancreatitis phenotypes.

The ensemble of mouse and human data emphasize the existence of a complex interaction between genetic and non-genetic factors. However, little is known about these interactions. Our results indicate that a genetic defect associated with increased susceptibility to pancreatic disease may at the same time reduce the penetrance or sensitivity to non-genetic risk factors that predispose to PDAC, such

## 2. Gut microbiota depletion induces a sub-inflammatory state and rescues genetic susceptibility to pancreatic disease in *Nr5a2*$^{+/-}$ mice

Increasing evidence supports the existence of a close connection between the gut microbiome and the pancreas, where one influences the other. Pancreatic secretions modify the composition of the gut microbiome, while the latter modulates pancreatic disease (Pan *et al.*, 2021; Schepis *et al.*, 2021). Although traditionally considered a sterile organ, recent studies have pointed to the existence of microbiota within the pancreas (Pushalkar *et al.*, 2018; Sethi *et al.*, 2018; Thomas *et al.*, 2018; Aykut *et al.*, 2019). The anatomic connection between the main pancreatic duct and the duodenum constitutes a possible route of migration of gut microbia to the pancreas (Pushalkar *et al.*, 2018),

although translocation may also occur via the mesenteric veins or lymph nodes (Diehl *et al.*, 2013). Under physiological conditions, the permeability of the intestinal epithelium is restricted by tight junctions. However, these critical structures can be damaged, compromising the intestinal barrier function and leading to bacterial translocation into the mesenteric circulation (Ulluwishewa *et al.*, 2011). Although a pancreatic microbiome can be identified in physiological conditions, an increase in the abundance of this community has been associated to pancreatic oncogenesis (Pushalkar *et al.*, 2018; Aykut *et al.*, 2019). In addition, intestinal homeostasis has been reported to modulate the pathogenesis of AP: commensal bacteria were reported to aggravate acute necrotizing pancreatitis through the induction of intestinal injury (Zheng *et al.*, 2019), intestinal permeability correlates with the severity of AP in humans (Ammori *et al.*, 1999), and probiotic treatment was recently reported to suppress experimental AP through the induction of intestinal homeostasis (Pan *et al.*, 2019).

Dysbiosis - an imbalance in the composition of the gut microbiome - is associated with multiple pancreatic diseases, such as acute (Zhu *et al.*, 2019) and chronic pancreatitis (Frost *et al.*, 2020), diabetes (Wen *et al.*, 2008; Qin *et al.*, 2012), and pancreatic cancer (Riquelme *et al.*, 2019; Kartal *et al.*, 2022). However, it is unclear whether these alterations are the cause or the consequence of pancreatic disease (Pan *et al.*, 2021; Kartal *et al.*, 2022). On the one hand, pancreatic disease could alter the gut microbiota by modulating acinar secretions. On the other hand, the gut microbiome has been found to migrate and shape the pancreatic microenvironment (Pushalkar *et al.*, 2018; Aykut *et al.*, 2019; Riquelme *et al.*, 2019). The best evidence supporting a causative link between gut microbiome dysbiosis and pancreatic disease – to our understanding – was provided by Riquelme et al. (2019) who, using human-into-mice fecal transplant experiments from short-term and long-term survival PDAC patients and control donors, were able to modulate the immune tumor microenvironment and affect tumor growth.

Based on the data described above, the gut microbiome can promote pancreatic disease through qualitative or quantitative changes in the composition of the pancreatic microbiome.

One of the main objectives of my work was to determine whether the gut microbiome could impact on the pancreatic phenotype of *Nr5a2*$^{+/-}$ mice. Administration of broad-

spectrum ABX depleted the gut microbiome (Fig. R4) and suppressed the effects of *Nr5a2* haploinsufficiency on mouse pancreas in basal conditions and upon induction of an AP, as indicated by transcriptomic and histologic analysis of the pancreas (Figs. R6 and R19). Using cohousing experiments to reconstitute the gut microbiome in ABX treated *Nr5a2*$^{+/-}$ mice, we were able to restore the sensitivity to pancreatic inflammation (Fig. R8), indicating that the effects of ABX were due to gut microbiome depletion.

ABX-mediated gut microbiome depletion had no effects on pancreas histology and serum amylase levels in basal conditions (Fig. R5). However, ABX administration resulted in the up-regulation of the acinar transcriptomic signature in basal conditions independently of the genotype, suggesting that it may promote exocrine differentiation (data not shown). I also explored the effects of gut microbiome depletion on the endocrine pancreas: an improved tolerance to glucose overload was observed only in *Nr5a2*$^{+/-}$ mice (data not shown). These effects could be mediated by NR5A2, since NR5A2 activation has been reported to improve glucose tolerance in *Nr5a2*$^{+/-}$ mice (Lee *et al.*, 2011) and PE and PG – two bacterial phospholipids – have been proposed to be NR5A2 ligands (Krylova *et al.*, 2005; Ortlund *et al.*, 2005; Wang *et al.*, 2005; Musille *et al.*, 2012; Sablin *et al.*, 2015).

NR5A2 has a crucial role in gut homeostasis (Fernandez-Marcos, Auwerx and Schoonjans, 2011) and its ablation in intestinal organoids was reported to increase epithelial permeability (Bayrer *et al.*, 2018). In addition, NR5A2 stimulates glucocorticoid production in the intestine (Mueller *et al.*, 2006), which not only regulate local immune responses but also improve epithelial barrier function (Boivin *et al.*, 2007). Considering that our experiments were conducted on germline heterozygous mice, we hypothesised that intestinal *Nr5a2* haploinsufficiency could contribute to pancreatic inflammation by increasing the permeability of the gut epithelium. Using FITC dextran assays, we found that neither *Nr5a2* heterozygosity nor the pancreatitis we induced compromised the permeability of the gut epithelium (Fig. R9A and R9B). Using FISH assays with a 16S rRNA-specific probe, we did not detect any differences in pancreatic bacterial abundance (Fig. R9C and R9D). However, these analyses are limited by the fact that a fine time-course was not performed.

We then hypothesised that *Nr5a2* heterozygosity could promote pancreatic inflammation by favouring dysbiosis. Analysis of the fecal microbiome revealed that alpha diversity (i.e. species richness and evenness within samples) and beta diversity (i.e. species richness across samples) were not altered in *Nr5a2*$^{+/-}$ mice, compared to *wt* controls (Fig. R11A and R11B). Differential abundance analysis of taxa showed that the fecal microbiomes from *wt* and *Nr5a2*$^{+/-}$ mice differed only in the abundance of three ASVs, while no differences were detected at any other taxonomic levels (Fig. R11C). One of the ASVs that was enriched in *Nr5a2*$^{+/-}$ mice (ASV3) belonged to the *Rikenella* genus, which was reported to be over-represented in an experimental mouse model of CP (Wu, Li and Chen, 2021). ASV1 and ASV2 were classified as part of the *Muribaculaceae* taxon, a poorly characterised family involved in carbohydrate degradation (Lagkouvardos *et al.*, 2019). Interestingly, these ASVs differed in a single nucleotide and were enriched in opposite genotypes, suggesting that the intestinal microenvironment of *wt* and *Nr5a2*$^{+/-}$ mice may offer a selective advantage for different species of the *Muribaculaceae* family. Importantly, this family was found to be enriched in an experimental mouse model of CP (Han *et al.*, 2019) and recently reported to promote pancreatic inflammation (Yang *et al.*, 2022). Whether differences in ASVs belonging to the *Muribaculaceae* family are biologically relevant is only speculative, since these ASVs were detected only in some of the mice (data not shown). In addition, while ASVs provide a more precise taxonomic resolution than operational taxonomic units (OTUs) for the analysis of microbial communities, they may split bacterial species into different clusters (Schloss, 2021). An imbalance in the fungal community, which cannot be explored using 16 rDNA sequencing, cannot be ruled out. Cohousing of *wt* and *Nr5a2*$^{+/-}$ mice failed to modulate the severity of pancreatitis (Figs. R8B, R8C and R8D), indicating that horizontal transmission factors (i.e. microbes) are not responsible for the increased sensitivity to pancreatic damage observed in *Nr5a2*$^{+/-}$ mice. Together, these results point to a limited role of bacterial dysbiosis to the phenotype of *Nr5a2*$^{+/-}$ mice.

A limitation of the microbiome analysis is that it was performed with cohoused mice, a practice that is well known to homogenise the gut microbiota (Liang *et al.*, 2020). The analyses were performed in these conditions because we postulated that a microbiome signature predisposing *Nr5a2*$^{+/-}$ mice to pancreatic inflammation should be present

under the same circumstances in which the *Nr5a2*$^{+/-}$ phenotype was initially described (i.e. using cohoused mice). Thus, we cannot exclude the possibility that *Nr5a2* haploinsufficiency may cause differences in the gut microbiome that are masked upon cohousing with *wt* mice. In fact, a SNP in *NR5A2* (rs7534666) was recently identified as the top genetic variant associated with alpha diversity in the gut microbiome in a GWAS (Kurilshikov *et al.*, 2021), suggesting that NR5A2 function shapes the composition of the gut microbiome in humans. Importantly, this SNP has not been reported to be associated to intestinal alterations (GWAS Catalog and PheGenI databases, accessed on 14/05/2022), indicating that its effect on gut microbiome diversity is not mediated by intestinal disease.

To recapitulate, I found that gut microbiome depletion rescued the effects of *Nr5a2* haploinsufficiency in mouse pancreas. To our knowledge, this is the first reported evidence of a genetic defect involved in pancreatic disease being completely rescued upon modulation of a non-genetic factor.

### *Exploring the causative link between the gut microbiome and severity of pancreatitis*

The causative links between gut microbiome dysbiosis and pancreatic disease have been poorly characterised. Our experiments provide a good scenario to identify bacterial taxa that predispose to pancreatic disease, since some of the mice used for the analysis of the gut microbiome were later exposed to pancreatitis, meaning that we could correlate damage with microbial abundance. Using differential abundance analysis to compare the gut microbiome from mice that displayed the highest damage during pancreatitis to their low damage counterparts, I identified a taxa signature that was over-represented in high damage *wt* and *Nr5a2*$^{+/-}$ mice prior to pancreatitis induction (Fig. R13). Importantly, one of the over-represented taxons in high-damage *Nr5a2*$^{+/-}$ mice, *Turicibacter* genus, has been reported to be enriched in patients with pancreatic cancer (Kim *et al.*, 2021), albeit in the absence of causal evidence to the association. While our analysis has several limitations (e.g. the low number of mice used), our results suggest that certain bacteria – such as those of the *Turicibacter* genus - may impact on pancreatic disease. To mitigate

the limitations, I will explore the correlation between bacterial abundance and the histopathological score, measured as a continuous variable.

## 3. Mitochondrial function: a mediator of the protective effects of gut microbiome depletion in *Nr5a2*$^{+/-}$ mice?

Despite the interest of analysing the role of the gut microbiome on disease, there is little or no data on the transcriptomic effects of depleting the gut microbiome. This is true in general, and more so in relationship to pancreatic disease. The RNA-seq studies performed in my thesis have enabled me to answer some of these questions. I have compared the transcriptomes of ABX-treated and control *wt* mice and have found that - despite the lack of major histological changes (Figs. R5A, R5B and R5C) profound alterations in gene expression can be demonstrated. GSEA analysis revealed an up-regulation of pathways related to digestive enzyme secretion in ABX-treated mice (e.g. mitochondrial function, protein synthesis, and RNA metabolism) (Fig. R16F). Together with the up-regulation of the acinar signature (data not shown), this suggests that gut microbiome depletion may increase enzyme production and acinar differentiation. This was not associated with increased pancreatic injury since serum amylase levels were within the normal range in ABX-treated *wt* mice (Fig. R5D). Differential expression analysis also revealed a down-regulation of pathways related to ECM organization, coagulation and – most notably – immune pathways (Fig. R16F). All immune pathways displayed a negative directionality of regulation in ABX-treated *wt* mice (Fig. R19), indicating that gut microbiome depletion induces a sub-inflammatory state in the pancreas and suggesting that the gut flora causes "basal pre-inflammation" in the pancreas.

We also explored the transcriptomic effects of depleting the gut microbiome in *Nr5a2*$^{+/-}$ mice. Our results indicated that the transcriptomic changes caused by gut microbiome depletion in *Nr5a2*$^{+/-}$ mice were milder than those detected in *wt* mice (Figs. R16B and R16C). While these results may have been influenced by the reduced number of mice used for the *Nr5a2*$^{+/-}$ comparisons, an analysis to test the effect of using the same number of mice than in the *wt* comparison does not support that the differences between

the effect observed in *wt* and *Nr5a2*$^{+/-}$ mice are due to sample size issues (data not shown).

Despite the lower number of transcriptomic alterations detected in *Nr5a2*$^{+/-}$ mice, the effects of gut microbiome depletion were comparable across genotypes, since most pathways were regulated in the same direction by ABX treatment in *wt* and *Nr5a2*$^{+/-}$ mice (Fig. R16E). At the gene level, the transcriptomic effects of ABX in *wt* and *Nr5a2*$^{+/-}$ mice overlapped in the up-regulation of a single gene (*Clec11a*), a C-type lectin receptor involved in hematopoietic differentiation and homeostasis (Fig. R16D) (Yue, Shen and Morrison, 2016). Interestingly, high CLEC11A expression is a favourable prognostic factor in pancreatic cancer in humans, according to the entry of this gene in the Protein Atlas.

ABX-mediated gut microbiome depletion protected *Nr5a2*$^{+/-}$ - but not *wt* – mice from the effects of inducing a mild AP (Fig. R6). To explore the impact at the transcriptomic level, we used RNA-seq. Gut microbiome depletion profoundly attenuated the effects of inducing a pancreatitis in *Nr5a2*$^{+/-}$ mice: while 6529 genes were deregulated in control mice, only 17 genes were deregulated in ABX-treated mice (Fig. R17B and R17C). This analysis may suffer from the lower number of mice used for the comparison including ABX-treated mice. To overcome this limitation, we plan to repeat the analysis reducing the number of mice used for the control condition comparison.

To identify mechanisms through which gut microbiome depletion may protect *Nr5a2*$^{+/-}$ - but not *wt* - mice from the damage caused by cerulein, I first explored the differences associated with pancreatitis induction in *wt* and *Nr5a2*$^{+/-}$ mice in mice harboring gut flora. As expected, the effects were profoundly higher in *Nr5a2*$^{+/-}$ than in *wt* mice: 630 genes and 47 pathways were deregulated in *wt* mice, compared with 6529 genes and 168 pathways in *Nr5a2*$^{+/-}$ mice (Fig. R17D). Overall, the transcriptomic effects of pancreatitis induction were highly consistent across genotypes, with a marked up-regulation of immune pathways and a down-regulation of amino acid metabolism. Interestingly, a few pathways displaying opposite changes across genotypes were identified. In *Nr5a2*$^{+/-}$ mice, mitochondrial and protein synthesis pathways were significantly down-regulated, while they were up-regulated in *wt* mice. This suggests that gut microbiome depletion may selectively protect *Nr5a2*$^{+/-}$ mice from pancreatitis by affecting mitochondrial function.

Mitochondrial activity plays a crucial role in acinar cells, since high protein-secreting cells have high energy requirements. Pathological conditions, including AP, can result in mitochondrial dysfunction and impaired cellular respiration, resulting in the accumulation of reactive oxygen species, ER stress and $Ca^{2+}$ clearance impairment, which eventually leads to intracellular activation of pancreatic enzymes and acinar injury (Gukovsky, Pandol and Gukovskaya, 2011; Biczo *et al.*, 2018; Lee and Papachristou, 2019; Zheng *et al.*, 2021). In this context, I propose a mechanism through which ABX-mediated gut microbiome depletion could selectively protect *Nr5a2*$^{+/-}$ mice from the effects of pancreatitis through the prevention of mitochondrial dysfunction (Fig. D3).

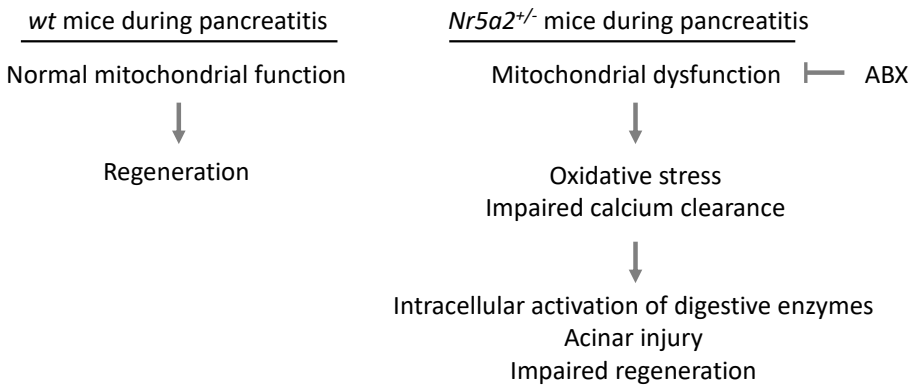


**Figure D3: Mechanism through which gut microbiome depletion could selectively protect *Nr5a2*$^{+/-}$ from pancreatitis through the inhibition of mitochondrial dysfunction.**

Genetic defects leading to mitochondrial dysfunction and oxidative stress may also cause acinar degeneration in basal conditions (Choi *et al.*, 2020, 2022), suggesting a possible mechanism through which *Nr5a2* haploinsufficiency may contribute to pancreatic disease. A cell-autonomous role of NR5A2 in mitochondrial function has been proposed (Michalek and Brunner, 2021). In fact, mitochondrial function is primarily regulated by PGC-1α, a known coactivator of NR5A2 (Mays *et al.*, 2017). *Nr5a2* deletion in mouse hepatocytes was recently reported to regulate mitochondrial biogenesis and function (Choi *et al.*, 2020), and NRH-25 - the *C. elegans* homolog – was found to modulate mitochondrial function in response to bacterial metabolites (Lin and Wang, 2017). In addition, NR5A2 regulates the expression of the mitochondrial proteins P450SCC and CYP11A1 in the ovary (Duggavathi *et al.*, 2008), and CYP11B1 and CYP11A1 in the intestinal epithelium (Mueller *et al.*, 2006). This suggests a scenario in which NR5A2 promotes mitochondrial function and bacterial metabolites modulate NR5A2 function.

This effect could also be mediated by bacterial metabolites acting as NR5A2 ligands (PE and PG). Experimental confirmation that the effects of *Nr5a2* haploinsufficiency, either in basal conditions or during pancreatitis, were mediated by altered mitochondrial function and oxidative stress, would suggest exploring the effect of antioxidant therapies in *Nr5a2*$^{+/-}$ mice and - possibly - in humans. This strategy has been reported to ameliorate acinar injury associated to a genetic defect that causes mitochondrial dysfunction and oxidative stress (Choi *et al.*, 2022). As mentioned in the introduction, NR5A2 has been proposed to have an oncogenic role in the pancreas, once a tumor has been stablished: it promotes proliferation of several PDAC cell lines *in vitro* (Benod *et al.*, 2011) and its overexpression is associated to a worse clinical outcome in human patients with pancreatic cancer (Dong *et al.*, 2011). Interestingly, mitochondria are also associated with cancer cell survival (Vyas, Zaganjor and Haigis, 2016), suggesting a mechanism through which NR5A2 may promote mitochondrial function and prevent pancreatic disease while contributing to tumor cell survival. The effects of NR5A2 on mitochondrial function and cancer cell survival have been reviewed by Michalek and Brunner (2020).

## 4. T cells could mediate the protective effects of gut microbiome depletion in *Nr5a2*$^{+/-}$ mice

The sub-inflammatory state induced by gut microbiome depletion in basal conditions suppressed pre-inflammation in *Nr5a2*$^{+/-}$ mice, suggesting that the protective effects of ABX could partially result from the inhibition of basal pre-inflammation. To determine whether this effect was mediated by specific TFs, I performed motif analysis on the promoters of genes in the leading edge of pathways that were down-regulated in ABX-treated mice. This unveiled motifs that were enriched in *wt* and/or *Nr5a2*$^{+/-}$ mice, including those for CEBPB, ELF3, PU.1, KLF14, IRF8, SPIB, ETS1, and ERG. Only the PU.1 and IRF8 motifs were present among those significantly enriched both in *wt* and *Nr5a2*$^{+/-}$ mice, pointing to their participation in the induction of the sub-inflammatory state in both mouse genotypes. The transcripts coding for PU.1 and IRF8 were down-regulated both in the pancreas of ABX-treated mice and in the intestine of GF mice (compared to normal mice), supporting that they may contribute to the effects of gut microbiome depletion. In addition, expression of both TFs displayed a positive correlation with signatures that reflected the effect of ABX in *wt* and *Nr5a2*$^{+/-}$ mice. Among them, PU.1

displayed the highest correlation (r = 0.81-0.82), suggesting that it may be the primary regulator of the anti-inflammatory effect of ABX.

PU.1 is a well-known regulator of immune cell development and differentiation (Li, Hao and Hu, 2020), leading to the hypothesis that the protective effects of gut microbiome depletion could be mediated through the modulation of the immune system prior to the induction of mild AP. I postulate two different scenarios: one in which gut microbiome depletion could affect the abundance or function of inflammatory cells involved in the pathophysiology of AP through an effect on PU.1 expression and another one in which an effect in the abundance of PU.1 expressing inflammatory cells could result in a reduction of PU.1 expression (Fig. D4).

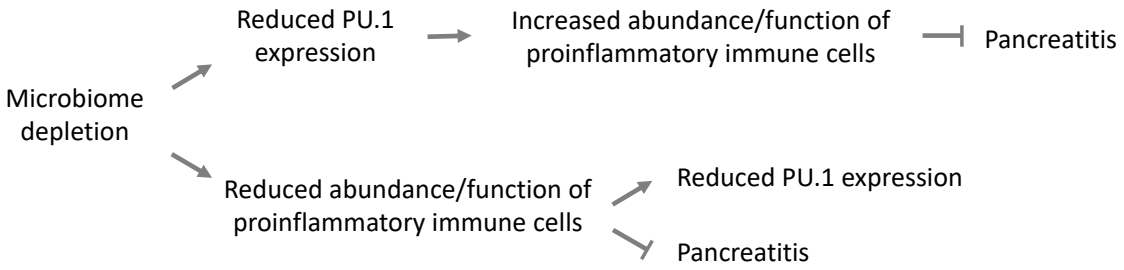


**Figure D4: Mechanisms through which gut microbiome depletion could protect from pancreatitis through the regulation of pro-inflammatory immune cells.**

Based on single cell RNA-seq data, PU.1 expression in the pancreas is restricted to the macrophage compartment (data not shown), suggesting that the effects of gut microbiome depletion on PU.1 expression could result from a reduction of the number of macrophages in the pancreatic microenvironment. This is consistent with the documented role of macrophages as modulators of the severity of pancreatitis (Xue and Habtezion, 2014; Sendler *et al.*, 2018; Wu *et al.*, 2018, 2020). During early stages of pancreatitis, inflammatory monocytes (CCR2+ expressing monocytes) are recruited from the bone marrow to the inflamed pancreas, where they differentiate into pro-inflammatory M1 macrophages (Wu *et al.*, 2020). The proliferation of tissue resident macrophages may also contribute. Chlodronate-mediated macrophage depletion during the M1-dominated phase has a protective effect on pancreatitis, while depletion during the M2-dominated resolution phase worsens the severity of AP (Wu *et al.*, 2020). Interestingly, the literature supports a role of the gut microbiome in macrophage

polarization. On one hand, LPS is a widely used method to polarise macrophages towards the M1 subtype *in vitro* (Li, Hao and Hu, 2020). On the other, gut microbiome dysbiosis (Kim *et al.*, 2014) and bacterial metabolites (Ji *et al.*, 2016) induce M2 polarization *in vivo*. Thus, an effect of the gut microbiome on resident monocyte/macrophage abundance could explain the sub-inflammatory state leading to pancreatitis protection. In addition, high levels of PU.1 were reported to induce hematopoietic cell differentiation into macrophages (Pospisil *et al.*, 2016), suggesting that microbiome depletion could cause a reduction in macrophage abundance through PU.1 down-regulation. PU.1 is also involved in macrophage polarization and is required for LPS-mediated *in vitro* activation of M1 macrophages (Li, Hao and Hu, 2020), further indicating that the gut microbiome could modulate pancreatic inflammation through an effect on macrophage function.

Mouse MCP-counter analysis revealed a down-regulation of T cell, B cell, memory B cell and monocyte/macrophages in microbiome-depleted mice. These immune cell populations were also up-regulated in the pancreas of *Nr5a2*$^{+/-}$ mice, compared to *wt* controls. While these results suggest that gut microbiome depletion decreases the abundance of these immune cell populations in the pancreas, no differences in the expression of CD45, F480 and PAX5 – markers used to assess leukocyte, macrophage and B cell infiltration respectively – were found across conditions, possibly due to the small proportion of immune cells present in basal pancreas. Alternatively, it may be function rather than cell numbers what is modulated by depletion of the gut flora. To acquire a better understanding of the effects of gut microbiome depletion on the abundance of immune cell populations, I immunoprofiled blood from *wt* and *Nr5a2*$^{+/-}$ mice under three different conditions: basal, post-ABX administration, and upon gut microbiome reconstitution. While gut microbiome depletion had no major effects on the percentage of B cells, monocytes/macrophages and neutrophils, it caused profound alterations in T and CD4+ T cell abundance, consistent with the evidence that CD4+ T cells play a crucial role in pancreatic inflammation (Zhou *et al.*, 2020). While monocytes/macrophages and neutrophils are the major immune populations that infiltrate the inflamed pancreas, CD4+ T cells influence the evolution of AP by migrating into the pancreas and inducing pro-inflammatory cytokine release (Zhou *et al.*, 2020). In addition, CD4+ T cells are expanded in peripheral blood from patients with chronic pancreatitis (Gansauge *et al.*,

2001). Recently, CD4+ T cell depletion was reported to protect from pancreatic inflammation in experimental models of AP (Glaubitz *et al.*, 2020). The results from our blood immunoprofiling revealed that gut microbiome depletion led to a significant decrease in the abundance of CD4+ that was rescued upon gut microbiome reconstitution. These populations were also increased in *Nr5a2*$^{+/-}$ mice in basal conditions and upon reconstitution, indicating an impact of *Nr5a2* haploinsufficieny on CD4+ T cell abundance. These results suggest a correlation between the abundance of these immune cells and pancreatic sensitization to inflammation, suggesting a possible mechanism though which i) *Nr5a2* heterozygosity could promote pancreatic inflammation, ii) gut microbiome depletion could selectively protect *Nr5a2*$^{+/-}$ mice from pancreatitis.

Since splenic CD4+ T cell activation was recently reported to correlate with the severity of AP in mice (Glaubitz *et al.*, 2020), we also immunoprofiled spleens from ABX-treated and control *wt* and *Nr5a2*$^{+/-}$ mice. While we failed to evaluate CD4+ T cell activation due to the lack of expression of the activation marker CD25 (data not shown), our results indicated that control *Nr5a2*$^{+/-}$ mice presented an increased percentage of CD4+ T cells ($P = 0.056$) compared to ABX-treated mice, indicating that microbiome depletion also decreases CD4+ T cell abundance in the spleen. In agreement with this, the gut microbiome has been found to shape CD4+ T cell populations in multiple tissues. Low PU.1 expression promotes T cell differentiation (Rothenberg, Hosokawa and Ungerbäck, 2019) but we cannot rule out that the effects of gut microbiome depletion on T cell levels may be mediated through PU.1. The increased abundance of splenic CD4+ T cell in control *Nr5a2*$^{+/-}$ mice further supports a role of NR5A2 in CD4+ T cell differentiation or survival. In line with this, recent studies have pointed to NR5A2 as a critical regulator of T cell function (Seitz *et al.*, 2019).

## 5. Which are the next steps?

Our results indicate that, while sensitising the pancreas to pancreatic disease, NR5A2 haploinsufficency reduces the penetrance or sensitivity to non-genetic risk factors that predispose for pancreatic cancer development, such as obesity, diabetes and liver steatosis. To validate these observations, we will assess the association of these metabolic

alterations and variability in the *NR5A2* gene in humans, and we will evaluate whether these well-known risk factors for pancreatic disease increase the risk of pancreatitis and pancreatic cancer development in human patients with altered NR5A2 function. If we validate the protective effects of NR5A2 in human data, we will aim to identify the mechanisms involved through the analysis of human transcriptomic data in multiple tissues.

On the other hand, we found that gut microbiome depletion suppresses the effects of NR5A2 haploinsufficency in mouse pancreas, indicating that the genetic defect can be modulated. While no major differences have been observed in the composition of the fecal microbiota between *wt* and *Nr5a2*$^{+/-}$ mice, subtle differences in the duodenum cannot be ruled out. We propose to explore this issue in greater detail, since variability in NR5A2 was recently associated to alpha diversity of the gut microbiome (Kurilshikov *et al.*, 2021). We have shown that the protective effects of gut microbiome depletion could be mediated by the regulation of mitochondrial function and inflammatory cells. We propose to perform a thorough analysis of mitochondrial function and to explore the possibility of suppressing the effects of NR5A2 haploinsufficency using antioxidant treatments. We will also explore the contribution of CD4+T cells to the *Nr5a2*$^{+/-}$ phenotype: we will explore the possibility to modulate inflammation in *Nr5a2*$^{+/-}$ mice using anti-CD4 monoclonal antibodies and attempt to rescue pre-inflammation in microbiome depleted *Nr5a2*$^{+/-}$ mice through adoptive CD4+ T cell transfer. In addition, it would be important to validate our observations in germ-free mice.

Overall, our results reveal a complex interaction between NR5A2 haploinsufficiency and non-genetic factors, in which NR5A2 haploinsufficiency may protect from the effects of specific non-genetic risk factors while sensitising to others. Understanding the mechanisms involved may provide an opportunity to act on modifiable factors to prevent pancreatic disease.

# CONCLUSIONS

1. *Wt* and *Nr5a2*$^{+/-}$ mice have a similar response to HFD administration, except that *Nr5a2*$^{+/-}$ males display an attenuated liver steatosis.

2. HFD administration promotes pancreatic inflammation in *wt* – but not *Nr5a2*$^{+/-}$ - male mice.

3. Administration of broad-spectrum ABX depletes the gut microbiome with no major effects on pancreas histology neither in *wt* nor in *Nr5a2*$^{+/-}$ mice, but it results in up-regulation of the acinar signature in mice of both genotypes.

4. ABX-mediated gut microbiome depletion induces a transcriptomic sub-inflammatory state in the pancreas, both in *wt* and *Nr5a2*$^{+/-}$ mice.

5. ABX-mediated gut microbiome depletion protects *Nr5a2*$^{+/-}$ mice from cerulein-induced pancreatic damage. *Nr5a2* heterozygosity in the gut epithelium and altered barrier function are not the mechanisms through which *Nr5a2* heterozygosity promotes pancreatic inflammation.

6. *Nr5a2*$^{+/-}$ mice have normal bacterial abundance in the pancreas and display a normal fecal microbiome composition and diversity.

7. An exploratory analysis suggests specific bacterial taxa that may predispose *wt* and *Nr5a2*$^{+/-}$ mice to cerulein-induced pancreatic damage.

8. *Nr5a2*$^{+/-}$ mice have elevated levels of circulating and splenic T and CD4+ T cells that are normalised upon ABX administration.

# CONCLUSIONES

1. La administración de una dieta grasa tiene efectos similares en ratones *wt* y *Nr5a2*$^{+/-}$, con la excepción de que los machos *Nr5a2*$^{+/-}$ presentan menos esteatosis hepática.

2. La administración de una dieta grasa induce inflamación pancreática en ratones macho *wt*, pero no *Nr5a2*$^{+/-}$.

3. La administración de antibióticos de amplio espectro elimina la microbiota intestinal sin causar efectos importantes en la histología del páncreas en ratones *wt* y *Nr5a2*$^{+/-}$, pero resulta en la inducción de la firma acinar en ambos genotipos.

4. La eliminación de la microbiota intestinal mediante el uso de antibióticos induce un estado sub-inflamatorio en el páncreas, tanto en ratones *wt* como en *Nr5a2*$^{+/-}$.

5. La eliminación de la microbiota intestinal mediante el uso de antibióticos protege a los ratones *Nr5a2*$^{+/-}$ del daño pancreático inducido por ceruleina. La heterocigosidad para *Nr5a2* en el epitelio intestinal o la alteración de la barrera intestinal no son los mecanismos a través de los cuales la heterocigosis para *Nr5a2* promueve inflamación pancreática.

6. Los ratones *Nr5a2*$^{+/-}$ tienen una cantidad normal de microbiota en el páncreas y no presentan alteraciones en la composición y diversidad de la microbiota fecal.

7. Un análisis exploratorio sugiere la existencia de taxones bacterianos concretos que podrían predisponer a los ratones *wt* y *Nr5a2*$^{+/-}$ al daño pancreático inducido por ceruleina.

8. Los ratones *Nr5a2*$^{+/-}$ tienen niveles elevados de células T y T CD4+ en sangre y en bazo, que se normalizan tras la administración de antibióticos.

# BIBLIOGRAPHY

Ahlgren, U. *et al.* (1998) 'β-Cell-specific inactivation of the mouse Ipf1/Pdx1 gene results in loss of the β-cell phenotype and maturity onset diabetes', *Genes & Development*, 12(12), pp. 1763–1768. doi: 10.1101/gad.12.12.1763.

Ahmed, A., Wong, R. J. and Harrison, S. A. (2015) 'Nonalcoholic Fatty Liver Disease Review: Diagnosis, Treatment, and Outcomes', *Clinical Gastroenterology and Hepatology*, 13(12), pp. 2062–2070. doi: 10.1016/j.cgh.2015.07.029.

Akshintala, V. S. *et al.* (2019) 'The Gut Microbiome in Pancreatic Disease', *Clinical Gastroenterology and Hepatology*, 17(2), pp. 290–295. doi: 10.1016/j.cgh.2018.08.045.

Albai, O., Roman, D. and Frandes, M. (2017) 'Hypertriglyceridemia, an important and independent risk factor for acute pancreatitis in patients with type 2 diabetes mellitus.', *Therapeutics and clinical risk management*, 13, pp. 515–522. doi: 10.2147/TCRM.S134560.

Ammori, B. J. *et al.* (1999) 'Early increase in intestinal permeability in patients with severe acute pancreatitis: correlation with endotoxemia, organ failure, and mortality.', *Journal of gastrointestinal surgery : official journal of the Society for Surgery of the Alimentary Tract*, 3(3), pp. 252–62. doi: 10.1016/s1091-255x(99)80067-5.

Arpaia, N. *et al.* (2013) 'Metabolites produced by commensal bacteria promote peripheral regulatory T-cell generation', *Nature*, 504(7480), pp. 451–455. doi: 10.1038/nature12726.

Arslan, A. A. *et al.* (2010) 'Anthropometric measures, body mass index, and pancreatic cancer: a pooled analysis from the Pancreatic Cancer Cohort Consortium (PanScan).', *Archives of internal medicine*, 170(9), pp. 791–802. doi: 10.1001/archinternmed.2010.63.

Aune, D. *et al.* (2012) 'Body mass index, abdominal fatness and pancreatic cancer risk: a systematic review and non-linear dose-response meta-analysis of prospective studies.', *Annals of oncology : official journal of the European Society for Medical Oncology*, 23(4), pp. 843–52. doi: 10.1093/annonc/mdr398.

Aune, D. *et al.* (2021) 'High Body Mass Index and Central Adiposity Is Associated with Increased Risk of Acute Pancreatitis: A Meta-Analysis.', *Digestive diseases and sciences*, 66(4), pp. 1249–1267. doi: 10.1007/s10620-020-06275-6.

Aykut, B. *et al.* (2019) 'The fungal mycobiome promotes pancreatic oncogenesis via activation of MBL', *Nature*. Springer US, 574(7777), pp. 264–267. doi: 10.1038/s41586-019-1608-2.

Bailey, P. *et al.* (2016) 'Genomic analyses identify molecular subtypes of pancreatic cancer', *Nature*. Nature Publishing Group, 531(7592), pp. 47–52. doi: 10.1038/nature16965.

Al Bander, Z. *et al.* (2020) 'The Gut Microbiota and Inflammation: An Overview.', *International journal of environmental research and public health*, 17(20). doi: 10.3390/ijerph17207618.

Banskota, S., Ghia, J.-E. and Khan, W. I. (2019) 'Serotonin in the gut: Blessing or a curse', *Biochimie*. Société Française de Biochimie et Biologie Moléculaire (SFBBM), 161, pp. 56–64. doi: 10.1016/j.biochi.2018.06.008.

Baquié, M. *et al.* (2011) 'The liver receptor homolog-1 (LRH-1) is expressed in human islets and protects β-cells against stress-induced apoptosis', *Human Molecular Genetics*. Oxford University Press, 20(14), pp. 2823–2833. doi: 10.1093/hmg/ddr193.

Bardeesy, N. and DePinho, R. A. (2002) 'Pancreatic cancer biology and genetics', *Nature Reviews Cancer*, 2(12), pp. 897–909. doi: 10.1038/nrc949.

Basturk, O. *et al.* (2015) 'A revised classification system and recommendations from the Baltimore consensus meeting for neoplastic precursor lesions in the pancreas', in *American*

*Journal of Surgical Pathology*. doi: 10.1097/PAS.0000000000000533.

Batterham, R. L. *et al.* (2006) 'Critical role for peptide YY in protein-mediated satiation and body-weight regulation', *Cell Metabolism*, 4(3), pp. 223–233. doi: 10.1016/j.cmet.2006.08.001.

Bayrer, J. R. *et al.* (2018) 'LRH-1 mitigates intestinal inflammatory disease by maintaining epithelial homeostasis and cell survival', *Nature Communications*. Springer US, pp. 1–10. doi: 10.1038/s41467-018-06137-w.

Beck-Nielsen, H. and Groop, L. C. (1994) 'Metabolic and genetic characterization of prediabetic states. Sequence of events leading to non-insulin-dependent diabetes mellitus.', *Journal of Clinical Investigation*, 94(5), pp. 1714–1721. doi: 10.1172/JCI117518.

Beer, R. L., Parsons, M. J. and Rovira, M. (2016) 'Centroacinar cells: At the center of pancreas regeneration', *Developmental Biology*, 413(1), pp. 8–15. doi: 10.1016/j.ydbio.2016.02.027.

Benedé-Ubieto, R. *et al.* (2020) 'Guidelines and Considerations for Metabolic Tolerance Tests in Mice.', *Diabetes, metabolic syndrome and obesity : targets and therapy*, 13, pp. 439–450. doi: 10.2147/DMSO.S234665.

Benitez, C. M., Goodyer, W. R. and Kim, S. K. (2012) 'Deconstructing pancreas developmental biology', *Cold Spring Harbor Perspectives in Biology*, 4(6), pp. 1–17. doi: 10.1101/cshperspect.a012401.

Benod, C. *et al.* (2011) 'Nuclear receptor liver receptor homologue 1 (LRH-1) regulates pancreatic cancer cell growth and proliferation', *Proceedings of the National Academy of Sciences*, 108(41), pp. 16927–16931. doi: 10.1073/pnas.1112047108.

Beres, T. M. *et al.* (2006) 'PTF1 Is an Organ-Specific and Notch-Independent Basic Helix-Loop-Helix Complex Containing the Mammalian Suppressor of Hairless (RBP-J) or Its Paralogue, RBP-L', *Molecular and Cellular Biology*, 26(1), pp. 117–130. doi: 10.1128/MCB.26.1.117-130.2006.

Bharti, R. and Grimm, D. G. (2021) 'Current challenges and best-practice protocols for microbiome analysis', *Briefings in Bioinformatics*, 22(1), pp. 178–193. doi: 10.1093/bib/bbz155.

Bianco, S. *et al.* (2015) 'LRH-1 controls proliferation in breast tumor cells by regulating CDKN1A gene expression', *Oncogene*, 34(34), pp. 4509–4518. doi: 10.1038/onc.2014.382.

Biankin, A. V. *et al.* (2012) 'Pancreatic cancer genomes reveal aberrations in axon guidance pathway genes', *Nature*, 491(7424), pp. 399–405. doi: 10.1038/nature11547.

Biczo, G. *et al.* (2018) 'Mitochondrial Dysfunction, Through Impaired Autophagy, Leads to Endoplasmic Reticulum Stress, Deregulated Lipid Metabolism, and Pancreatitis in Animal Models', *Gastroenterology*, 154(3), pp. 689–703. doi: 10.1053/j.gastro.2017.10.012.

Blaine, S. A. *et al.* (2010) 'Adult pancreatic acinar cells give rise to ducts but not endocrine cells in response to growth factor signaling', *Development*, 137(14). doi: 10.1242/dev.048421.

Boivin, M. A. *et al.* (2007) 'Mechanism of glucocorticoid regulation of the intestinal tight junction barrier.', *American journal of physiology. Gastrointestinal and liver physiology*, 292(2), pp. G590-8. doi: 10.1152/ajpgi.00252.2006.

Bonadonna, R. C. *et al.* (1990) 'Obesity and insulin resistance in humans: a dose-response study.', *Metabolism: clinical and experimental*, 39(5), pp. 452–9. doi: 10.1016/0026-0495(90)90002-t.

Botrugno, O. A. *et al.* (2004) 'Synergy between LRH-1 and beta-catenin induces G1 cyclin-mediated cell proliferation.', *Molecular cell*, 15(4), pp. 499–509. doi: 10.1016/j.molcel.2004.07.009.

Bouchard, M. F., Taniguchi, H. and Viger, R. S. (2005) 'Protein Kinase A-Dependent Synergism between GATA Factors and the Nuclear Receptor, Liver Receptor Homolog-1, Regulates Human Aromatase (CYP19) PII Promoter Activity in Breast Cancer Cells', *Endocrinology*, 146(11), pp. 4905–4916. doi: 10.1210/en.2005-0187.

Boulias, K. (2004) 'Functional role of G9a-induced histone methylation in small heterodimer partner-mediated transcriptional repression', *Nucleic Acids Research*, 32(20), pp. 6096–6103. doi: 10.1093/nar/gkh947.

Brembeck, F. H. *et al.* (2003) 'The mutant K-ras oncogene causes pancreatic periductal lymphocytic infiltration and gastric mucous neck cell hyperplasia in transgenic mice', *Cancer Research*, 63(9), pp. 2005–2009.

Burris, T. P., Busby, S. A. and Griffin, P. R. (2012) 'Targeting Orphan Nuclear Receptors for Treatment of Metabolic Diseases and Autoimmunity', *Chemistry & Biology*, 19(1), pp. 51–59. doi: 10.1016/j.chembiol.2011.12.011.

Calori, G. *et al.* (2011) 'Prevalence, Metabolic Features, and Prognosis of Metabolically Healthy Obese Italian Individuals', *Diabetes Care*, 34(1), pp. 210–215. doi: 10.2337/dc10-0665.

Carrasco, M. *et al.* (2012) 'GATA4 and GATA6 control mouse pancreas organogenesis', *Journal of Clinical Investigation*, 122(10), pp. 3504–3515. doi: 10.1172/JCI63240.

Carrière, C. *et al.* (2011) 'Acute pancreatitis accelerates initiation and progression to pancreatic cancer in mice expressing oncogenic Kras in the Nestin cell lineage', *PLoS ONE*, 6(11). doi: 10.1371/journal.pone.0027725.

Case, R. M. (1978) 'Synthesis, intracellular transport and discharge of exportable proteins in the pancreatic acinar cell and other cells.', *Biological reviews of the Cambridge Philosophical Society*, pp. 211–347. doi: 10.1111/j.1469-185x.1978.tb01437.x.

Chalkiadaki, A. and Talianidis, I. (2005) 'SUMO-Dependent Compartmentalization in Promyelocytic Leukemia Protein Nuclear Bodies Prevents the Access of LRH-1 to Chromatin', *Molecular and Cellular Biology*, 25(12), pp. 5095–5105. doi: 10.1128/MCB.25.12.5095-5105.2005.

Chanda, D., Xie, Y.-B. and Choi, H.-S. (2010) 'Transcriptional corepressor SHP recruits SIRT1 histone deacetylase to inhibit LRH-1 transactivation', *Nucleic Acids Research*, 38(14), pp. 4607–4619. doi: 10.1093/nar/gkq227.

Chen, Q. *et al.* (2018) 'Association between NR5A2 and the risk of pancreatic cancer, especially among Caucasians: a meta-analysis of case-control studies', *OncoTargets and Therapy*. Dove Medical Press Ltd., 11, pp. 2709–2723. doi: 10.2147/OTT.S157759.

Chen, S. M., Xiong, G. S. and Wu, S. M. (2012) 'Is obesity an indicator of complications and mortality in acute pancreatitis? An updated meta-analysis', *Journal of Digestive Diseases*, 13(5), pp. 244–251. doi: 10.1111/j.1751-2980.2012.00587.x.

Chirgwin, J. M. *et al.* (1979) 'Isolation of biologically active ribonucleic acid from sources enriched in ribonuclease.', *Biochemistry*, 18(24), pp. 5294–9. doi: 10.1021/bi00591a005.

Choi, J. *et al.* (2022) 'Estrogen-Related Receptor γ maintains pancreatic acinar cell function and identity by regulating cellular metabolism', *Gastroenterology*. AGA Institute, (May), pp. 1–18. doi: 10.1053/j.gastro.2022.04.013.

Choi, S. *et al.* (2020) 'Methyl-Sensing Nuclear Receptor Liver Receptor Homolog-1 Regulates Mitochondrial Function in Mouse Hepatocytes.', *Hepatology (Baltimore, Md.)*, 71(3), pp. 1055–1069. doi: 10.1002/hep.30884.

Cobo-Vuilleumier, N., Lorenzo, Petra I, *et al.* (2018) 'LRH-1 agonism favours an immune-islet dialogue which protects against diabetes mellitus', *Nature Communications*, 9(1), p. 1488. doi: 10.1038/s41467-018-03943-0.

Cobo-Vuilleumier, N., Lorenzo, Petra I., *et al.* (2018) 'LRH-1 agonism favours an immune-islet dialogue which protects against diabetes mellitus', *Nature Communications*, 9(1), p. 1488. doi: 10.1038/s41467-018-03943-0.

Cobo-Vuilleumier, N. and Gauthier, B. R. (2020) 'Time for a paradigm shift in treating type 1 diabetes mellitus: coupling inflammation to islet regeneration', *Metabolism: Clinical and Experimental*. W.B. Saunders, p. 154137. doi: 10.1016/j.metabol.2020.154137.

Cobo, I. *et al.* (2018) 'Transcriptional regulation by NR5A2 links differentiation and inflammation in the pancreas', *Nature*, 554(7693), pp. 533–537. doi: 10.1038/nature25751.

Consortium, Gte. (2017) 'Genetic effects on gene expression across human tissues', *Nature*, 550(7675), pp. 204–213. doi: 10.1038/nature24277.

Coste, A. *et al.* (2007) 'LRH-1-mediated glucocorticoid synthesis in enterocytes protects against inflammatory bowel disease.', *Proceedings of the National Academy of Sciences of the United States of America*, 104(32), pp. 13098–103. doi: 10.1073/pnas.0702440104.

Dassaye, R., Naidoo, S. and Cerf, M. E. (2016) 'Transcription factor regulation of pancreatic organogenesis, differentiation and maturation', *Islets*. Taylor & Francis, 8(1), pp. 13–34. doi: 10.1080/19382014.2015.1075687.

David, L. A. *et al.* (2014) 'Diet rapidly and reproducibly alters the human gut microbiome', *Nature*, 505(7484), pp. 559–563. doi: 10.1038/nature12820.

Dawson, D. W. *et al.* (2013) 'High-fat, high-calorie diet promotes early pancreatic neoplasia in the conditional KrasG12D mouse model.', *Cancer prevention research (Philadelphia, Pa.)*, 6(10), pp. 1064–73. doi: 10.1158/1940-6207.CAPR-13-0065.

Decker, K. *et al.* (2006) 'Gata6 is an important regulator of mouse pancreas development', *Developmental Biology*. Academic Press Inc., 298(2), pp. 415–429. doi: 10.1016/j.ydbio.2006.06.046.

DeFronzo, R. A. *et al.* (2015) 'Type 2 diabetes mellitus', *Nature Reviews Disease Primers*, 1(1), p. 15019. doi: 10.1038/nrdp.2015.19.

Delaspre, F. *et al.* (2015) 'Centroacinar Cells Are Progenitors That Contribute to Endocrine Pancreas Regeneration.', *Diabetes*, 64(10), pp. 3499–509. doi: 10.2337/db15-0153.

Desai, B. M. *et al.* (2007) 'Preexisting pancreatic acinar cells contribute to acinar cell, but not islet beta cell, regeneration.', *The Journal of clinical investigation*, 117(4), pp. 971–7. doi: 10.1172/JCI29988.

Diehl, G. E. *et al.* (2013) 'Microbiota restricts trafficking of bacteria to mesenteric lymph nodes by CX3CR1hi cells', *Nature*, 494(7435), pp. 116–120. doi: 10.1038/nature11809.

Dobszai, D. *et al.* (2019) 'Body-mass index correlates with severity and mortality in acute pancreatitis: A meta-analysis.', *World journal of gastroenterology*, 25(6), pp. 729–743. doi: 10.3748/wjg.v25.i6.729.

Dolenšek, J., Rupnik, M. S. and Stožer, A. (2015) 'Structural similarities and differences between the human and the mouse pancreas', *Islets*. Taylor and Francis Inc., 7(1), p. e1024405. doi: 10.1080/19382014.2015.1024405.

Dong, X. *et al.* (2011) 'Abstract 4672: Overexpression of NR5A2/LRH1 in pancreatic cancer and

possible association with clinical outcome', in *Epidemiology*. American Association for Cancer Research, pp. 4672–4672. doi: 10.1158/1538-7445.AM2011-4672.

Drouin, J. (2014) 'Minireview: Pioneer Transcription Factors in Cell Fate Specification', *Molecular Endocrinology*, 28(7), pp. 989–998. doi: 10.1210/me.2014-1084.

Duggavathi, R. *et al.* (2008) 'Liver receptor homolog 1 is essential for ovulation', *Genes and Development*, 22(14). doi: 10.1101/gad.472008.

Ellis, C., Ramzy, A. and Kieffer, T. J. (2017) 'Regenerative medicine and cell-based approaches to restore pancreatic function', *Nature Reviews Gastroenterology & Hepatology*. Nature Publishing Group, 14(10), pp. 612–628. doi: 10.1038/nrgastro.2017.93.

Ezeh, K. J. and Ezeudemba, O. (2021) 'Hyperlipidemia: A Review of the Novel Methods for the Management of Lipids', *Cureus*. doi: 10.7759/cureus.16412.

Falender, A. E. *et al.* (2003) 'Differential expression of steroidogenic factor-1 and FTF/LRH-1 in the rodent ovary', *Endocrinology*, 144(8). doi: 10.1210/en.2002-0137.

Fang, S. *et al.* (2007) 'Coordinated Recruitment of Histone Methyltransferase G9a and Other Chromatin-Modifying Enzymes in SHP-Mediated Regulation of Hepatic Bile Acid Metabolism', *Molecular and Cellular Biology*, 27(4), pp. 1407–1424. doi: 10.1128/MCB.00944-06.

Fassio, E. *et al.* (2004) 'Natural history of nonalcoholic steatohepatitis: a longitudinal study of repeat liver biopsies.', *Hepatology (Baltimore, Md.)*, 40(4), pp. 820–6. doi: 10.1002/hep.20410.

Fayard, E. *et al.* (2003) 'Liver Receptor Homolog 1 Controls the Expression of Carboxyl Ester Lipase', *Journal of Biological Chemistry*, 278(37), pp. 35725–35731. doi: 10.1074/jbc.M302370200.

Fayard, E., Auwerx, J. and Schoonjans, K. (2004) 'LRH-1: an orphan nuclear receptor involved in development, metabolism and steroidogenesis', *Trends in Cell Biology*, 14(5), pp. 250–260. doi: 10.1016/j.tcb.2004.03.008.

Feingold, K. R. (2021) 'Introduction to Lipids and Lipoproteins', *Endotext*, (2).

Fendrich, V. *et al.* (2008) 'Hedgehog signaling is required for effective regeneration of exocrine pancreas.', *Gastroenterology*, 135(2), pp. 621–31. doi: 10.1053/j.gastro.2008.04.011.

Fernandez-Marcos, P. J., Auwerx, J. and Schoonjans, K. (2011) 'Emerging actions of the nuclear receptor LRH-1 in the gut', *Biochimica et Biophysica Acta (BBA) - Molecular Basis of Disease*, 1812(8), pp. 947–955. doi: 10.1016/j.bbadis.2010.12.010.

Von Figura, G. *et al.* (2014) 'Nr5a2 maintains acinar cell differentiation and constrains oncogenic Kras-mediated pancreatic neoplastic initiation', *Gut*, 63(4), pp. 656–664. doi: 10.1136/gutjnl-2012-304287.

Fitzgerald, K. A. and Kagan, J. C. (2020) 'Toll-like Receptors and the Control of Immunity', *Cell*, 180(6), pp. 1044–1066. doi: 10.1016/j.cell.2020.02.041.

Flandez, M. *et al.* (2014) 'Nr5a2 heterozygosity sensitises to, and cooperates with, inflammation in KRas G12V - driven pancreatic tumourigenesis', *Gut*, 63(4), pp. 647–655. doi: 10.1136/gutjnl-2012-304381.

Forsmark, C. and Pham, A. (2018) 'Chronic pancreatitis: Review and update of etiology, risk factors, and management', *F1000Research*, 7. doi: 10.12688/f1000research.12852.1.

Fox, C. S. *et al.* (2007) 'Genome-wide association to body mass index and waist circumference: the Framingham Heart Study 100K project.', *BMC medical genetics*, 8 Suppl 1, p. S18. doi:

10.1186/1471-2350-8-S1-S18.

Frost, F. *et al.* (2020) 'The Gut Microbiome in Patients With Chronic Pancreatitis Is Characterized by Significant Dysbiosis and Overgrowth by Opportunistic Pathogens', *Clinical and Translational Gastroenterology*, 11(9), p. e00232. doi: 10.14309/ctg.0000000000000232.

Fujitani, Y. *et al.* (2006) 'Targeted deletion of a cis -regulatory region reveals differential gene dosage requirements for Pdx1 in foregut organ differentiation and pancreas formation', *Genes & Development*, 20(2), pp. 253–266. doi: 10.1101/gad.1360106.

Fung, T. C., Olson, C. A. and Hsiao, E. Y. (2017) 'Interactions between the microbiota, immune and nervous systems in health and disease', *Nature Neuroscience*, 20(2), pp. 145–155. doi: 10.1038/nn.4476.

Gan, S. I. (2006) 'Hypertriglyceridemia-induced pancreatitis: A case-based review', *World Journal of Gastroenterology*, 12(44), p. 7197. doi: 10.3748/wjg.v12.i44.7197.

Gandhi, S. *et al.* (2022) 'Chronic pancreatitis is a risk factor for pancreatic cancer and incidence increases with duration of disease: A systematic review and meta-analysis.', *Clinical and translational gastroenterology*. doi: 10.14309/ctg.0000000000000463.

Gannon, M. *et al.* (2008) 'pdx-1 function is specifically required in embryonic β cells to generate appropriate numbers of endocrine cell types and maintain glucose homeostasis', *Developmental Biology*. Academic Press Inc., 314(2), pp. 406–417. doi: 10.1016/j.ydbio.2007.10.038.

Gansauge, F. *et al.* (2001) 'Distributional and functional alterations of immunocompetent peripheral blood lymphocytes in patients with chronic pancreatitis.', *Annals of surgery*, 233(3), pp. 365–70. doi: 10.1097/00000658-200103000-00010.

Gao, T. *et al.* (2014) 'Pdx1 Maintains β Cell Identity and Function by Repressing an α Cell Program', *Cell Metabolism*, 19(2), pp. 259–271. doi: 10.1016/j.cmet.2013.12.002.

Gasslander, T. *et al.* (1990) 'Proliferative Response of Different Exocrine Pancreatic Cell Types to Hormonal Stimuli', *Scandinavian Journal of Gastroenterology*, 25(11), pp. 1103–1110. doi: 10.3109/00365529008998541.

Genkinger, J. M. *et al.* (2011) 'A pooled analysis of 14 cohort studies of anthropometric factors and pancreatic cancer risk.', *International journal of cancer*, 129(7), pp. 1708–17. doi: 10.1002/ijc.25794.

Glaubitz, J. *et al.* (2020) 'Experimental pancreatitis is characterized by rapid T cell activation, Th2 differentiation that parallels disease severity, and improvement after CD4+ T cell depletion', *Pancreatology*, 20(8), pp. 1637–1647. doi: 10.1016/j.pan.2020.10.044.

Goodger, R. L. *et al.* (2016) 'Impact of metabolic comorbidities on outcomes of patients with acute pancreatitis: a scoping review.', *Panminerva medica*, 58(1), pp. 86–93. Available at: http://www.ncbi.nlm.nih.gov/pubmed/26633700.

Goodwin, B. *et al.* (2000) 'A Regulatory Cascade of the Nuclear Receptors FXR, SHP-1, and LRH-1 Represses Bile Acid Biosynthesis', *Molecular Cell*, 6(3), pp. 517–526. doi: 10.1016/S1097-2765(00)00051-4.

Gordon, S. (2002) 'Pattern Recognition Receptors', *Cell*, 111(7), pp. 927–930. doi: 10.1016/S0092-8674(02)01201-1.

Grady, T. *et al.* (1996) 'Edema and intrapancreatic trypsinogen activation precede glutathione depletion during caerulein pancreatitis', *American Journal of Physiology*, 271(1 PART 1).

Graña, O. *et al.* (2018) 'Nextpresso: Next Generation Sequencing Expression Analysis Pipeline', *Current Bioinformatics*, 13(6), pp. 583–591. doi: 10.2174/1574893612666170810153850.

Grapin-Botton, A. (2005) 'Ductal cells of the pancreas', *International Journal of Biochemistry and Cell Biology*. Elsevier Ltd, pp. 504–510. doi: 10.1016/j.biocel.2004.07.010.

Grimont, A., Leach, S. D. and Chandwani, R. (2022) 'Uncertain Beginnings: Acinar and Ductal Cell Plasticity in the Development of Pancreatic Cancer', *Cellular and Molecular Gastronterology and Hepatology*, 13(2), pp. 369–382. doi: 10.1016/j.jcmgh.2021.07.014.

Gu, P. *et al.* (2005) 'Orphan Nuclear Receptor LRH-1 Is Required To Maintain Oct4 Expression at the Epiblast Stage of Embryonic Development', *Molecular and Cellular Biology*, 25(9). doi: 10.1128/mcb.25.9.3492-3505.2005.

Guerra, C. *et al.* (2003) 'Tumor induction by an endogenous K-ras oncogene is highly dependent on cellular context', *Cancer Cell*, 4(2), pp. 111–120. doi: 10.1016/S1535-6108(03)00191-0.

Guerra, C. *et al.* (2007) 'Chronic Pancreatitis Is Essential for Induction of Pancreatic Ductal Adenocarcinoma by K-Ras Oncogenes in Adult Mice', *Cancer Cell*, 11(3), pp. 291–302. doi: 10.1016/j.ccr.2007.01.012.

Guerra, C. *et al.* (2011) 'Pancreatitis-induced inflammation contributes to pancreatic cancer by inhibiting oncogene-induced senescence', *Cancer Cell*, 19(6). doi: 10.1016/j.ccr.2011.05.011.

Gukovskaya, A. S. *et al.* (1997) 'Pancreatic acinar cells produce, release, and respond to tumor necrosis factor-α. Role in regulating cell death and pancreatitis', *Journal of Clinical Investigation*, 100(7), pp. 1853–1862. doi: 10.1172/JCI119714.

Gukovsky, I., Pandol, S. J. and Gukovskaya, A. S. (2011) 'Organellar Dysfunction in the Pathogenesis of Pancreatitis', *Antioxidants & Redox Signaling*, 15(10), pp. 2699–2710. doi: 10.1089/ars.2011.4068.

Gupta, S. *et al.* (2019) 'Amplicon sequencing provides more accurate microbiome information in healthy children compared to culturing', *Communications Biology*, 2(1), p. 291. doi: 10.1038/s42003-019-0540-1.

Gutch, M. *et al.* (2015) 'Assessment of insulin sensitivity/resistance', *Indian Journal of Endocrinology and Metabolism*, 19(1), p. 160. doi: 10.4103/2230-8210.146874.

Haghikia, A. *et al.* (2015) 'Dietary Fatty Acids Directly Impact Central Nervous System Autoimmunity via the Small Intestine', *Immunity*, 43(4), pp. 817–829. doi: 10.1016/j.immuni.2015.09.007.

Hah, N. *et al.* (2013) 'Enhancer transcripts mark active estrogen receptor binding sites', *Genome Research*, 23(8), pp. 1210–1223. doi: 10.1101/gr.152306.112.

Hahn, S. A. *et al.* (1996) 'DPC4, a candidate tumor suppressor gene at human chromosome 18q21.1', *Science*, 271(5247). doi: 10.1126/science.271.5247.350.

Halangk, W. *et al.* (2000) 'Role of cathepsin B in intracellular trypsinogen activation and the onset of acute pancreatitis', *Journal of Clinical Investigation*, 106(6), pp. 773–781. doi: 10.1172/JCI9411.

Hale, M. A. *et al.* (2005) 'The homeodomain protein PDX1 is required at mid-pancreatic development for the formation of the exocrine pancreas', *Developmental Biology*, 286(1), pp. 225–237. doi: 10.1016/j.ydbio.2005.07.026.

Hale, M. A. *et al.* (2014) 'The nuclear hormone receptor family member NR5A2 controls aspects of multipotent progenitor cell formation and acinar differentiation during pancreatic

organogenesis', *Development*, 141(16), pp. 3123–3133. doi: 10.1242/dev.109405.

Han, B. and Logsdon, C. D. (1999) 'Cholecystokinin induction of mob-1 chemokine expression in pancreatic acinar cells requires NF-kappaB activation.', *The American journal of physiology*, 277(1), pp. C74-82. doi: 10.1152/ajpcell.1999.277.1.C74.

Han, M.-M. *et al.* (2019) 'The alterations of gut microbiota in mice with chronic pancreatitis.', *Annals of translational medicine*, 7(18), p. 464. doi: 10.21037/atm.2019.08.18.

Haschek-Hock, W. M. *et al.* (2022) 'NEW: Haschek and Rousseaux's Handbook of Toxicologic Pathology, Volume 1: Principles and Practice of Toxicologic Pathology, 4th Edition - 2021.', *International journal of toxicology*, p. 10915818221099126. doi: 10.1177/10915818221099126.

Hattori, T. *et al.* (2014) 'LRH-1 heterozygous knockout mice are prone to mild obesity.', *Endocrine journal*, 61(5), pp. 471–80. doi: 10.1507/endocrj.ej14-0017.

Hayashi, K. Y. *et al.* (2003) 'Differentiation and proliferation of endocrine cells in the regenerating rat pancreas after 90% pancreatectomy', *Archives of Histology and Cytology*, 66(2), pp. 163–174. doi: 10.1679/aohc.66.163.

Heng, J. C. D. *et al.* (2010) 'The Nuclear Receptor Nr5a2 Can Replace Oct4 in the Reprogramming of Murine Somatic Cells to Pluripotent Cells', *Cell Stem Cell*, 6(2). doi: 10.1016/j.stem.2009.12.009.

Hingorani, S. R. *et al.* (2003) 'Preinvasive and invasive ductal pancreatic cancer and its early detection in the mouse', *Cancer Cell*, 4(6), pp. 437–450. doi: 10.1016/S1535-6108(03)00309-X.

Hong, Y. *et al.* (2020) 'High-Fat Diet Aggravates Acute Pancreatitis via TLR4-Mediated Necroptosis and Inflammation in Rats', *Oxidative Medicine and Cellular Longevity*, 2020, pp. 1–10. doi: 10.1155/2020/8172714.

Hou, S. *et al.* (2019) 'Fatty liver disease is associated with the severity of acute pancreatitis:A systematic review and meta-analysis', *International Journal of Surgery*, 65, pp. 147–153. doi: 10.1016/j.ijsu.2019.04.003.

Houbracken, I. *et al.* (2011) 'Lineage Tracing Evidence for Transdifferentiation of Acinar to Duct Cells and Plasticity of Human Pancreas', *Gastroenterology*, 141(2), pp. 731-741.e4. doi: 10.1053/j.gastro.2011.04.050.

Houbracken, I. and Bouwens, L. (2017) 'Acinar cells in the neonatal pancreas grow by self-duplication and not by neogenesis from duct cells', *Scientific Reports*. Springer US, 7(1), p. 12643. doi: 10.1038/s41598-017-12721-9.

Hruban, R. H. *et al.* (2000) 'Progression model for pancreatic cancer.', *Clinical cancer research : an official journal of the American Association for Cancer Research*, 6(8), pp. 2969–72. Available at: http://www.ncbi.nlm.nih.gov/pubmed/10955772.

Huang, S.-C., Lee, C. and Chung, B. (2014) 'Tumor Necrosis Factor Suppresses NR5A2 Activity and Intestinal Glucocorticoid Synthesis to Sustain Chronic Colitis', *Science Signaling*, 7(314). doi: 10.1126/scisignal.2004786.

Jensen, J. N. *et al.* (2005) 'Recapitulation of elements of embryonic development in adult mouse pancreatic regeneration', *Gastroenterology*, 128(3), pp. 728–741. doi: 10.1053/j.gastro.2004.12.008.

Ji, J. *et al.* (2016) 'Microbial metabolite butyrate facilitates M2 macrophage polarization and function.', *Scientific reports*, 6, p. 24838. doi: 10.1038/srep24838.

Jin, K. and Xiang, M. (2019) 'Transcription factor Ptf1a in development, diseases and

reprogramming', *Cellular and Molecular Life Sciences*. Springer International Publishing, 76(5), pp. 921–940. doi: 10.1007/s00018-018-2972-z.

Johnson, C. L. *et al.* (2004) 'Mist1 is necessary for the establishment of granule organization in serous exocrine cells of the gastrointestinal tract', *Mechanisms of Development*, 121(3). doi: 10.1016/j.mod.2004.01.003.

Jones, S. *et al.* (2008) 'Core signaling pathways in human pancreatic cancers revealed by global genomic analyses', *Science*, 321(5897). doi: 10.1126/science.1164368.

Jonsson, J. *et al.* (1994) 'Insulin-promoter-factor 1 is required for pancreas development in mice', *Nature*, 371(6498), pp. 606–609. doi: 10.1038/371606a0.

Kalisz, M. *et al.* (2020) 'HNF1A recruits KDM6A to activate differentiated acinar cell programs that suppress pancreatic cancer', *The EMBO Journal*, 39(9). doi: 10.15252/embj.2019102808.

Kanda, M. *et al.* (2012) 'Presence of somatic mutations in most early-stage pancreatic intraepithelial neoplasia', *Gastroenterology*, 142(4), pp. 730–733. doi: 10.1053/j.gastro.2011.12.042.

Kang, S. H. *et al.* (2013) 'Identification of metabolically active proteobacterial and archaeal communities in the rumen by DNA- and RNA-derived 16S rRNA gene', *Journal of Applied Microbiology*, 115(3). doi: 10.1111/jam.12270.

Kanwar, P. and Kowdley, K. V. (2016) 'The Metabolic Syndrome and Its Influence on Nonalcoholic Steatohepatitis', *Clinics in Liver Disease*, pp. 225–243. doi: 10.1016/j.cld.2015.10.002.

Karlsson, F. H. *et al.* (2013) 'Gut metagenome in European women with normal, impaired and diabetic glucose control.', *Nature*, 498(7452), pp. 99–103. doi: 10.1038/nature12198.

Kartal, E. *et al.* (2022) 'A faecal microbiota signature with high specificity for pancreatic cancer.', *Gut*. doi: 10.1136/gutjnl-2021-324755.

Kawaguchi, Y. *et al.* (2002) 'The role of the transcriptional regulator Ptf1a in converting intestinal to pancreatic progenitors', *Nature Genetics*, 32(1), pp. 128–134. doi: 10.1038/ng959.

Kawasaki, T. and Kawai, T. (2014) 'Toll-Like Receptor Signaling Pathways', *Frontiers in Immunology*, 5(461), pp. 1–8. doi: 10.3389/fimmu.2014.00461.

Khatua, B., El-Kurdi, B. and Singh, V. P. (2017) 'Obesity and pancreatitis', *Current Opinion in Gastroenterology*, 33(5), pp. 374–382. doi: 10.1097/MOG.0000000000000386.

Kichaev, G. *et al.* (2019) 'Leveraging Polygenic Functional Enrichment to Improve GWAS Power.', *American journal of human genetics*, 104(1), pp. 65–75. doi: 10.1016/j.ajhg.2018.11.008.

Kidd, M. *et al.* (2009) 'IL1beta- and LPS-induced serotonin secretion is increased in EC cells derived from Crohn's disease.', *Neurogastroenterology and Motility*, 21(4), pp. 439–50. doi: 10.1111/j.1365-2982.2008.01210.x.

Kim, J. R. *et al.* (2021) 'Microbiome Markers of Pancreatic Cancer Based on Bacteria-Derived Extracellular Vesicles Acquired from Blood Samples: A Retrospective Propensity Score Matching Analysis.', *Biology*, 10(3). doi: 10.3390/biology10030219.

Kim, W. Y. and Sharpless, N. E. (2006) 'The Regulation of INK4/ARF in Cancer and Aging', *Cell*. doi: 10.1016/j.cell.2006.10.003.

Kim, Y.-G. *et al.* (2014) 'Gut Dysbiosis Promotes M2 Macrophage Polarization and Allergic Airway Inflammation via Fungi-Induced PGE2', *Cell Host & Microbe*, 15(1), pp. 95–102. doi: 10.1016/j.chom.2013.12.010.

Knopp, J. L., Holder-Pearson, L. and Chase, J. G. (2019) 'Insulin Units and Conversion Factors: A Story of Truth, Boots, and Faster Half-Truths', *Journal of Diabetes Science and Technology*, 13(3), pp. 597–600. doi: 10.1177/1932296818805074.

Krapp, A. *et al.* (1998) 'The bHLH protein PTF1-p48 is essential for the formation of the exocrine and the correct spatial organization of the endocrine pancreas', *Genes & Development*, 12(23), pp. 3752–3763. doi: 10.1101/gad.12.23.3752.

Krylova, I. N. *et al.* (2005) 'Structural Analyses Reveal Phosphatidyl Inositols as Ligands for the NR5 Orphan Receptors SF-1 and LRH-1', *Cell*, 120(3), pp. 343–355. doi: 10.1016/j.cell.2005.01.024.

Kurilshikov, A. *et al.* (2021) 'Large-scale association analyses identify host factors influencing human gut microbiome composition', *Nature Genetics*, 53(2), pp. 156–165. doi: 10.1038/s41588-020-00763-1.

Lagkouvardos, I. *et al.* (2019) 'Sequence and cultivation study of Muribaculaceae reveals novel species, host preference, and functional potential of this yet undescribed family', *Microbiome*, 7(1), p. 28. doi: 10.1186/s40168-019-0637-2.

Lai, T.-C. and Hu, M.-C. (2019) 'Regulation of liver receptor homologue-1 by DDB2 E3 ligase activity is critical for hepatic glucose metabolism', *Scientific Reports*, 9(1), p. 5304. doi: 10.1038/s41598-019-41411-x.

Lankisch, P. G. *et al.* (2002) 'What is the risk of alcoholic pancreatitis in heavy drinkers?', *Pancreas*. doi: 10.1097/00006676-200211000-00015.

Larraufie, P. *et al.* (2017) 'TLR ligands and butyrate increase Pyy expression through two distinct but inter-regulated pathways', *Cellular Microbiology*, 19(2), p. e12648. doi: 10.1111/cmi.12648.

Larsson, S. C., Orsini, N. and Wolk, A. (2007) 'Body mass index and pancreatic cancer risk: A meta-analysis of prospective studies.', *International journal of cancer*, 120(9), pp. 1993–8. doi: 10.1002/ijc.22535.

Lazarus, K. A. *et al.* (2012) 'Therapeutic potential of Liver Receptor Homolog-1 modulators', *The Journal of Steroid Biochemistry and Molecular Biology*, 130(3–5), pp. 138–146. doi: 10.1016/j.jsbmb.2011.12.017.

Lebrun, L. J. *et al.* (2017) 'Enteroendocrine L Cells Sense LPS after Gut Barrier Injury to Enhance GLP-1 Secretion', *Cell Reports*. Elsevier B.V., 21(5), pp. 1160–1168. doi: 10.1016/j.celrep.2017.10.008.

Lee, J. M. *et al.* (2011) 'A nuclear-receptor-dependent phosphatidylcholine pathway with antidiabetic effects.', *Nature*, 474(7352), pp. 506–10. doi: 10.1038/nature10111.

Lee, P. J. and Papachristou, G. I. (2019) 'New insights into acute pancreatitis', *Nature Reviews Gastroenterology & Hepatology*, 16(8), pp. 479–496. doi: 10.1038/s41575-019-0158-2.

Lee, Y.-K. *et al.* (2006) 'Phosphorylation of the Hinge Domain of the Nuclear Hormone Receptor LRH-1 Stimulates Transactivation', *Journal of Biological Chemistry*, 281(12), pp. 7850–7855. doi: 10.1074/jbc.M509115200.

Lee, Y.-K. *et al.* (2008) 'Liver receptor homolog-1 regulates bile acid homeostasis but is not essential for feedback regulation of bile acid synthesis.', *Molecular endocrinology (Baltimore, Md.)*, 22(6), pp. 1345–56. doi: 10.1210/me.2007-0565.

Lee, Y.-K. and Moore, D. D. (2002) 'Dual Mechanisms for Repression of the Monomeric Orphan Receptor Liver Receptor Homologous Protein-1 by the Orphan Small Heterodimer Partner',

*Journal of Biological Chemistry*, 277(4), pp. 2463–2467. doi: 10.1074/jbc.M105161200.

Leech, C. A. *et al.* (2011) 'Molecular physiology of glucagon-like peptide-1 insulin secretagogue action in pancreatic β cells', *Progress in Biophysics and Molecular Biology*. Elsevier Ltd, 107(2), pp. 236–247. doi: 10.1016/j.pbiomolbio.2011.07.005.

Leeson, T. S. and Leeson, R. (1986) 'Close association of centroacinar/ductular and insular cells in the rat pancreas.', *Histology and histopathology*, 1(1), pp. 33–42. Available at: http://www.ncbi.nlm.nih.gov/pubmed/2980100.

Lemercier, C. *et al.* (1997) 'Mist1: A novel basic helix-loop-helix transcription factor exhibits a developmentally regulated expression pattern', *Developmental Biology*, 182(1). doi: 10.1006/dbio.1996.8454.

Li, D. and Wu, M. (2021) 'Pattern recognition receptors in health and diseases', *Signal Transduction and Targeted Therapy*, 6(1), p. 291. doi: 10.1038/s41392-021-00687-0.

Li, G., Hao, W. and Hu, W. (2020) 'Transcription factor PU.1 and immune cell differentiation (Review)', *International Journal of Molecular Medicine*, 46(6), pp. 1943–1950. doi: 10.3892/ijmm.2020.4763.

Li, M. *et al.* (1998) 'Cloning and characterization of a novel human hepatocyte transcription factor, hB1F, which binds and activates enhancer II of hepatitis B virus', *Journal of Biological Chemistry*, 273(44). doi: 10.1074/jbc.273.44.29022.

Liang, W. *et al.* (2020) 'FAM3D is essential for colon homeostasis and host defense against inflammation associated carcinogenesis.', *Nature communications*, 11(1), p. 5912. doi: 10.1038/s41467-020-19691-z.

Lim, S. M. *et al.* (2015) 'Association between Obesity Indices and Insulin Resistance among Healthy Korean Adolescents: The JS High School Study', *PLOS ONE*. Edited by V. Sanchez-Margalet, 10(5), p. e0125238. doi: 10.1371/journal.pone.0125238.

Lin, C.-C. J. and Wang, M. C. (2017) 'Microbial metabolites regulate host lipid metabolism through NR5A-Hedgehog signalling.', *Nature cell biology*, 19(5), pp. 550–557. doi: 10.1038/ncb3515.

Liou, G.-Y. *et al.* (2013) 'Macrophage-secreted cytokines drive pancreatic acinar-to-ductal metaplasia through NF-κB and MMPs', *Journal of Cell Biology*, 202(3), pp. 563–577. doi: 10.1083/jcb.201301001.

Logsdon, C. D. and Ji, B. (2013) 'The role of protein synthesis and digestive enzymes in acinar cell injury', *Nature Reviews Gastroenterology & Hepatology*, 10(6), pp. 362–370. doi: 10.1038/nrgastro.2013.36.

López de Maturana, E. *et al.* (2021) 'A multilayered post-GWAS assessment on genetic susceptibility to pancreatic cancer', *Genome Medicine*. Genome Medicine, 13(1), pp. 1–18. doi: 10.1186/s13073-020-00816-4.

Lotta, L. A. *et al.* (2018) 'Association of Genetic Variants Related to Gluteofemoral vs Abdominal Fat Distribution With Type 2 Diabetes, Coronary Disease, and Cardiovascular Risk Factors.', *JAMA*, 320(24), pp. 2553–2563. doi: 10.1001/jama.2018.19329.

Love, M. I., Huber, W. and Anders, S. (2014) 'Moderated estimation of fold change and dispersion for RNA-seq data with DESeq2.', *Genome biology*, 15(12), p. 550. doi: 10.1186/s13059-014-0550-8.

Lu, T. T. *et al.* (2000) 'Molecular Basis for Feedback Regulation of Bile Acid Synthesis by Nuclear

Receptors', *Molecular Cell*, 6(3), pp. 507–515. doi: 10.1016/S1097-2765(00)00050-2.

Lüttges, J. *et al.* (2001) 'Allelic loss is often the first hit in the biallelic inactivation of the p53 and DPC4 genes during pancreatic carcinogenesis', *American Journal of Pathology*, 158(5). doi: 10.1016/S0002-9440(10)64123-5.

MacDonald, R. J., Swift, G. H. and Real, F. X. (2010) 'Transcriptional control of acinar development and homeostasis', *Progress in Molecular Biology and Translational Science*, 97(C), pp. 1–40. doi: 10.1016/B978-0-12-385233-5.00001-5.

Magenheim, J. *et al.* (2011) 'Blood vessels restrain pancreas branching, differentiation and growth', *Development*, 138(21), pp. 4743–4752. doi: 10.1242/dev.066548.

Maitra, A. and Hruban, R. H. (2008) 'Pancreatic cancer', *Annual Review of Pathology: Mechanisms of Disease*, 3(2), pp. 157–188. doi: 10.1146/annurev.pathmechdis.3.121806.154305.

Malayil, L. *et al.* (2020) 'Metabolically-active bacteria in reclaimed water and ponds revealed using bromodeoxyuridine DNA labeling coupled with 16S rRNA and shotgun sequencing', *Water Research*, 184. doi: 10.1016/j.watres.2020.116185.

Malumbres, M. and Barbacid, M. (2003) 'RAS oncogenes: The first 30 years', *Nature Reviews Cancer*. doi: 10.1038/nrc1097.

Mameishvili, E. *et al.* (2019) 'Aldh1b1 expression defines progenitor cells in the adult pancreas and is required for Kras-induced pancreatic cancer', *Proceedings of the National Academy of Sciences of the United States of America*, 116(41), pp. 20679–20688. doi: 10.1073/pnas.1901075116.

Mangelsdorf, D. J. *et al.* (1995) 'The nuclear receptor superfamily: The second decade', *Cell*, 83(6), pp. 835–839. doi: 10.1016/0092-8674(95)90199-X.

el Marjou, F. *et al.* (2004) 'Tissue-specific and inducible Cre-mediated recombination in the gut epithelium.', *Genesis (New York, N.Y. : 2000)*, 39(3), pp. 186–93. doi: 10.1002/gene.20042.

Martin, A. M. *et al.* (2019) 'The Influence of the Gut Microbiome on Host Metabolism Through the Regulation of Gut Hormone Release', *Frontiers in Physiology*, 10(428), pp. 1–11. doi: 10.3389/fphys.2019.00428.

Martinelli, P., Cañamero, M., del Pozo, N., *et al.* (2013) 'Gata6 is required for complete acinar differentiation and maintenance of the exocrine pancreas in adult mice.', *Gut*, 62(10), pp. 1481–8. doi: 10.1136/gutjnl-2012-303328.

Martinelli, P., Cañamero, M., Del Pozo, N., *et al.* (2013) 'Gata6 is required for complete acinar differentiation and maintenance of the exocrine pancreas in adult mice', *Gut*, 62(10), pp. 1481–1488. doi: 10.1136/gutjnl-2012-303328.

Martinelli, P. *et al.* (2016) 'The acinar regulator Gata6 suppresses KRasG12V-driven pancreatic tumorigenesis in mice', *Gut*, 65(3), pp. 476–486. doi: 10.1136/gutjnl-2014-308042.

Masui, T. *et al.* (2007) 'Early pancreatic development requires the vertebrate Suppressor of Hairless (RBPJ) in the PTF1 bHLH complex', *Genes & Development*, 21(20), pp. 2629–2643. doi: 10.1101/gad.1575207.

Masui, T. *et al.* (2008) 'Transcriptional Autoregulation Controls Pancreatic Ptf1a Expression during Development and Adulthood', *Molecular and Cellular Biology*. American Society for Microbiology, 28(17), pp. 5458–5468. doi: 10.1128/MCB.00549-08.

Masui, T. *et al.* (2010) 'Replacement of Rbpj With Rbpjl in the PTF1 Complex Controls the Final Maturation of Pancreatic Acinar Cells', *Gastroenterology*. W.B. Saunders, 139(1), pp. 270–280.

doi: 10.1053/j.gastro.2010.04.003.

Mata, A. J. and Jasul, G. (2017) 'Prevalence of metabolic syndrome and its individual features across different (Normal, overweight, pre-obese and obese) body mass index (BMI) categories in a tertiary hospital in the Philippines', *Journal of the ASEAN Federation of Endocrine Societies*, 32(2). doi: 10.15605/jafes.032.02.04.

Mataki, C. *et al.* (2007) 'Compromised intestinal lipid absorption in mice with a liver-specific deficiency of liver receptor homolog 1.', *Molecular and cellular biology*, 27(23), pp. 8330–9. doi: 10.1128/MCB.00852-07.

Matthews, D. R. *et al.* (1985) 'Homeostasis model assessment: insulin resistance and beta-cell function from fasting plasma glucose and insulin concentrations in man.', *Diabetologia*, 28(7), pp. 412–9. doi: 10.1007/BF00280883.

Mayerle, J. *et al.* (2005) 'Extracellular cleavage of E-cadherin by leukocyte elastase during acute experimental pancreatitis in rats', *Gastroenterology*, 129(4), pp. 1251–1267. doi: 10.1053/j.gastro.2005.08.002.

Mays, S. G. *et al.* (2017) 'Structure and Dynamics of the Liver Receptor Homolog 1-PGC1α Complex.', *Molecular pharmacology*, 92(1), pp. 1–11. doi: 10.1124/mol.117.108514.

McFarlane, S. I., Banerji, M. and Sowers, J. R. (2001) 'Insulin resistance and cardiovascular disease.', *The Journal of clinical endocrinology and metabolism*, 86(2), pp. 713–8. doi: 10.1210/jcem.86.2.7202.

Michalek, S. and Brunner, T. (2021) 'Nuclear-mitochondrial crosstalk: On the role of the nuclear receptor liver receptor homolog-1 (NR5A2) in the regulation of mitochondrial metabolism, cell survival, and cancer', *IUBMB Life*, 73(3), pp. 592–610. doi: 10.1002/iub.2386.

Minoguchi, S. *et al.* (1997) 'RBP-L, a transcription factor related to RBP-Jkappa', *Molecular and Cellular Biology*, 17(5), pp. 2679–2687. doi: 10.1128/MCB.17.5.2679.

Miyaki, M. and Kuroki, T. (2003) 'Role of Smad4 (DPC4) inactivation in human cancer', *Biochemical and Biophysical Research Communications*. doi: 10.1016/S0006-291X(03)01066-0.

Miyazaki, S., Tashiro, F. and Miyazaki, J. (2016) 'Transgenic Expression of a Single Transcription Factor Pdx1 Induces Transdifferentiation of Pancreatic Acinar Cells to Endocrine Cells in Adult Mice', *PLOS ONE*. Edited by F. X. Real, 11(8), p. e0161190. doi: 10.1371/journal.pone.0161190.

Molero, X. *et al.* (2007) 'Pancreas transcription factor 1α expression is regulated in pancreatitis', *European Journal of Clinical Investigation*, 37(10), pp. 791–801. doi: 10.1111/j.1365-2362.2007.01856.x.

Molero, X. *et al.* (2012) 'Gene expression dynamics after murine pancreatitis unveils novel roles for Hnf1α in acinar cell homeostasis', *Gut*, 61(8), pp. 1187–1196. doi: 10.1136/gutjnl-2011-300360.

Morris, J. P. *et al.* (2010) 'Beta-catenin blocks Kras-dependent reprogramming of acini into pancreatic cancer precursor lesions in mice.', *The Journal of clinical investigation*, 120(2), pp. 508–20. doi: 10.1172/JCI40045.

Morris, J. P., Wang, S. C. and Hebrok, M. (2010) 'KRAS, Hedgehog, Wnt and the twisted developmental biology of pancreatic ductal adenocarcinoma', *Nature Reviews Cancer*. doi: 10.1038/nrc2899.

Moskaluk, C. A., Hruban, R. H. and Kern, S. E. (1997) 'p16 and K-ras gene mutations in the intraductal precursors of human pancreatic adenocarcinoma', *Cancer Research*, 57(11).

Mueller, M. *et al.* (2006) 'The nuclear receptor LRH-1 critically regulates extra-adrenal glucocorticoid synthesis in the intestine.', *The Journal of experimental medicine*, 203(9), pp. 2057–62. doi: 10.1084/jem.20060357.

Musille, P. M. *et al.* (2012) 'Antidiabetic phospholipid–nuclear receptor complex reveals the mechanism for phospholipid-driven gene regulation', *Nature Structural & Molecular Biology*, 19(5), pp. 532–537. doi: 10.1038/nsmb.2279.

Nagasao, J. *et al.* (2005) 'Morphological Changes in the Rat Endocrine Pancreas within 12 h of Intravenous Streptozotocin Administration', *Anatomia, Histologia, Embryologia: Journal of Veterinary Medicine Series C*, 34(1), pp. 42–47. doi: 10.1111/j.1439-0264.2004.00566.x.

Nishida, C. *et al.* (2004) 'Appropriate body-mass index for Asian populations and its implications for policy and intervention strategies', *The Lancet*, 363(9403). doi: 10.1016/S0140-6736(03)15268-3.

Nitta, M. *et al.* (1999) 'CPF: An orphan nuclear receptor that regulates liver-specific expression of the human cholesterol 7α-hydroxylase gene', *Proceedings of the National Academy of Sciences of the United States of America*, 96(12). doi: 10.1073/pnas.96.12.6660.

Notta, F. *et al.* (2016) 'A renewed model of pancreatic cancer evolution based on genomic rearrangement patterns', *Nature*, 538(7625). doi: 10.1038/nature19823.

Notta, F., Hahn, S. A. and Real, F. X. (2017) 'A genetic roadmap of pancreatic cancer: Still evolving', *Gut*, 66(12). doi: 10.1136/gutjnl-2016-313317.

O'Konski, M. S. and Pandol, S. J. (1993) 'Cholecystokinin jmv-180 and caerulein effects on the pancreatic acinar cell cytoskeleton', *Pancreas*, 8(5). doi: 10.1097/00006676-199309000-00018.

OECD Obesity Update (2017) 'Obesity Update 2017', *Diabetologe*, 13(5).

Ohlsson, H., Karlsson, K. and Edlund, T. (1993) 'IPF1, a homeodomain-containing transactivator of the insulin gene.', *The EMBO Journal*, 12(11), pp. 4251–4259. doi: 10.1002/j.1460-2075.1993.tb06109.x.

Ortlund, E. A. *et al.* (2005) 'Modulation of human nuclear receptor LRH-1 activity by phospholipids and SHP', *Nature Structural & Molecular Biology*, 12(4), pp. 357–363. doi: 10.1038/nsmb910.

Pan, F. C. and Wright, C. (2011) 'Pancreas organogenesis: From bud to plexus to gland', *Developmental Dynamics*, 240(3), pp. 530–565. doi: 10.1002/dvdy.22584.

Pan, L. *et al.* (2019) 'Clostridium butyricum Strains Suppress Experimental Acute Pancreatitis by Maintaining Intestinal Homeostasis', *Molecular Nutrition & Food Research*, p. 1801419. doi: 10.1002/mnfr.201801419.

Pan, L. *et al.* (2021) 'Gut microbiota in pancreatic diseases: possible new therapeutic strategies', *Acta Pharmacologica Sinica*, 42(7), pp. 1027–1039. doi: 10.1038/s41401-020-00532-0.

Parét, J. F. *et al.* (2001) 'The Mouse Fetoprotein Transcription Factor (FTF) Gene Promoter Is Regulated by Three GATA Elements with Tandem E Box and Nkx Motifs, and FTF in Turn Activates the Hnf3β, Hnf4α, and Hnf1α Gene Promoters', *Journal of Biological Chemistry*, 276(16). doi: 10.1074/jbc.M010737200.

Patterson, R. E. *et al.* (2004) 'A comprehensive examination of health conditions associated with obesity in older adults', *American Journal of Preventive Medicine*, 27(5). doi: 10.1016/j.amepre.2004.08.001.

Petersen, G. M. *et al.* (2010) 'A GWAS identifies pancreatic cancer ssceptibility loci chromosomes 13q22.1, 1q32.1 and 5p15.33', *Nature Genetics*, 42(3), pp. 224–228. doi: 10.1038/ng.522.A.

Petitprez, F. *et al.* (2020) 'The murine Microenvironment Cell Population counter method to estimate abundance of tissue-infiltrating immune and stromal cell populations in murine samples using gene expression.', *Genome medicine*, 12(1), p. 86. doi: 10.1186/s13073-020-00783-w.

Philip, B. *et al.* (2013) 'A high-fat diet activates oncogenic Kras and COX2 to induce development of pancreatic ductal adenocarcinoma in mice.', *Gastroenterology*, 145(6), pp. 1449–58. doi: 10.1053/j.gastro.2013.08.018.

Pin, C. L. *et al.* (2001) 'The bHLH transcription factor Mist1 is required to maintain exocrine pancreas cell organization and acinar cell identity', *Journal of Cell Biology*, 155(3). doi: 10.1083/jcb.200105060.

Pospisil, V. *et al.* (2016) 'Graded PU.1 Levels Regulate Granulocyte Vs. Macrophage Genes Via Multiple Enhancer Elements', *Blood*, 128(22), pp. 403–403. doi: 10.1182/blood.V128.22.403.403.

Pulit, S. L. *et al.* (2019) 'Meta-analysis of genome-wide association studies for body fat distribution in 694 649 individuals of European ancestry.', *Human molecular genetics*, 28(1), pp. 166–174. doi: 10.1093/hmg/ddy327.

Puri, S. and Hebrok, M. (2010) 'Cellular Plasticity within the Pancreas— Lessons Learned from Development', *Developmental Cell*. Cell Press, 18(3), pp. 342–356. doi: 10.1016/j.devcel.2010.02.005.

Pushalkar, S. *et al.* (2018) 'The pancreatic cancer microbiome promotes oncogenesis by induction of innate and adaptive immune suppression', *Cancer Discovery*, 8(4), pp. 403–416. doi: 10.1158/2159-8290.CD-17-1134.

Qin, J. *et al.* (2012) 'A metagenome-wide association study of gut microbiota in type 2 diabetes.', *Nature*, 490(7418), pp. 55–60. doi: 10.1038/nature11450.

Rahib, L. *et al.* (2014) 'Projecting cancer incidence and deaths to 2030: The unexpected burden of thyroid, liver, and pancreas cancers in the united states', *Cancer Research*. doi: 10.1158/0008-5472.CAN-14-0155.

Rahman, M. S. *et al.* (2021) 'Role of insulin in health and disease: An update', *International Journal of Molecular Sciences*. doi: 10.3390/ijms22126403.

Rao, A. *et al.* (2016) 'Inhibition of ileal bile acid uptake protects against nonalcoholic fatty liver disease in high-fat diet-fed mice.', *Science translational medicine*, 8(357), p. 357ra122. doi: 10.1126/scitranslmed.aaf4823.

Rausa, F. M. *et al.* (1999) 'The nuclear receptor fetoprotein transcription factor is coexpressed with its target gene HNF-3β in the developing murine liver intestine and pancreas', *Mechanisms of Development*, 89(1–2), pp. 185–188. doi: 10.1016/S0925-4773(99)00209-9.

Rawla, P., Sunkara, T. and Gaduputi, V. (2019) 'Epidemiology of Pancreatic Cancer: Global Trends, Etiology and Risk Factors', *World Journal of Oncology*, 10(1). doi: 10.14740/wjon1166.

Real, F. X. (2003) 'A "catastrophic hypothesis" for pancreas cancer progression', *Gastroenterology*. doi: 10.1016/S0016-5085(03)00389-5.

Real, F. X., Cibrián-Uhalte, E. and Martinelli, P. (2008) 'Pancreatic Cancer Development and Progression: Remodeling the Model', *Gastroenterology*, 135(3), pp. 724–728. doi: 10.1053/j.gastro.2008.07.033.

Reddy, S. K. (2013) 'Nonalcoholic fatty liver disease is associated with benign gastrointestinal disorders', *World Journal of Gastroenterology*, 19(45), p. 8301. doi: 10.3748/wjg.v19.i45.8301.

Redston, M. S. *et al.* (1994) 'p53 mutations in pancreatic carcinoma and evidence of common involvement of homocopolymer tracts in DNA microdeletions.', *Cancer research*, 54(11), pp. 3025–33. Available at: http://www.ncbi.nlm.nih.gov/pubmed/8187092.

Reich, M. *et al.* (2006) 'GenePattern 2.0.', *Nature genetics*, 38(5), pp. 500–1. doi: 10.1038/ng0506-500.

Reikvam, D. H. *et al.* (2011) 'Depletion of murine intestinal microbiota: Effects on gut mucosa and epithelial gene expression', *PLoS ONE*, 6(3), pp. 1–13. doi: 10.1371/journal.pone.0017996.

Riquelme, E. *et al.* (2019) 'Tumor Microbiome Diversity and Composition Influence Pancreatic Cancer Outcomes', *Cell*, 178(4), pp. 795-806.e12. doi: 10.1016/j.cell.2019.07.008.

Rogers, G. B. *et al.* (2016) 'From gut dysbiosis to altered brain function and mental illness: mechanisms and pathways', *Molecular Psychiatry*. Nature Publishing Group, 21(6), pp. 738–748. doi: 10.1038/mp.2016.50.

Roshan-Moniri, M. *et al.* (2014) 'Orphan nuclear receptors as drug targets for the treatment of prostate and breast cancers', *Cancer Treatment Reviews*, 40(10), pp. 1137–1152. doi: 10.1016/j.ctrv.2014.10.005.

Rothenberg, E. V., Hosokawa, H. and Ungerbäck, J. (2019) 'Mechanisms of Action of Hematopoietic Transcription Factor PU.1 in Initiation of T-Cell Development', *Frontiers in Immunology*, 10. doi: 10.3389/fimmu.2019.00228.

Rouse, R. *et al.* (2014) 'High fat diet and GLP-1 drugs induce pancreatic injury in mice', *Toxicology and Applied Pharmacology*. Elsevier B.V., 276(2), pp. 104–114. doi: 10.1016/j.taap.2014.01.021.

Rudzki, L. *et al.* (2021) 'Gut microbiota-derived vitamins – underrated powers of a multipotent ally in psychiatric health and disease', *Progress in Neuro-Psychopharmacology and Biological Psychiatry*, 107(110240), p. 110240. doi: 10.1016/j.pnpbp.2020.110240.

Rukstalis, J. M. *et al.* (2003) 'Exocrine specific expression of connexin32 is dependent on the basic helix-loop-helix transcription factor Mist1', *Journal of Cell Science*. doi: 10.1242/jcs.00631.

Sablin, E. P. *et al.* (2003) 'Structural Basis for Ligand-Independent Activation of the Orphan Nuclear Receptor LRH-1', *Molecular Cell*, 11(6), pp. 1575–1585. doi: 10.1016/S1097-2765(03)00236-3.

Sablin, E. P. *et al.* (2015) 'Structure of Liver Receptor Homolog-1 (NR5A2) with PIP3 hormone bound in the ligand binding pocket', *Journal of Structural Biology*, 192(3), pp. 342–348. doi: 10.1016/j.jsb.2015.09.012.

Saluja, A. K. *et al.* (1989) 'Experimental pancreatitis is mediated by low-affinity cholecystokinin receptors that inhibit digestive enzyme secretion', *Proceedings of the National Academy of Sciences of the United States of America*, 86(22), pp. 8968–71. doi: 10.1073/pnas.86.22.8968.

Sankaran, S. J. *et al.* (2015) 'Frequency of Progression From Acute to Chronic Pancreatitis and Risk Factors: A Meta-analysis', *Gastroenterology*, 149(6), pp. 1490-1500.e1. doi: 10.1053/j.gastro.2015.07.066.

Sarafidis, P. A. and Lasaridis, A. N. (2006) 'Actions of peroxisome proliferator-activated receptors-gamma agonists explaining a possible blood pressure-lowering effect.', *American journal of hypertension*, 19(6), pp. 646–53. doi: 10.1016/j.amjhyper.2005.12.017.

Schaffer, A. E. *et al.* (2010) 'Nkx6 Transcription Factors and Ptf1a Function as Antagonistic Lineage Determinants in Multipotent Pancreatic Progenitors', *Developmental Cell*, 18(6), pp. 1022–1029. doi: 10.1016/j.devcel.2010.05.015.

Schepis, T. *et al.* (2021) 'Microbiota in Pancreatic Diseases: A Review of the Literature.', *Journal of clinical medicine*, 10(24). doi: 10.3390/jcm10245920.

Schloss, P. D. (2021) 'Amplicon Sequence Variants Artificially Split Bacterial Genomes into Separate Clusters.', *mSphere*, 6(4), p. e0019121. doi: 10.1128/mSphere.00191-21.

Schoonjans, K. *et al.* (2002) 'Liver receptor homolog 1 controls the expression of the scavenger receptor class B type I', *EMBO Reports*. doi: 10.1093/embo-reports/kvf238.

Schutte, M. *et al.* (1997) 'Abrogation of the Rb/p16 tumor-suppressive pathway in virtually all pancreatic carcinomas', *Cancer Research*, 57(15), pp. 3126–3130.

Seitz, C. *et al.* (2019) 'The orphan nuclear receptor LRH-1/NR5a2 critically regulates T cell functions', *Science Advances*, 5(7), pp. 1–12. doi: 10.1126/sciadv.aav9732.

Sendler, M. *et al.* (2018) 'Cathepsin B-Mediated Activation of Trypsinogen in Endocytosing Macrophages Increases Severity of Pancreatitis in Mice', *Gastroenterology*, 154(3), pp. 704-718.e10. doi: 10.1053/j.gastro.2017.10.018.

Seol, W., Choi, H. S. and Moore, D. D. (1996) 'An orphan nuclear hormone receptor that lacks a DNA binding domain and heterodimerizes with other receptors.', *Science*, 272(5266), pp. 1336–9. doi: 10.1126/science.272.5266.1336.

Sethi, V. *et al.* (2018) 'Gut Microbiota Promotes Tumor Growth in Mice by Modulating Immune Response.', *Gastroenterology*, 155(1), pp. 33-37.e6. doi: 10.1053/j.gastro.2018.04.001.

Sever, R. and Glass, C. K. (2013) 'Signaling by Nuclear Receptors', *Cold Spring Harbor Perspectives in Biology*, 5(3), pp. a016709–a016709. doi: 10.1101/cshperspect.a016709.

Shannon, P. *et al.* (2003) 'Cytoscape: a software environment for integrated models of biomolecular interaction networks.', *Genome research*, 13(11), pp. 2498–504. doi: 10.1101/gr.1239303.

Shi, G. *et al.* (2009) 'Loss of the Acinar-Restricted Transcription Factor Mist1 Accelerates Kras-Induced Pancreatic Intraepithelial Neoplasia', *Gastroenterology*, 136(4), pp. 1368–1378. doi: 10.1053/j.gastro.2008.12.066.

Shin, D.-J. and Osborne, T. F. (2008) 'Peroxisome Proliferator-activated Receptor-γ Coactivator-1α Activation of CYP7A1 during Food Restriction and Diabetes Is Still Inhibited by Small Heterodimer Partner', *Journal of Biological Chemistry*, 283(22), pp. 15089–15096. doi: 10.1074/jbc.M710452200.

Da Silva Xavier, G. (2018) 'The Cells of the Islets of Langerhans', *Journal of Clinical Medicine*, 7(3), p. 54. doi: 10.3390/jcm7030054.

Sinaiko, A. R. *et al.* (2001) 'Insulin resistance syndrome in childhood: Associations of the euglycemic insulin clamp and fasting insulin with fatness and other risk factors', *The Journal of Pediatrics*, 139(5), pp. 700–707. doi: 10.1067/mpd.2001.118535.

Sinaiko, A. R. and Caprio, S. (2012) 'Insulin resistance', *The Journal of pediatrics*, 161(1), pp. 11–5. doi: 10.1016/j.jpeds.2012.01.012.

Siveke, J. T. *et al.* (2008) 'Notch Signaling Is Required for Exocrine Regeneration After Acute Pancreatitis', *Gastroenterology*, 134(2). doi: 10.1053/j.gastro.2007.11.003.

Slack, J. M. (1995) 'Developmental biology of the pancreas', *Development*, 121(6), pp. 1569–1580. doi: 10.1242/dev.121.6.1569.

Smeets, X. J. N. M. *et al.* (2019) 'The association between obesity and outcomes in acute pancreatitis: an individual patient data meta-analysis.', *European journal of gastroenterology & hepatology*, 31(3), pp. 316–322. doi: 10.1097/MEG.0000000000001300.

Smith, P. M. *et al.* (2013) 'The Microbial Metabolites, Short-Chain Fatty Acids, Regulate Colonic T reg Cell Homeostasis', *Science*, 341(6145), pp. 569–573. doi: 10.1126/science.1241165.

Solanki, N. S., Barreto, S. G. and Saccone, G. T. P. (2012) 'Acute pancreatitis due to diabetes: The role of hyperglycaemia and insulin resistance', in *Pancreatology*, pp. 234–239. doi: 10.1016/j.pan.2012.01.003.

Stanger, B. Z. and Hebrok, M. (2013) 'Control of cell identity in pancreas development and regeneration', *Gastroenterology*, 144(6). doi: 10.1053/j.gastro.2013.01.074.

Stein, S. *et al.* (2014) 'SUMOylation-Dependent LRH-1/PROX1 Interaction Promotes Atherosclerosis by Decreasing Hepatic Reverse Cholesterol Transport', *Cell Metabolism*, 20(4), pp. 603–613. doi: 10.1016/j.cmet.2014.07.023.

Stein, S. and Schoonjans, K. (2015) 'Molecular basis for the regulation of the nuclear receptor LRH-1', *Current Opinion in Cell Biology*. Elsevier Ltd, 33, pp. 26–34. doi: 10.1016/j.ceb.2014.10.007.

Storz, P. (2017) 'Acinar cell plasticity and development of pancreatic ductal adenocarcinoma', *Nature Reviews Gastroenterology & Hepatology*, 14(5), pp. 296–304. doi: 10.1038/nrgastro.2017.12.

Strobel, O. *et al.* (2007) 'In Vivo Lineage Tracing Defines the Role of Acinar-to-Ductal Transdifferentiation in Inflammatory Ductal Metaplasia', *Gastroenterology*, 133(6). doi: 10.1053/j.gastro.2007.09.009.

Su, K. H., Cuthbertson, C. and Christophi, C. (2006) 'Review of experimental animal models of acute pancreatitis', *HPB*. doi: 10.1080/13651820500467358.

Sun, Y., Demagny, H. and Schoonjans, K. (2021) 'Emerging functions of the nuclear receptor LRH-1 in liver physiology and pathology', *Biochimica et Biophysica Acta (BBA) - Molecular Basis of Disease*. Elsevier B.V., 1867(8), p. 166145. doi: 10.1016/j.bbadis.2021.166145.

Tachibana, M. *et al.* (2002) 'G9a histone methyltransferase plays a dominant role in euchromatic histone H3 lysine 9 methylation and is essential for early embryogenesis', *Genes & Development*, 16(14), pp. 1779–1791. doi: 10.1101/gad.989402.

Teta, M. *et al.* (2007) 'Growth and Regeneration of Adult β Cells Does Not Involve Specialized Progenitors', *Developmental Cell*, 12(5), pp. 817–826. doi: 10.1016/j.devcel.2007.04.011.

The Cancer Genome Atlas Research Network and Raphael, B. J. (2017) 'Integrated Genomic Characterization of Pancreatic Ductal Adenocarcinoma The Cancer Genome Atlas Research Network *', *Cancer Cell*, 32(2)(2).

Thomas, R. M. *et al.* (2018) 'Intestinal microbiota enhances pancreatic carcinogenesis in preclinical models', 39(8), pp. 1068–1078. doi: 10.1093/carcin/bgy073.

Thursby, E. and Juge, N. (2017) 'Introduction to the human gut microbiota', *Biochemical Journal*, 474(11), pp. 1823–1836. doi: 10.1042/BCJ20160510.

Tilg, H. and Moschen, A. R. (2010) 'Evolution of inflammation in nonalcoholic fatty liver disease: the multiple parallel hits hypothesis.', *Hepatology (Baltimore, Md.)*, 52(5), pp. 1836–46. doi:

10.1002/hep.24001.

Tsuru, H. *et al.* (2020) 'HFD-induced hepatic lipid accumulation and inflammation are decreased in Factor D deficient mouse.', *Scientific reports*, 10(1), p. 17593. doi: 10.1038/s41598-020-74617-5.

Turnbaugh, P. J. *et al.* (2009) 'A core gut microbiome in obese and lean twins.', *Nature*. Nature Publishing Group, 457(7228), pp. 480–4. doi: 10.1038/nature07540.

Turner, N. C. and Clapham, J. C. (1998) 'Insulin resistance, impaired glucose tolerance and non-insulin-dependent diabetes, pathologic mechanisms and treatment: Current status and therapeutic possibilities', *Progress in Drug Research*. Basel: Birkhäuser Basel, 51, pp. 33–94. doi: 10.1007/978-3-0348-8845-5_2.

Ulluwishewa, D. *et al.* (2011) 'Regulation of Tight Junction Permeability by Intestinal Bacteria and Dietary Components 1 , 2', pp. 769–776. doi: 10.3945/jn.110.135657.769.

Venteclef, N. *et al.* (2010) 'GPS2-dependent corepressor/SUMO pathways govern anti-inflammatory actions of LRH-1 and LXRβ in the hepatic acute phase response', *Genes & Development*, 24(4), pp. 381–395. doi: 10.1101/gad.545110.

Vich Vila, A. *et al.* (2018) 'Gut microbiota composition and functional changes in inflammatory bowel disease and irritable bowel syndrome', *Science Translational Medicine*, 10(472). doi: 10.1126/scitranslmed.aap8914.

Vonlaufen, A., Wilson, J. S. and Apte, M. V. (2008) 'Molecular mechanisms of pancreatitis: Current opinion', *Journal of Gastroenterology and Hepatology*, 23(9), pp. 1339–1348. doi: 10.1111/j.1440-1746.2008.05520.x.

Vyas, S., Zaganjor, E. and Haigis, M. C. (2016) 'Mitochondria and Cancer', *Cell*, 166(3), pp. 555–566. doi: 10.1016/j.cell.2016.07.002.

Waddell, N. *et al.* (2015) 'Whole genomes redefine the mutational landscape of pancreatic cancer', *Nature*, 518(7540), pp. 495–501. doi: 10.1038/nature14169.

Wang, W. *et al.* (2005) 'The crystal structures of human steroidogenic factor-1 and liver receptor homologue-1', *Proceedings of the National Academy of Sciences*, 102(21), pp. 7505–7510. doi: 10.1073/pnas.0409482102.

Wang, Z. *et al.* (2017) 'Changes in metabolically active bacterial community during rumen development, and their alteration by rhubarb root powder revealed by 16s rRNA amplicon sequencing', *Frontiers in Microbiology*, 8(FEB). doi: 10.3389/fmicb.2017.00159.

Weger, B. D. *et al.* (2019) 'The Mouse Microbiome Is Required for Sex-Specific Diurnal Rhythms of Gene Expression and Metabolism', *Cell Metabolism*, 29(2), pp. 362-382.e8. doi: 10.1016/j.cmet.2018.09.023.

Weiss, F. U., Laemmerhirt, F. and Lerch, M. M. (2019) 'Etiology and Risk Factors of Acute and Chronic Pancreatitis', *Visceral Medicine*, 35(2), pp. 73–81. doi: 10.1159/000499138.

Wen, L. *et al.* (2008) 'Innate immunity and intestinal microbiota in the development of Type 1 diabetes', *Nature*, 455(7216), pp. 1109–1113. doi: 10.1038/nature07336.

Whitcomb, D. C. and Lowe, M. E. (2007) 'Human Pancreatic Digestive Enzymes', *Digestive Diseases and Sciences*, 52(1), pp. 1–17. doi: 10.1007/s10620-006-9589-z.

Whitley, E. M. (2014) 'Comparative Pancreatic Pathology', in *Pathobiology of Human Disease*. Elsevier, pp. 1101–1123. doi: 10.1016/B978-0-12-386456-7.03415-8.

WHO (2020) *Fact Sheet: Obesity and Overweight*, *World Health Organization*.

Wiese, M. L. *et al.* (2021) 'Excess Body Weight and Pancreatic Disease', *Visceral Medicine*, 37(4), pp. 281–286. doi: 10.1159/000517147.

Wilentz, R. E. *et al.* (2000) 'Loss of expression of Dpc4 in pancreatic intraepithelial neoplasia: Evidence that DPC4 inactivation occurs late in neoplastic progression', *Cancer Research*, 60(7).

Williams, J. A. (2010) 'Regulation of acinar cell function in the pancreas', *Current Opinion in Gastroenterology*, 26(5), pp. 478–483. doi: 10.1097/MOG.0b013e32833d11c6.

Wu, C., Li, M. and Chen, W. (2021) 'Characteristics of Gut Microbiota in Cerulein-Induced Chronic Pancreatitis.', *Diabetes, metabolic syndrome and obesity : targets and therapy*, 14, pp. 285–294. doi: 10.2147/DMSO.S291822.

Wu, J. *et al.* (2018) 'Carbon Monoxide Impairs CD11b + Ly-6C hi Monocyte Migration from the Blood to Inflamed Pancreas via Inhibition of the CCL2/CCR2 Axis', *The Journal of Immunology*, 200(6), pp. 2104–2114. doi: 10.4049/jimmunol.1701169.

Wu, J. *et al.* (2020) 'Macrophage phenotypic switch orchestrates the inflammation and repair/regeneration following acute pancreatitis injury.', *EBioMedicine*, 58, p. 102920. doi: 10.1016/j.ebiom.2020.102920.

Xu, C. *et al.* (2015) 'Influence of Fatty Liver on the Severity and Clinical Outcome in Acute Pancreatitis', *PLOS ONE*. Edited by Z. Rakonczay, 10(11), p. e0142278. doi: 10.1371/journal.pone.0142278.

Xu, M. *et al.* (2018) 'Obesity and Pancreatic Cancer', *Pancreas*, 47(2), pp. 158–162. doi: 10.1097/MPA.0000000000000974.

Xu, T. *et al.* (2021) 'Free Fatty Acid Increases the Expression of NLRP3-Caspase1 in Adipose Tissue Macrophages in Obese Severe Acute Pancreatitis', *Digestive Diseases and Sciences*. Springer US, (0123456789). doi: 10.1007/s10620-021-07027-w.

Xuan, S. *et al.* (2012) 'Pancreas-specific deletion of mouse Gata4 and Gata6 causes pancreatic agenesis', *Journal of Clinical Investigation*, 122(10), pp. 3516–3528. doi: 10.1172/JCI63352.

Xue, J. and Habtezion, A. (2014) 'Carbon monoxide–based therapy ameliorates acute pancreatitis via TLR4 inhibition', *Journal of Clinical Investigation*, 124(1), pp. 437–447. doi: 10.1172/JCI71362.

Yang, A. X. *et al.* (2022) 'Pathobionts from chemically disrupted gut microbiota induce insulin-dependent diabetes in mice', pp. 1–46.

Yatsuji, S. *et al.* (2009) 'Clinical features and outcomes of cirrhosis due to non-alcoholic steatohepatitis compared with cirrhosis caused by chronic hepatitis C', *Journal of Gastroenterology and Hepatology*, 24(2), pp. 248–254. doi: 10.1111/j.1440-1746.2008.05640.x.

Ye, C. *et al.* (2019) 'Obesity Aggravates Acute Pancreatitis via Damaging Intestinal Mucosal Barrier and Changing Microbiota Composition in Rats.', *Scientific reports*, 9(1), p. 69. doi: 10.1038/s41598-018-36266-7.

Yengo, L. *et al.* (2018) 'Meta-analysis of genome-wide association studies for height and body mass index in ~700000 individuals of European ancestry.', *Human molecular genetics*, 27(20), pp. 3641–3649. doi: 10.1093/hmg/ddy271.

Yoon, S. B. *et al.* (2017) 'Impact of Fatty Liver on Acute Pancreatitis Severity.', *Gastroenterology research and practice*, 2017, p. 4532320. doi: 10.1155/2017/4532320.

Yue, R., Shen, B. and Morrison, S. J. (2016) 'Clec11a/osteolectin is an osteogenic growth factor

that promotes the maintenance of the adult skeleton.', *eLife*, 5. doi: 10.7554/eLife.18782.

Zerem, E. (2014) 'Treatment of severe acute pancreatitis and its complications', *World Journal of Gastroenterology*, 20(38), p. 13879. doi: 10.3748/wjg.v20.i38.13879.

Zhang, M. *et al.* (2016) 'Three new pancreatic cancer susceptibility signals identified on chromosomes 1q32.1, 5p15.33 and 8q24.21', *Oncotarget*, 7(41), pp. 66328–66343. doi: 10.18632/oncotarget.11041.

Zheng, D., Liwinski, T. and Elinav, E. (2020) 'Interaction between microbiota and immunity in health and disease', *Cell Research*, 30(6), pp. 492–506. doi: 10.1038/s41422-020-0332-7.

Zheng, J. *et al.* (2019) 'Commensal Escherichia coli aggravates acute necrotizing pancreatitis through targeting of intestinal epithelial cells', *Applied and Environmental Microbiology*, 85(12), pp. 1–25. doi: 10.1128/AEM.00059-19.

Zheng, Z. *et al.* (2021) 'A narrative review of acute pancreatitis and its diagnosis, pathogenetic mechanism, and management', *Annals of Translational Medicine*, 9(1). doi: 10.21037/atm-20-4802.

Zhou, Q. *et al.* (2007) 'A Multipotent Progenitor Domain Guides Pancreatic Organogenesis', *Developmental Cell*, 13(1), pp. 103–114. doi: 10.1016/j.devcel.2007.06.001.

Zhou, Q. *et al.* (2020) 'T Lymphocytes: A Promising Immunotherapeutic Target for Pancreatitis and Pancreatic Cancer?', *Frontiers in Oncology*, 10. doi: 10.3389/fonc.2020.00382.

Zhu, Y. *et al.* (2019) 'Gut microbiota dysbiosis worsens the severity of acute pancreatitis in patients and mice', *Journal of Gastroenterology*, 54(4), pp. 347–358. doi: 10.1007/s00535-018-1529-0.

Zhu, Z. *et al.* (2020) 'Shared genetic and experimental links between obesity-related traits and asthma subtypes in UK Biobank.', *The Journal of allergy and clinical immunology*, 145(2), pp. 537–549. doi: 10.1016/j.jaci.2019.09.035.